

UNCLASSIFIED

AD 282 119

*Reproduced
by the*

ARMED SERVICES TECHNICAL INFORMATION AGENCY
ARLINGTON HALL STATION
ARLINGTON 12, VIRGINIA



UNCLASSIFIED

NOTICE: When government or other drawings, specifications or other data are used for any purpose other than in connection with a definitely related government procurement operation, the U. S. Government thereby incurs no responsibility, nor any obligation whatsoever; and the fact that the Government may have formulated, furnished, or in any way supplied the said drawings, specifications, or other data is not to be regarded by implication or otherwise as in any manner licensing the holder or any other person or corporation, or conveying any rights or permission to manufacture, use or sell any patented invention that may in any way be related thereto.

282 119

U. S. A R M Y
TRANSPORTATION RESEARCH COMMAND
FORT EUSTIS, VIRGINIA

TCREC Technical Report 62-28

AN EXPERIMENTAL INVESTIGATION OF THE RESPONSE
CHARACTERISTICS OF TWO MAN-CARRYING
GROUND EFFECT MACHINES

Task 9R99-01-005-02
Contract DA 44-177-TC-733

April 1962

Prepared By:

KELLETT AIRCRAFT CORPORATION
Willow Grove, Pennsylvania



282 119

CATALOGED BY ASTIA
AS AD NO.

NOX


FOREWORD


Stability and control studies of the ground effect machine (GEM) have in the past been hampered by the scarcity of experimental data on large-scale machines. This is especially true in the area of dynamic stability measuring response of the machine to control inputs and terrain discontinuities.

This report of dynamic stability tests of two widely different types of GEM's is an initial effort to obtain data with which to compare the theoretical predictions of vehicle response. The lack of correlation between predicted and measured pitch and heave frequency response indicates that some revisions of theory are necessary.

As larger and more sophisticated GEM's become available, it is the intent of this Command to obtain similar data on these machines. It is believed that these data will be useful to industry in refining the methods of predicting characteristics of GEM designs.

APPROVED:


WILLIAM D. HINSHAW
PROJECT ENGINEER


EARL A. WIRTH
CWO-4
Adjutant

Task 9R99-01-005-02

Contract DA 44-177-TC-733

April 1962

AN EXPERIMENTAL INVESTIGATION OF THE RESPONSE
CHARACTERISTICS OF TWO MAN-CARRYING
GROUND EFFECT MACHINES

Prepared by

KELLETT AIRCRAFT CORPORATION
Willow Grove, Pennsylvania

for

U. S. ARMY TRANSPORTATION RESEARCH COMMAND
FORT EUSTIS, VIRGINIA

PREFACE

This report presents the results of an experimental investigation of the dynamic response characteristics of two man-carrying ground effect machines. The project was performed under Contract No. DA 44-177-TC-733 with the United States Army Transportation Research Command, Fort Eustis, Virginia. Mr. W. Hinshaw was the Army Project Engineer and his assistance is hereby gratefully acknowledged. The work was performed under the direction of Dr. A. A. Perlmutter, Manager of Research Engineering of the Kellett Aircraft Corporation, and was conducted through the period from May 1960 through January 1961. The contributions to the success of this program of the following Kellett personnel is gratefully acknowledged:

Mr. J. de la Cierva, Head, Electronics Section
Mr. M. George, Test Engineer
Mr. R. DeRogatis, Test Engineer

Acknowledgement is also made to the Princeton University Department of Aeronautical Engineering for their cooperation during the P-GEM test program.

CONTENTS

	<u>Page</u>
PREFACE	iii
TABLE OF CONTENTS	v
LIST OF ILLUSTRATIONS	vi
LIST OF SYMBOLS	xi
SUMMARY	1
I. INTRODUCTION	2
II. DISCUSSION OF THE TEST RESULTS	3
1. Princeton GEM Tests	3
2. "Hula Hoop" Tests	7
III. CORRELATION WITH THEORY	9
1. Current Theories	9
2. The Effect of Air Cushion Flow	11
IV. CONCLUSIONS AND RECOMMENDATIONS	17
V. REFERENCES	18
APPENDICES	
A. The Physical Parameters of the Test Vehicles	20
B. The Instrumentation	25
C. The Test Program Summary	28
D. Illustrations	35

LIST OF ILLUSTRATIONS

<u>FIGURE</u>	<u>TITLE</u>	<u>PAGE</u>
1	The Princeton University 20-Foot Diameter Ground Effect Machine	36
2	The TRECOM "Hula Hoop"	37
3	P-GEM Low Altitude Response to a Longitudinal Disturbance (External Push-Down)	38
4	P-GEM Response to a Longitudinal Disturbance (External Push-Down) At a Height of 12 Inches	39
5	P-GEM Low Altitude Response to a Lateral Disturbance (External Push-Down)	40
6	P-GEM Response to a Lateral Disturbance (External Push-Down) At a Height of 14 Inches	41
7	Effect of Increased Moment of Inertia on the Longitudinal Response Characteristics of the P-GEM	42
8	P-GEM Low Speed Response to a Longitudinal Disturbance	43
9	P-GEM Medium Speed Response to a Longitudinal Control Pulse	44
10	P-GEM High Speed Response to a Longitudinal Control Pulse	45
11	P-GEM Response to a Forward Control Step Input	46
12	P-GEM Response to a Lateral Control Input	47
13	P-GEM Response to an Aft Control Input	48
14	P-GEM Response to a Yaw Control Step Input at Zero Forward Speed	49

<u>FIGURE</u>	<u>TITLE</u>	<u>PAGE</u>
15	P-GEM Low Speed Response to a Yaw Control Input	50
16	P-GEM Medium Speed Response to a Yaw Control Input	51
17	Variation of P-GEM Altitude With Brake Horsepower	52
18	Operating Altitude of the P-GEM As a Function of Forward Speed At a Constant Power of About 160 H.P.	53
19	Response of the P-GEM Crossing a 4-Foot Wide By 2-Foot Deep Ditch	54
20	Low Speed Crossing of the P-GEM Over a 4-Foot Wide x 4-Foot Deep Ditch	55
21	Medium Speed Crossing of the P-GEM Over a 4-Foot Wide x 4-Foot Deep Ditch	56
22	High Speed Crossing of the P-GEM Over a 4-Foot Wide x 4-Foot Deep Ditch	57
23	Response of the P-GEM Crossing a 2-Foot Wide x 2-Foot Deep Ditch	58
24	Low Speed Crossing of the P-GEM Over a 3-Inch Thick x 6-Inch High Fence	59
25	High Speed Crossing of the P-GEM Over a 3-Inch Thick x 6-Inch High Fence	60
26	Low Speed Crossing of the P-GEM Over a 3-Inch Thick x 12-Inch High Fence	61
27	High Speed Crossing of the P-GEM Over a 3-Inch Thick x 12-Inch High Fence	62
28	Low Speed Crossing of the P-GEM Over a 24-Inch Thick x 6-Inch High Fence	63
29	Medium Speed Crossing of the P-GEM Over a 24-Inch Thick x 6-Inch High Fence	64
30	Low Speed Crossing of the P-GEM Over a 24-Inch Thick x 12-Inch High Fence	65

<u>FIGURE</u>	<u>TITLE</u>	<u>PAGE</u>
31	Medium Speed Crossing of the P-GEM Over a 24-Inch Thick x 12-Inch High Fence	66
32	Low Speed Crossing of the P-GEM Over a Series of 2-Foot Wide x 1-Foot Deep Ditches	67
33	Medium Speed Crossing of the P-GEM Over a Series of 2-Foot Wide x 1-Foot Deep Ditches	68
34	High Speed Crossing of the P-GEM Over a Series of 2-Foot Wide x 1-Foot Deep Ditches	69
35	Low Speed Crossing of the P-GEM Over a Series of 4-Foot Wide x 2-Foot Deep Ditches	70
36	Medium Speed Crossing of the P-GEM Over a Series of 4-Foot Wide x 2-Foot Deep Ditches	71
37	High Speed Crossing of the P-GEM Over a Series of 4-Foot Wide x 2-Foot Deep Ditches	72
38	"Hula-Hoop" Response to an External Longitudinal Disturbance	73
39	"Hula-Hoop" Response to Longitudinal Control Pulses at Low Forward Speed	74
40	"Hula-Hoop" Response to an External Heave Disturbance	75
41	"Hula-Hoop" Response to an External Yaw Disturbance	76
42	"Hula-Hoop" Response to Longitudinal Control Inputs	77
43a	"Hula-Hoop" Response to Lateral Control Inputs	78
43b	"Hula-Hoop" Response to a Yaw Control Input	79

<u>FIGURE</u>	<u>TITLE</u>	<u>PAGE</u>
44	Effect of Gross Weight on the Hovering Altitude of the "Hula-Hoop"	80
45	Comparison of Theory With Test Data of the Heave Frequency of the P-GEM	81
46	The Rotational Cushion Flow	82
47	Variation of P_B/P_b with y/r	83
48	Yaw Control Installation	84
49	"Hula-Hoop" Roll Vane Installation	85
50	Percent of Longitudinal Stick Travel vs. Thrust Rotor Collective Pitch Angle, "Hula-Hoop"	86
51	Percent of Lateral Stick Travel vs. Roll Vane Angle, "Hula-Hoop"	87
52	Oscillograph Recorder and Bridge Balance Boxes Installed on the P-GEM	88
53	Vertical and Directional Gyros Installed on the P-GEM	89
54	Position Indicator Wiring Diagram	90
55	Installation of Control Panel on P-GEM	91
56	Instrumentation Cart Utilized in the Flight Testing of the "Hula-Hoop"	92
57a & b	A Schematic Representation of the Test Tracks Utilized in the P-GEM Tests	93 & 94
58	Series of 10 Ditches 8 Feet Apart 2 Feet Wide by 1 Foot Deep, 30 Feet Long	95
59	Series of 10 Ditches 10 Feet Apart 2 Feet Wide by 1 Foot Deep, 30 Feet Long	96
60	Individual Ditch 4 Feet Wide x 4 Feet Deep x 30 Feet Long	97

<u>FIGURE</u>	<u>TITLE</u>	<u>PAGE</u>
61	Individual Hole 4 Feet by 4 Feet by 4 Feet Deep	98
62	Wooden Fence, 12 Inches High, 24 Inches Thick and 30 Feet Long	99
63	Plowed Field .75 Foot Deep x 1.5-Foot Spacing Negotiated by the P-GEM	100

LIST OF SYMBOLS

d	Vehicle Base Diameter, ft.
g	Acceleration of Gravity, ft./sec. ²
h	Algebraic Average of the Distance From Forward and Rearward Height Sensors to Obstacles Directly Beneath These Sensors, ft. (See also additional comments in Section 1.4)
h_e	Equilibrium Height, ft. (See Reference 8)
I_{xx}	Vehicle Mass Moment of Inertia in Roll, slug-ft. ²
I_{yy}	Vehicle Mass Moment of Inertia in Pitch, slug-ft. ²
I_{zz}	Vehicle Mass Moment of Inertia in Yaw, slug-ft. ²
P_a	Ambient Static Pressure, lb./ft. ²
P_b	Static Pressure at Point B, lb./ft. ² (Reference Figure 46)
P_b	Vehicle Base Pressure, lb./ft. ²
P_T	Total Pressure, lb./ft. ²
P_{Tj}	Total Pressure at the Nozzle Exit, lb./ft. ²
r	Vehicle Base Radius, ft.
t_e	Nozzle Thickness, ft.
V_A	Velocity at Point A, ft./sec. (Reference Figure 46)
W	Vehicle Gross Weight, lb.
$\bar{X}, \bar{X}_t, \dots$	Longitudinal Distance of Vehicle Components From Center of Gravity, Perpendicular to Main Rotor Axis of Rotation, ft.

$\bar{y}, \bar{y}_v \dots$	Lateral Distance of Vehicle Components From Center of Gravity, Perpendicular to Main Rotor Axis of Rotation, ft.
$\bar{z}, \bar{z}_t \dots$	Distance of Vehicle Components From Center of Gravity, Parallel to the Main Rotor Axis of Rotation, ft.
α	Vehicle Pitch Angle, Degrees, Positive Nose-Up
γ	Ratio of Specific Heats (AIR = 1.4)
ρ	Air Density, slug/ft. ²
σ	Solidity Ratio, $\frac{\text{No. of Blades} \times \text{Chord Length}}{\pi \times \text{Rotor Radius}}$
ϕ	Vehicle Roll Angle, Degrees, Positive When Pilot's Right Hand Down
ψ	Vehicle Yaw Angle, Degrees, Positive to Pilot's Left
ω_h	Heave Frequency, radians/sec.
ω_α	Pitch Frequency, radians/sec.

SUMMARY

An experimental investigation was performed of the dynamic response characteristics of the Princeton 20-foot annular jet Ground Effect Machine and the U. S. Army Transportation Research Command 15-foot "Hula-Hoop". The tests ranged from dynamic stability and control responses to performance and for the P-GEM also the operation over specially prepared test tracks simulating various conditions of rough terrain. The P-GEM successfully negotiated all prepared obstacles. The calculated values of frequency and damping ratio from existing two-dimensional theories are found to be inadequate for the prediction of the dynamic characteristics of the test vehicles.

I. INTRODUCTION

In recent years a considerable number of investigations have been performed on various aspects of the operation of Ground Effect Machines. Particular emphasis has been placed on the evaluation of the parameters that affect the performance, and the stability and control characteristics of these vehicles. Whereas analyses on performance have resulted in significant advances, much still remains to be done in the areas of stability and control. The present project was undertaken to shed further light on the handling qualities of GEMs and for this purpose two man-carrying machines were instrumented and their response characteristics were recorded. The test vehicles were the 20-foot annular GEM built by the Princeton University for the U. S. Army Transportation Corps, shown in Figure 1, and the Hula-Hoop shown in Figure 2. The "Hula-Hoop" consists of an experimental de Lackner Aerocycle modified by the U. S. Army TRECOM by the addition of a circular duct or hoop around the two co-axial rotors and a reversible pitch thrust fan in the longitudinal direction.

Section II of this report is a discussion of the test results. Section III correlates these data with the available theoretical analyses. Conclusions and recommendations are presented in Section IV. The physical parameters of the test vehicles, the test instrumentation and a summary of the test program are presented in Appendices A, B, and C, respectively.

A sixteen-mm color film supplements the data presented in this report. This film is available on loan from U. S. Army TRECOM, Fort Eustis, Virginia.

II. DISCUSSION OF THE TEST RESULTS

The test results of each of the two test vehicles are discussed separately. The first series of tests were performed with the 20-foot annular jet Princeton GEM. The tests with this vehicle were divided into four major categories:

- a. Dynamic Stability
- b. Response to Control Inputs
- c. Performance
- d. Rough Terrain

The tests performed with the "Hula-Hoop" were concerned mostly with the first two of the above test categories.

1. Princeton GEM Tests

1.1 Dynamic Stability

Tests were performed to determine the transient response of the vehicle to different types of pulse disturbances. In the zero velocity tests the disturbance was obtained by a manual push-down of the vehicle by one of the test engineers. In the forward speed tests the disturbances were obtained by:

- a.) Stick pulse
- b.) Single ditch or hole

Figures 3 and 4 show the response to a longitudinal disturbance at zero forward speed. It is seen from Figure 3 that, at low altitude, the machine is quite stable. The normal acceleration response consists of a rapidly decaying oscillation with a frequency of about 1.0 cycle/second. In the figures linear acceleration is defined as positive when upward, forward, or starboard along the centroidal principal axes, respectively. The pitch response appears to be a nonperiodic decaying motion. At a higher altitude, Figure 4, the frequency of the normal acceleration is again about 1 cycle/second, and the vehicle assumed a new pitch attitude, while starting to move forward. Roll disturbances at zero forward speed, presented in Figures 5 and 6, show a similar behavior as the pitch disturbances. At low height the attitude response is stable and the machine returns to its previous equilibrium position. At higher altitudes the machine attains a

new attitude equilibrium position in the direction in which it was disturbed, and transverse motion ensues.

These zero speed tests seem to indicate that there does not exist strong coupling between normal acceleration and attitude, the former being stable at all altitudes, the latter being dynamically unstable at the higher test altitudes. Figure 5 and 6 also show the trace of the vehicle altitude. It is noted that these traces indicate a height variation that is, in general, compatible with the vehicle attitude response. The effect of an increase in moment of inertia is shown in Figure 7. An additional weight of 114 lbs. was placed at two locations on the longitudinal axis, thereby increasing I_{yy} from 1540 to 1730 slug-ft.². The pitch response for this test showed an oscillatory tendency with a frequency of about 0.25 cycle/second.

Forward speed test data are presented in Figures 8 through 10. Figure 8 is the response of the vehicle passing at 9 feet/second over a single hole of 2-foot depth and 4-foot width. Figures 9 and 10 are longitudinal stick pulse responses at 15 and 22 feet/second, respectively. The test records indicate that the pitch attitude does not return to its predisturbance equilibrium position. On the other hand, the motion is not unstable in the sense that its magnitude continuously increases with time. It is also interesting to note that the pitch motion exhibits more waviness than in the hovering tests. In the visual film records of these tests the change of trim attitude is barely perceptible and the responses to the disturbances appear to decay rapidly. From the above, as well as from other tests made, it is shown that the heaving motion is oscillatory with a frequency of about 1 cycle/second for all test speeds. The pitch motion is aperiodic at zero speed and has what may be a nonlinear oscillatory shape of about 0.25-.40 cycle/second for the forward speed tests.

1.2 Control Response

Figure 11 shows the response of the P-GEM to a forward stick step at zero forward speed. This test was performed with the pusher propeller inoperative. A maximum longitudinal acceleration of 0.04 g was obtained. This is 50% larger than would be expected, considering the tilt angle of the machine. A speed of 12 feet/second was obtained in 10 seconds. The pitch angle change was limited to about one degree.

Figure 12 is a similar control step to the right. Initial roll velocity was about 2 degrees per second. The velocity instrumentation was inoperative during this test, but it is estimated that a sideward velocity of 10 feet/second was obtained after 10 seconds. Another control response is shown in Figure 13, where the machine is brought to a stop from a forward speed of 16.5 feet/second. The above responses represent the controllability of the P-GEM as resulting from vehicle tilting. Yaw control responses are shown in Figures 14, 15 and 16 for forward velocities of 0, 13 and 20 feet/second, respectively. Yaw control is obtained by locating a rudder surface in the airflow of the pusher propeller. As a result there exists a strong coupling between yaw, pitch and forward motion. The effect of the pusher propeller is seen in Figures 15 and 16 where there is a rapid increase in yaw attitude when the thrust engine power is increased. The rate of yaw is highest for the zero trim speed test, with a maximum value of 30 degrees/second. This value is reduced to about 10 degrees per second for the forward speed tests.

1.3 Performance

The variation of brake horsepower with hover altitude is shown in Figure 17. In the range of altitudes tested the power increase is nearly linear with altitude.

The variation of operating altitude with forward speed at constant power of about 160 HP is presented in Figure 18. The average loss of altitude with increasing forward speed is seen to be about 2 inches for every 10 feet/second.

A maximum forward speed of about 50 feet/second (34 m.p.h.) was attained. During that particular test the machine experienced a sharp pitch-up exceeding 15 degrees.

The P-GEM was operated up and down 5-degree inclines, and exhibited adequate control capability during these tests.

No accurate measurements were obtained for the radius of turn for different forward speeds.

1.4 Rough Terrain

Test runs were made over individual holes and ditches of various widths and depths, series of ditches, individual fences, plowed fields, and general cross-country conditions. It was determined that individual holes with a planform area to vehicle base area ratio of less than 0.05 had only a negligible effect on the motion of the vehicle passing over the holes. The response of the machine traversing individual ditches, however, was quite pronounced. Figure 19 presents the response of the P-GEM crossing a single ditch 4-foot wide x 2-foot deep at a speed of 8 feet/second. Figure 20 presents a similar crossing over a 4-foot wide x 4-foot deep ditch. During the crossing of the deeper ditch, the machine front and rear ends collided with the ground, resulting in 0.1 g values of rearward acceleration. The pitch attitude changes were also more severe for the deeper ditch. The effect of forward speed on the ditch crossing characteristics of the P-GEM are obtained by comparing Figure 20 with Figures 21 and 22. It is noted that, whereas the peak magnitude of the normal acceleration tends to increase with forward speed, the opposite occurs insofar as the peak magnitudes of the pitch attitude is concerned. The longitudinal accelerations are indicative of ground impacts. The effect of ditch width is demonstrated by comparing Figures 19 and 23. The normal acceleration peaks are considerably smaller for the narrower ditch shown in Figure 23. The altitude traces for these tests provide qualitative information only, insofar as vehicle height from average ground level is concerned. The altimeter utilized two conductive surfaces, attached to the vehicle base, which together with the ground completed a variable capacitive circuit. The altitude traces indicate the relative distance between these surfaces and the obstacle, such as the bottom of a ditch or the top of a fence, rather than the relative distance of the vehicle base from the ground surrounding these obstacles. The peaks in Figures 20 and 22 are representative of the ditch depths, and not of vehicle altitude. It should be noted, however, that over flat terrain the altitude indicated corresponds to the distance between the center of the vehicle's base and the ground.

The effects of fence height and forward speeds are shown in Figures 24 through 27. As expected, increased speed and fence height results in increased magnitudes of normal acceleration peaks and pitch attitude displacements. Similar effects are demonstrated in Figures 28 through 31 for 24-inch-wide fences. The longitudinal acceleration peaks correspond to ground impacts.

The responses of the P-GEM passing at three different speeds over a series of ten 2-foot wide x 1-foot deep ditches are shown in Figures 32, 33 and 34. At the low speed run, Figure 32, the heave response frequency is identical to the disturbance frequency. As speed increases, however, the machine tends to oscillate at its natural frequency in heave which is about 1 cycle/second. The pitch response was of insignificant magnitude for all speeds.

The results of similar tests over a series of 4-foot wide x 2-foot deep ditches are shown in Figures 35, 36 and 37. At low speed, Figure 35, there occurred significant pitch attitude changes with a frequency close to that of the disturbance frequency. The increasing of the forward speed resulted in a decrease of the pitch response in both magnitude and frequency. The pitch attitude frequency during these higher speed runs was about 2/3 of a cycle/second. Maximum normal acceleration peaks of .27 g were recorded and the altitude peak changes were about equal in magnitude to the operating height of 10 inches.

The test vehicle was operated over plowed fields with various directions of incidence relative to the furrows, and no significant effects on the motion of the machine were detected.

Operation over ground with different grass heights did not affect the hover altitude at constant engine r.p.m.

Similarly, the operation of the machine over and along steps and up and down moderate slopes did not pose any difficulties.

In summary, the P-GEM was capable of passing over all prepared obstacles. The most severe conditions were encountered when the disturbance frequency, as for example caused by a series of ditches, approached the natural heaving frequency of the vehicle (about 1 cycle/second). The ditches were at 10-foot intervals, and hence the "critical speed" over the ditches was about 10 feet/second.

2. The "Hula-Hoop" Tests

The tests with the "Hula-Hoop" covered the areas of dynamic stability, responses to control inputs, and hovering performance. A typical zero speed response

to an external longitudinal push-down is presented in Figure 38. The response to longitudinal stick pulses at low forward speed is shown in Figure 39. The pitch attitude motion for these tests were oscillatory at a frequency of about .2 cycle/second. Two other zero speed records, not presented here, show an aperiodic pitch attitude response, and, hence, caution should be exercised in the interpretation of these pitch data. On the other hand, the nearly neutrally stable heave oscillation is a characteristic feature of this test vehicle. Figure 40 more clearly illustrates this heave response to a vertical disturbance. The heave frequency is about 0.45 cycle/second. Figure 41 presents the response to a yaw disturbance. The "Hula-Hoop" at zero speed is seen to be neutrally stable in yaw and possesses zero yaw damping. The response to longitudinal control inputs is shown in Figure 42. Maximum rates of pitch of 3.5 degrees per second were attained. Similar responses in roll and yaw are shown in Figures 43a and 43b, respectively. Maximum rates achieved were 2 degrees/second in roll and 12.5 degrees/second in yaw. The maximum control moments measured were 55 foot-pounds in roll and 155 foot-pounds in pitch.

Two types of hovering performance tests were performed. In the first series of tests, the changes in altitude were obtained at $W = 834$ pounds and varying rpm, and the results are presented in Appendix C, Section II-C. The second series of tests consisted of the variation of gross weight at constant rpm, and the resulting equilibrium altitudes are shown in Figure 44.

III. CORRELATION WITH THEORY

1. Current Theories

Existing theories are mostly concerned with the static performance of ground effect vehicles, and specifically with the prediction of the vehicle base pressure as a function of operating altitude. These theories range from a simple momentum relation, Reference 1, to a more exact momentum theory in Reference 2, and to a potential flow solutions of a bifurcated jet with given upstream conditions, Reference 3. These analyses were for the two-dimensional symmetric case. In the analysis of the non symmetric case, corresponding, say, to a change in attitude, the available theories generally assume that the pressure varies linearly across the base from jet to jet with the base pressures near each jet evaluated by the two-dimensional symmetric theory. The symmetric theories all have one thing in common, namely, they postulate that the pressure across the base is constant for any given operating condition. Several controlled model tests, however, have shown that the pressure varies across the base. Both References 4 and 5 show that there exist pressure reductions on the base plate in the vicinity of the jet nozzles. This nonuniformity is generally ascribed to the existence of a "vortex"-type flow of the air trapped under the base plate. It is believed that the effect of these nonuniformities of base pressure on the stability characteristics is of significance, and warrants further investigation.

Work on dynamics of GEMs is reported in References 6 through 9. References 6, 8 and 9 formulate theories that are based on the concept of the unbalanced jet. This concept is concerned with the capability of jets to adjust to varying boundary conditions. For example, a jet curving from the nozzle to a path tangent with the ground surface does so under the influence of the pressure difference across the jet. If the nozzle height is increased, and assuming the pressure difference to remain constant, the jet will be parallel with the ground at a distance above the ground plane. There results an outflow of air from the cushion, which tends to reduce the base pressure, and hence the vehicle will experience a downward or stabilizing acceleration. As the vehicle height increases, however, the density of the trapped air decreases and so does the pressure. This reduction in pressure causes the jets to assume a new flow path which, depending on the relative

strength of these two effects, can result in the cushion air mass to be augmented, reduced or remain constant. The application of this analysis to the coupled heave and pitch motion as reported in Reference 8 results in a conclusion that uncompartmented, annular jets are never stable. This is, obviously, at variance with experience for low values of h/d . Furthermore, at the higher values of h/d , an incremental change in attitude angle will only insignificantly affect the equilibrium heights of the nozzles and hence is not expected to affect appreciably the jet flow boundary conditions. It is therefore believed that both the volume effect and the jet unbalance effect decrease in importance at the higher values of h/d . Yet, at these values the annular jet vehicles experience a strong static and dynamic instability. This leads toward the conclusion that a dynamic analysis of annular jets should include other, more influential phenomena, as, for instance, the base pressure variation as influenced by air flow inside the pressurized cushion. An analysis along these lines has been reported in Reference 9. That investigation considers the flow pattern under the base plate to be of a vortex type. The result of that study does not agree with the test data of Reference 5. One of the reasons for this disagreement is believed to be connected with the assumption of vortex flow. It is much more plausible, as also recognized in Reference 9, that the flow is rotational, and any future analysis of such rotational flow is believed to be worthwhile. To summarize, the existing theories result in the following conclusions:

a.) For the balanced case from References 6, or 8, the uncoupled heave mode is neutrally stable and is oscillatory

with a frequency, $\omega_h = \sqrt{\frac{g}{h_e}}$ radians/second (1)

The uncoupled pitch mode is an unstable oscillation with a

frequency, $\omega_\alpha = \sqrt{\frac{WR^2}{3I_{yy}h_e}}$ radians/second (2)

b.) For the unbalanced case, from Reference 8, the uncoupled heave mode has a frequency,

$$\omega_h = \sqrt{\frac{g}{h_e} - \frac{g^2 (B-1)^2}{4h_e^2 a_m^2 \beta^2}} \quad (3)$$

where

$$\beta = \frac{P_b - P_a}{P_b - P_a} \quad (4)$$

$$a_m = \frac{2}{r} \sqrt{\frac{P_b}{2\rho}} \left[\frac{\left(\frac{P_b}{P_{ij}}\right)^{1/2}}{1 + \left(1 - \frac{P_b}{P_{ij}}\right)^{1/2} + \frac{3}{4} \left(\frac{P_b}{P_{ij}}\right)^{1/2}} \right] \quad (5)$$

with a damping ratio,

$$\frac{C}{C_r} = \frac{\frac{B-1}{2(a_m B)}}{\sqrt{B/h}} \quad (6)$$

Calculations show that the unbalanced jet values are essentially identical to the balanced values for the frequencies and damping ratios. A comparison of the thus calculated values of ω_h and ω_α with the experimental

values is presented in Figure 45. It is seen that the experimental data show that the heave frequency is only insignificantly affected by altitude and speed. Whereas the theory predicts the heave oscillation to be undamped, the previously discussed test records show significant damping at all test altitudes. Also, the theory predicts the pitch motion to be oscillatory and with a higher frequency than that of the heave motion, whereas no concrete evidence of this was found from the test data.

The theory presented in Reference 9 is an extension of that of Reference 8 to the three-dimensional case. The basic shortcomings of the theory of Reference 8, therefore, also exist with that of Reference 9. In addition, the three-dimensional theory presented in Reference 9 requires a very complex calculation procedure and as such is not very suitable for the evaluation of the effects on stability of the various design parameters.

No stability theories are in existence for vehicles of the type of the "Hula-Hoop". The experimental heave frequency lies between 4 and 5 radians/second, as is also shown on Figure 45.

2. The Effect of Air Cushion Flow

As mentioned in previous paragraphs, it is believed that the air flow under the vehicle base significantly affects both the performance and the stability of annular jet GEMs. It has further been indicated that this flow is rotational, as opposed to the vortex type, i.e., the velocity decreases as the flow core is approached.

A rigorous rotational analysis of the flow beneath the base, even for the symmetric condition, is not an easy task. In what follows, an attempt has been made to investigate this rotational flow with a semi-empirical method. The resulting analysis, though not being rigorous from an

analytical point of view, determines some qualitative effects on performance and stability of the air cushion rotational flow.

For the symmetric condition, the flow is considered to follow stream paths as shown on Figure 46. Figure 46 also presents the notation to be used in the analysis.

The following assumptions are made:

1. There exists a stagnation point, O, located a distance $h/2$ below the base and a distance, η , along the base from the inboard nozzle edge.
2. Along any line OB, the velocity is parallel to the baseplate and has a magnitude that increases linearly with the distance from point O.
3. The mass flow per unit time crossing any radial line from point O, is constant with position angle, θ .
4. Incompressible flow equations are applicable.
5. The pressure at point A is given from the rotational flow equation,

$$p_A = \frac{1}{2} \rho V_A^2$$

6. The pressure at a point on the base very far from point A is equal to the base pressure, p_b , as calculated from theories that do not account for the rotational cushion flow.

With the above assumptions and the notation shown on Figure 46, the analysis proceeds as follows:

The velocity at a distance r_A from O along OA, is

$$V_{r_A} = \dot{\theta}_A r_A \quad (7)$$

In particular,

$$V_A = \dot{\theta}_A \left(\frac{h}{2} \right) \quad (8)$$

The velocity at a distance r_b from 0 along OB, is given by

$$V_{r_b} = \frac{r_b}{R_b} V_B = \left(\frac{r_b}{R_b} \right) R_b \dot{\theta}_B . \quad (9)$$

From the geometry of Figure 46,

$$X = R_b \sin \theta_B . \quad (10)$$

Differentiating (10) with respect to time,

$$\dot{X} = \dot{R}_b \sin \theta_B + R_b \dot{\theta}_B \cos \theta_B . \quad (11)$$

Also,

$$X^2 = \left(\frac{h}{2} \right)^2 + R_b^2 . \quad (12)$$

It follows that

$$\dot{R}_b = \frac{X}{R_b} \dot{X} . \quad (13)$$

Substituting Equation (13) into Equation (11) and solving for \dot{X} ,

$$\dot{X} = R_b \left(\frac{R_b}{h/2} \right) \dot{\theta}_B . \quad (14)$$

The mass per unit time crossing the line OB is

$$\left(\frac{dm}{dt} \right)_B = \int_0^{R_b} \rho \dot{X} \frac{r_b}{R_b} dr_b = \rho \frac{R_b^2}{2} \left(\frac{R_b}{h/2} \right) \dot{\theta}_B . \quad (15)$$

Similarly the mass per unit time crossing the line OA is

$$\left(\frac{dm}{dt} \right)_A = \rho \frac{(h/2)^2}{2} \dot{\theta}_A . \quad (16)$$

Equating Equations (15) and (16), solving for $\dot{\theta}_B$, and substituting this into Equation (14)

$$\dot{x} = \left(\frac{h/2}{R_B}\right) \frac{h}{2} \dot{\theta}_A = \left(\frac{h/2}{R_B}\right) V_A. \quad (17)$$

The pressure at the point B is given by Bernoulli's equation, and utilizing Equations (12) and (17)

$$p_B = p_T - \frac{1}{2} \rho V_B^2.$$

$$p_B = p_T - \frac{1}{2} \rho V_A^2 \left[\frac{1}{1 + \left(\frac{x}{h/2}\right)^2} \right]. \quad (18)$$

For large values of $\frac{x}{h/2}$, p_B has been assumed to equal p_b . It follows that $p_T = p_b$. Also the pressure at point A, p_A , equals the dynamic pressure $\frac{1}{2} \rho V_A^2$. It follows that

$$p_B = p_b \left[\frac{\frac{1}{2} + \left(\frac{x}{h/2}\right)^2}{1 + \left(\frac{x}{h/2}\right)^2} \right]. \quad (19)$$

As seen from Figure 46 the distance of any point, B, for the edge of the jet is given by

$$y = x + \eta \quad (20)$$

Introducing Equation (20) into Equation (19)

$$p_B = p_b \left[\frac{\frac{1}{2} + \left(\frac{y-\eta}{h/d}\right)^2}{1 + \left(\frac{y-\eta}{h/d}\right)^2} \right]. \quad (21)$$

The variation of the pressure ratio $\frac{p_B}{p_b}$ with $\frac{y}{r}$

for several values of h/d is shown in Figure 47. A number of test points from Reference 5 are also presented. The distance between the nozzle inner edge and the pressure loss peak, η , varies with h/d . For very low values of h/d , this distance is approximately equal to $h/2$. As the ratio h/d is increased, the test data of Reference 5 show that

the value of η is continuously reduced from $h/2$. This relative reduction may be associated with the flow curvature of the jet. In the theoretical curves on Figure 47, the experimental values of η have been utilized. The theory is seen to agree reasonably well with the experimental data. It is noted that for low values of h/d , the local base pressure, p_b , becomes the no-flow base pressure, p_b , before the vehicle centerline is reached. This is not so for the higher values of h/d . This pressure distribution implies that the average base pressure is less than p_b . The reduction can be evaluated by integrating Equation (21) with $\frac{y}{r}$ from 0 to 1. It follows that

$$p_{b,av} = p_b \left[1 - \frac{h/d}{2} \left\{ \tan^{-1} \left(\frac{1 - \eta/r}{h/d} \right) + \tan^{-1} \left(\frac{\eta/r}{h/d} \right) \right\} \right] \quad (22)$$

For the range of h/d under consideration, Equation (22) can be closely approximated by

$$\begin{aligned} p_{b,av} &= p_b (1 - h/d) \\ &= p_b (1 - \frac{t_c/d}{t_c/h}) \end{aligned} \quad (23)$$

Equation (23) implies that as a result of the rotational flow there exists a theoretical lift loss equal in percent to one hundred times the value of ratio h/d . Equation (23) also implies that for any fixed geometry parameter t_c/d , the loss decreases with increasing t_c/h . This is in agreement with the experimental data of Reference 10.

The above analysis is limited to the symmetric two-dimensional problem of annular jet performance. For this type of analysis to apply also for stability predictions, the method must be extended to the nonsymmetric case. Thus, the data of actual flow experiments should be taken into account insofar as the behavior of the rotational flow cores is concerned. Reference 5 indicates, for example, that an inclination of the vehicle base results in a detachment of the core from the base at the higher edge, whereas the core under the

lower edge of the base assumes an elliptical shape. These phenomena together with Equation (21) can be used to explain qualitatively the different stability characteristics of annular jets at low values of h/d as compared to the higher values of this parameter.

It is noted that Equation (16) consists of two factors. The first factor is the pressure, p_b , as obtained from the

standard theories. This pressure is known to possess a large, stable slope, $\frac{dp}{dh}$, at low values of h/d . This

stable slope reduces with increasing h/d . The second factor of Equation (21) has been shown to result in only narrow pressure loss regions for low values of h/d . The pressure loss region, however, is also seen from Figure 47, to increase with increasing values of h/d . Furthermore, the previously mentioned phenomena of detachment and flattening of the cores of the rotational flow at the high and low base ends, respectively, results in an unstable pressure variation, which increases in severity with increasing h/d . The base pressure distribution is seen, therefore, to be made up of one factor that is stable, but of decreasing importance as h/d increases, and another unstable factor that increases in importance with h/d .

The above qualitative analysis appears to explain the pitch stability characteristics of annular GEMs and hence, provides a promising avenue for further investigations.

IV. CONCLUSIONS AND RECOMMENDATIONS

Instrumented dynamic response tests were performed with two types of ground effect machines. The Princeton 20-foot GEM was also tested over specially prepared test tracks in order to simulate various conditions of rough terrain. It was found that the P-GEM was capable of successfully negotiating all prepared obstacles, thus emphasizing the potential of this type of vehicle for Army all-purpose-ground-proximity vehicles. The test data presented in this report can be utilized for correlation with analysis. Existing analyses, however, are found to be inadequate for such correlation. It is recommended that tests, similar to those performed in this program, be made also with other ground effect machines to form a reservoir of full scale test data for correlation with theories that eventually will be formulated. It is also recommended that increased effort be devoted to the formulation of a dynamic stability theory which will lead to a better understanding of the effects of the various design parameters on the handling qualities of ground effect machines.

V. REFERENCES

1. Chaplin, H. R., "Theory of the Annular Nozzle in Proximity to the Ground", David Taylor Model Basin Aero Report 923, July 1957.
2. Stanton - Jones, R., "Some Design Problems of Hovercraft", Institute of Aerospace Sciences, Preprint No. 61-45, January 1961.
3. Ehrich, F. F., "The Curtain Jet", Journal of the Aerospace Sciences, Volume 28, Number 11, November 1961.
4. Poisson-Quentin, P., "Study of a Current Plan for a Ground Effect Platform", Symposium on Ground Effect Phenomena, Princeton University Pg. 1, October 1959.
5. Nixon, W. B. and Sweeney T. C., "Some Qualitative Characteristics of a Two-Dimensional Peripheral Jet", Department of Aeronautical Engineering, Princeton University, Report No. 484, September 1959.
6. Tulin, M. P., "On the Vertical Motions of Edge Jet Vehicles", Symposium on Ground Effect Phenomena, Princeton University, Pg. 119, October 1959.
7. Tinajero, A. A. and Fresh, J. N., "Aerodynamic Response on a 7-foot Ground Effect Machine Flying Over Uneven Surfaces", David Taylor Model Basin, Aero Report 982, June 1960.
8. Eames, M. C., "Fundamentals of the Stability of Peripheral Jet Vehicles", Volume 1-3, Pneumodynamics Corporation, November 1960.
9. Anderson, B. W., "Stability Work Under O.N.R. Contract NOnv 3173, AiResearch Manufacturing Corporation, December 1961.
10. Carmichael, B. H., "Hovering Two-Dimensional Annular Jet Performance Experiments" Aeroneutronic, Division of Ford Motor Company, Report No. U-1053, November 1960.
11. Sweeney, T. E., Nixon, W. B., "Some Notes on the P-GEM, Report No. 537, Princeton University, January 1961.

V. REFERENCES

1. Chaplin, H. R., "Theory of the Annular Nozzle in Proximity to the Ground", David Taylor Model Basin Aero Report 923, July 1957.
2. Stanton - Jones, R., "Some Design Problems of Hovercraft", Institute of Aerospace Sciences, Preprint No. 61-45, January 1961.
3. Ehrich, F. F., "The Curtain Jet", Journal of the Aerospace Sciences, Volume 28, Number 11, November 1961.
4. Poisson-Quentin, P., "Study of a Current Plan for a Ground Effect Platform", Symposium on Ground Effect Phenomena, Princeton University Pg. 1, October 1959.
5. Nixon, W. B. and Sweeney T. C., "Some Qualitative Characteristics of a Two-Dimensional Peripheral Jet", Department of Aeronautical Engineering, Princeton University, Report No. 484, September 1959.
6. Tulin, M. P., "On the Vertical Motions of Edge Jet Vehicles", Symposium on Ground Effect Phenomena, Princeton University, Pg. 119, October 1959.
7. Tinajero, A. A. and Fresh, J. N., "Aerodynamic Response on a 7-foot Ground Effect Machine Flying Over Uneven Surfaces", David Taylor Model Basin, Aero Report 982, June 1960.
8. Eames, M. C., "Fundamentals of the Stability of Peripheral Jet Vehicles", Volume 1-3, Pneumodynamics Corporation, November 1960.
9. Anderson, B. W., "Stability Work Under O.N.R. Contract NONv 3173, AiResearch Manufacturing Corporation, December 1961.
10. Carmichael, B. H., "Hovering Two-Dimensional Annular Jet Performance Experiments" Aeroneutronic, Division of Ford Motor Company, Report No. U-1053, November 1960.
11. Sweeney, T. E., Nixon, W. B., "Some Notes on the P-GEM, Report No. 537, Princeton University, January 1961.

12. Sweeney, T. E., Nixon, W. B., "Preliminary Flight Experiments With the Princeton University Twenty-Foot Ground Effect Machine", Report No. 506 Princeton University, January 1960.

APPENDIX A
TEST VEHICLES

Two vehicles were used in conjunction with this test program.

1. The Princeton University 20-foot-diameter peripheral jet ground effect machine, shown in Figure 1.

2. The "Hula-Hoop", Figure 2, a DeLackner Aerocycle modified by the U. S. Army Transportation Research Command and Kellett Aircraft Corporation.

The following are the pertinent characteristics of the Princeton GEM with additional information on this vehicle to be found in References 11 and 12:

Empty Weight 1380 lb..
(Including 105 lb.. instrumentation)

Gross Weight 1680 lb..

Mass Moments of Inertia at Gross Weight:

Roll $I_{xx} = 737 \text{ slug-ft.}^2$

Pitch $I_{yy} = 1540 \text{ slug-ft.}^2$

Yaw $I_{zz} = 1542 \text{ slug-ft.}^2$

Centroids:

$\bar{x} = 0.3 \text{ in. fwd. of } \angle \text{ propeller}$

$\bar{y} = 0.7 \text{ in. to right of } \angle \text{ propeller (view looking down)}$

$\bar{z} = 18.1 \text{ in. above base of vehicle}$

Geometry:

Planform	Circular
Diameter (over-all)	20 ft.
Diameter (base)	18 ft. 2 in.

Nozzle Inclination	45 degrees
Nozzle Area	19.3 ft. ²
Inlet Ring	19.0 ft. ²

Percent of Total Nozzle Area Utilized for Control:

Longitudinal	24.4%
Lateral	31.4%
Main Propeller Diameter (4 Rigid Blades)	4.75 ft.
Rear Engine Propeller Diameter (2 Rigid Blades)	3.50 ft.
Rudder Area	10.1 ft. ²

Engine HP:

Main Engine (Lycoming Model No. VO 360-AA)	
Maximum HP at 2900 RPM	180
Operating HP at 2700 RPM	132
Rear Engine (Nelson Model No. H63C)	
Maximum HP at 3500 RPM (approx.)	30

Hours Flown in conjunction with this program,
12.5 hours

The Hula Hoop, as previously mentioned, is a DeLackner Aerocycle modified by the U. S. Army TRECOM. To the original Aerocycle TRECOM added a 15 ft. diameter duct with a flexible section at the bottom, and a variable pitch thrust rotor driven by the main engine and controlled with longitudinal stick motion.

Kellett Aircraft Corporation improved the "Hula-Hoop" yaw controls by adding 8 ducts along the skirt, 4 in each direction. These ducts turned the air flow from an axial to a tangential direction and utilizing the momentum of the air provided a control yawing moment on the vehicle. The rudder pedal travel closed micro switches which in turn activated solenoids that opened or closed these ducts. Photographs of this installation are shown in Figure 48.

A roll control system was also installed on the Hula-Hoop by Kellett Aircraft Corporation. Four vanes were added, 2 on either side, which, utilizing the drag forces induced by the air flow, provided the necessary control forces and moments. A photograph showing the installation for one set of these vanes is presented in Figure 49.

A summary of the Hula Hoop parameters are as follows:

Empty Weight	640 lb..
(including 26.4 lb.. instrumentation)	

Gross Weight	834 lb..
(including pilot, fuel, ballast)	

Mass Moments of Inertia at Gross Weight:

Roll $I_{xx} = 194 \text{ slug-ft.}^2$

Pitch $I_{yy} = 236 \text{ slug-ft.}^2$

Yaw $I_{zz} = 376 \text{ slug-ft.}^2$

Centroids:

\bar{x} and \bar{y} on ϕ of shaft

$\bar{z} = 2.10 \text{ ft.}$ above bottom of landing skids

Geometry:

Main Rotor (Two 2 Bladed counter rotating rotors)

Diameter	15.0 ft.
Hub Diameter	1.08 ft.
Chord (average)	0.50 ft.
σ	.085
Blade Pitch Settings at	0.75 Radius
Upper	8.67'
Lower	12.33°
Gear Ratio Rotor to Engine	10.3 : 1

Thrust Rotor (2 Blades)

Diameter	4.25 ft.
Hub Diameter	.79 ft.
σ	.0885

Total collective Pitch Travel 9.58° Forward, 12.5° Aft. Figure 50 is a plot of percent of longitudinal stick travel vs. collective pitch of thrust rotor. Distances from the ϕ propeller to the C.G. are $\bar{x}_\phi = -1.87$ ft., $\bar{z}_\phi = 3.0$ ft. Gear Ratio of rotor to engine is 1:2.5.

Hoop

Inside Diameter	15.1 ft.
Hoop Length (including flexible skirt)	2.5 ft.
Hoop Thickness	.34 ft.

Roll Vanes, Total of 4, 2 on each side

Chord	.75 ft.
Span	5.25 ft.
Total Area	15.8 ft. ²

Vane total travel, 0° , to 45° with the vertical. Figure 51 shows the relationship between lateral stick travel and roll vane angle.

Distance from vane centers to C.G.	$\bar{y}_v = 6.15$ ft.
	$\bar{z}_v = 1.58$ ft.

Yaw Ducts

Total of 8, 4 in each direction	
Total exit area in one direction	.805 ft. ²
Distance from C.G. to ϕ Ducts,	8.177 ft.

Engine

Modified Mercury Outboard Engine

**Rated at 40 HP at 5500 RPM
42 HP at 5800 RPM**

**Hours flown in the premodified and modified state
5 hours.**

APPENDIX B

INSTRUMENTATION

Provisions were made for oscillographic recording of time histories for the following flight data:

<u>Item</u>	<u>Measurement</u>
1	Longitudinal stick position
2	Lateral stick position
3	Rudder position (P-GEM only)
4	Fuselage pitch attitude
5	Fuselage roll attitude
6	Fuselage yaw attitude
7	Normal acceleration at center of gravity
8	Longitudinal acceleration at center of gravity
9	Lateral acceleration at center of gravity
10	Vehicle altitude (P-GEM only)
11	Vehicle position with respect to obstacles (P-GEM only)
12	Yaw duct vane position (Hula-Hoop only)

The above measurements were obtained by using analog type transducers which are described below. The signals were fed into two six channel bridge balance and calibrating units, and subsequently recorded on a twelve channel recording oscillograph, Consolidated Electrodynamics Model CEC-5118, all shown in Figure 52.

A strain gage type transducer was used to obtain position measurements (Items 1, 2, 3). This consisted of a double cantilever strain gaged beam assembly operated by a cam, and linked to the control system of the machine. In the P-GEM, because the controls consisted of a pulley and cable system, the stick position indicated represents a trend and cannot be used as an absolute value. The control system of the "Hula Hoop", however, consisted of a rigid linkage, so that any position indicated can be accepted as a true position within an accuracy of 2% of total travel.

Three Statham linear accelerometers Model D-2-275, were used to determine all linear accelerations (Items 7, 8, 9). The accelerometers were calibrated to $\pm 1g$ with a repeatability of 96%. In addition, they were also checked, by using a turntable, in the g ranges which were comparable to the actual g's experienced in

this test program. The correlation between predicted and indicated g's, at the range of .10 g was within 98%.

Pitch and roll were measured with a Giannini vertical gyro Model 3111G-1, wired in free gyro configuration. Yaw was measured with a Giannini directional gyro Model 3211G-1. Figure 53 is a photograph showing the gyros mounted on the Princeton GEM. The vertical gyro sensitivity was increased, so that full trace deflection occurred at $\pm 17^\circ$, a value 50% greater than the maximum angles expected from the vehicles being tested. In calibrating, it was discovered that the gyro had an excessive drift rate, particularly in the roll axis, where the average drift rate measured was $1.25^\circ/\text{min}$. From calibrations, it was also determined that the indicated readings were accurate to within $\pm 1/4$ of one degree.

The directional gyro has an electrical signal output for angles to $\pm 90^\circ$. The values obtained were within $\pm 1^\circ$. The gyro was linear up to an angle of 60° , and beyond this point its output was non-linear. Any readings beyond 60° were corrected for this non-linearity.

The vehicle position with respect to the obstacles was determined by using a resistive network designed to adapt the change in ground resistance to the galvanometer sensitivity. The change in resistance was accomplished by placing a steel wire a few inches over the ground just before each obstacle. Two conductive probes extending from the front of the vehicle completed the circuit and fed the signal into the recorder. By placing wires at fixed intervals along a track, the above principle was also used to determine vehicle average velocity. Figure 54 is a schematic diagram of the instrument.

It should be noted that the conductive probes had to be long enough, so that they would make contact with the stainless steel wire, regardless of the vehicle's attitude or height. As a result, the position of the vehicle relative to the obstacles can only be determined within ± 1 ft. Consequently, the velocities indicated would also be subject to this error. Therefore, the average velocity over any two wires 25 ft. apart would be accurate to within 4%.

The yaw duct vane position was determined by utilizing the change in current drawn by the vane activating solenoids. A fraction of the current operating each set of ducts was fed into the galvo by means of a shunt, and recorded in two different channels of the recorder to identify control direction.

The measurement of altitude was accomplished by using a capacitive altimeter. The instrument consisted of a Hall bridge circuit operated near its balance point. The readings of the altimeter were not linear due to the non-linearity of the change in reactance of the sensor with the altitude, and also due to the non-linear output of the unbalanced bridge. The altitude indication, however, was useful if considered from a qualitative point of view. Figure 55 shows the altimeter circuit housed in the control panel, and its installation on the Princeton GEM.

An umbilical instrumentation system was used with the Hula-Hoop, due to weight problems. The recorder, bridge balance boxes, and power source were mounted externally utilizing a 100 foot multiple cable to transmit the signals from the sensors to the recorder, as shown in Figure 56.

Shunt type resistance calibrations were taken for each channel during initial calibration, also before and after each flight to standardize results. In addition, total stick travel was recorded before and after flights, during ground check of instrumentation, to establish reference points.

APPENDIX C

TEST PROGRAM SUMMARY

The performance and handling qualities of the P-GEM were adequate for the performing of an extensive test program, including dynamic stability, control response tests, performance and operation over rough terrain. A similar test program was performed with the "Hula-Hoop", except that, because of the limited performance and controllability of this machine and the resulting safety considerations, the rough terrain tests were excluded.

In the following a list is presented of the tests performed with the two vehicles, as well as a brief description of the obstacles negotiated by the P-GEM. A schematic of the test tracks utilized in the testing of the P-GEM is presented in Figures 57a and 57b.

It should be noted that most of the tests described below were repeated at least twice to insure repeatability of data obtained.

I. Tests Performed With the Princeton GEM

A. Dynamic Stability

- 1.0 Hover with fixed stick
- 1.01 Manual rolling moment input from left side.
h = 6 in. 2050 RPM, W = 1680 lb..
- 1.02 Manual pitching moment input from the front.
h = 6 in. 2050 RPM, W = 1680 lb..
- 1.03 Manual pitching moment input from the front.
h = 6 in. 2500 RPM, W = 1795 lb..
- 1.04 Manual pitching moment input from the front.
h = 8.5 in. 2800 RPM, W = 1795 lb..
- 1.05 Manual rolling moment input from left side
h = 12 in. 2700 RPM, W = 1680 lb..
- 1.06 Manual pitching moment input from the front
h = 12 in. 2700 RPM, W = 1680 lb..

2.0 Forward Speed at 2700 RPM
h = 12 in. W = 1680 lb..

2.01 Stick pulse aft at 10 mph

2.02 Stick pulse aft at 20 mph

B. Response to Control Inputs, W = 1680 lb..

1.0 Hover with fixed stick at 2700 RPM,
h = 12 in.

1.01 Stick step forward until $V_{FWD} = 10$ mph

1.02 Stick step right until $V_{RT} = 10$ mph

1.03 Full left rudder with rear engine at 3500 RPM

2.0 Forward speed at 2700 RPM
h = 12 in.

2.01 Stick step aft from 10 mph to 0 mph

2.02 Stick step aft from 20 mph to 0 mph

2.03 Full left rudder from 10 mph

2.04 Full left rudder from 20 mph

C. Performance (W = 1680 lb . except as noted)

1.0 Control stick moments at 2700 RPM
h = 12 in.

1.10 Longitudinal stick motion to balance moment
due to weight added on front 7.63 ft. from
C.G.

1.11 $W_f = 0$ lb..

1.12 $W_r = 19.56$ lb..

1.13 $W_r = 37.44$ lb..

1.14 $W_f = 17.44$ lb..

1.20 Lateral stick motion to balance moment due
to weight added on left side 9 ft. from C.G.

1.21 $W_l = 0$ lb..

1.22 $W_l = 10$ lb..

1.23 $W_L = 24.56 \text{ lb.}$

1.24 $W_L = 47.44 \text{ lb.}$

2.0 Altitude vs. engine RPM in hovering

2.01 RPM = 2050 h = 6.5 in. W = 1680 lb.

2.02 RPM = 2500 h = 9.5 in. W = 1680 lb.

2.03 RPM = 2900 h = 14.5 in. W = 1680 lb.

2.05 RPM = 2050 h = 6.0 in. W = 1795 lb.

2.06 RPM = 2500 h = 8.0 in. W = 1795 lb.

2.07 RPM = 2900 h = 13.5 in. W = 1795 lb.

3.0 Altitude vs. forward speed at 2900 RPM
W = 1680 lb.

3.01 Slow speed approximately 8 MPH

3.02 Medium speed approximately 15 MPH

3.03 High speed approximately 30 MPH

4.0 Maximum Acceleration

4.01 Main engine RPM 2500 thrust engine RPM
3500 stick step forward

4.02 Main engine RPM 2900 thrust engine RPM
3500 stick step forward

D. Rough Terrain

1.0 A series of 10 ditches 8 ft. apart 2 ft.
wide 1 ft. deep x 30 ft. long shown in
Figure 58

1.01 Low forward speed 2700 RPM fixed stick

1.02 Medium forward speed 2700 RPM fixed stick

1.03 High forward speed 2700 RPM fixed stick

2.0 A series of 10 ditches 10 ft. apart 4 ft.
wide x 2 ft. deep 30 ft. long shown in
Figure 59

- 2.1 Low forward speed 2900 RPM fixed stick
- 2.2 Medium forward speed 2900 RPM fixed stick
- 2.3 High forward speed 2900 RPM fixed stick
- 3.0 Individual ditch 2 ft. wide x 2 ft. deep x 30 ft. long
- 3.01 Low forward speed 2900 RPM fixed stick
- 3.02 High forward speed 2900 RPM fixed stick
- 4.0 Individual ditch 4 ft. wide x 2 ft. deep x 30 ft. long
- 4.01 Low forward speed 2900 RPM fixed stick
- 4.02 High forward speed 2900 RPM fixed stick
- 5.0 Individual ditch 4 ft. wide x 4 ft. deep x 30 ft. long as shown in Figure 60
- 5.01 Low forward speed 2900 RPM fixed stick
- 5.02 Medium forward speed 2900 RPM fixed stick
- 5.03 High forward speed 2900 RPM fixed stick
- 6.0 Individual hole 4 ft. x 4 ft. x 2 ft. deep
- 6.01 Low forward speed 2900 RPM fixed stick
- 6.02 High forward speed 2900 RPM fixed stick
- 7.0 Individual hole 4 ft. x 4 ft. x 4 ft. deep as shown in Figure 61
- 7.01 Low speed 2900 RPM fixed stick
- 7.02 High speed 2900 RPM fixed stick
- 8.0 Single fence 3 in. thick x 6 in. high x 30 ft. long
- 8.01 Low forward speed 2900 RPM fixed stick
- 8.02 High forward speed 2900 RPM fixed stick

- 9.0 Single fence 3 in. thick x 6 in. high x 30 ft. long
 - 9.01 Low forward speed 2900 RPM fixed stick
 - 9.02 High forward speed 2900 RPM fixed stick
- 10.0 Single fence 24 in. thick x 6 in. high x 30 ft. long
 - 10.01 Low forward speed 2900 RPM fixed stick
 - 10.02 High forward speed 2900 RPM fixed stick
- 11.0 Single fence 24 in. thick x 12 in. high x 30 ft. long as shown in Figure 62
 - 11.01 Low forward speed 2900 RPM fixed stick
 - 11.02 High forward speed 2900 RPM fixed stick
- 12.0 Grass
 - 12.01 Hover in 7-8 in. grass 2700 RPM
- 13.0 Slopes
 - 13.01 Flight over 3° slope - medium speed downward
 - 13.02 Flight over 5° slope up - low speed - stop, turn 180° and descend slope 2700 RPM
- 14.0 Plowed field (shown in Figure 63)
 - 14.01 Flight perpendicular to furrows - 2700 RPM
 - 14.02 Flight parallel to furrows - 2700 RPM

II. Tests Performed With the Hula-Hoop

A. Dynamic Stability (W = 834 lb.)

- 1.0 Hover with fixed stick
 - 1.01 Manual pitching moment input from the front at 3 in. altitude
 - 1.02 Manual rolling moment, input from the right at 5 in. altitude

1.03 Manual pitching moment input from the front,
5 in. altitude

1.04 Manual heaving disturbance, 5 in. altitude

1.05 Manual disturbance in yaw 5 in. altitude

2.0 Forward Speed

2.01 Stick pulse aft at 5 MPH

B. Response to Control Inputs

1.0 From hover at 5 in. altitude 5900 RPM

1.01 Stick step forward

1.02 Stick step forward then aft to stop

1.03 Stick step right

1.04 Stick step left

1.05 Full left then full right rudder

C. Performance

1.0 Altitude vs. engine RPM W = 834 lb..

1.01 RPM 5500 h = 2 in.

1.02 RPM 5700 h = 3 in.

1.03 RPM 5900 h = 5 in.

2.0 Altitude vs. weight at 5800 RPM

2.01 W = 776 lb..

2.02 W = 826 lb..

2.03 W = 851 lb..

2.04 W = 866 lb..

2.05 W = 888 lb..

2.06 W = 918 lb..

3.0 Control stick moments at 5900 RPM h = 5 in.

3.10 Longitudinal stick (weight added on front)
7.72 ft. from C.G.

3.11 $W_f = 0$ lb.

3.12 $W_f = 2$ lb..

3.13 $W_f = 5$ lb..

3.14 $W_f = 10$ lb..

3.15 $W_f = 15$ lb..

3.16 $W_f = 20$ lb..

3.20 Lateral stick (weight added on right side)
7.72 ft. from C.G.

3.21 $W_r = 0$ lb.

3.22 $W_r = 1$ lb.

3.23 $W_r = 2$ lb.

3.24 $W_r = 3$ lb.

3.25 $W_r = 5$ lb.

3.26 $W_r = 7$ lb.

APPENDIX D

This Appendix contains illustrations, photographs and graphs of flight test records.

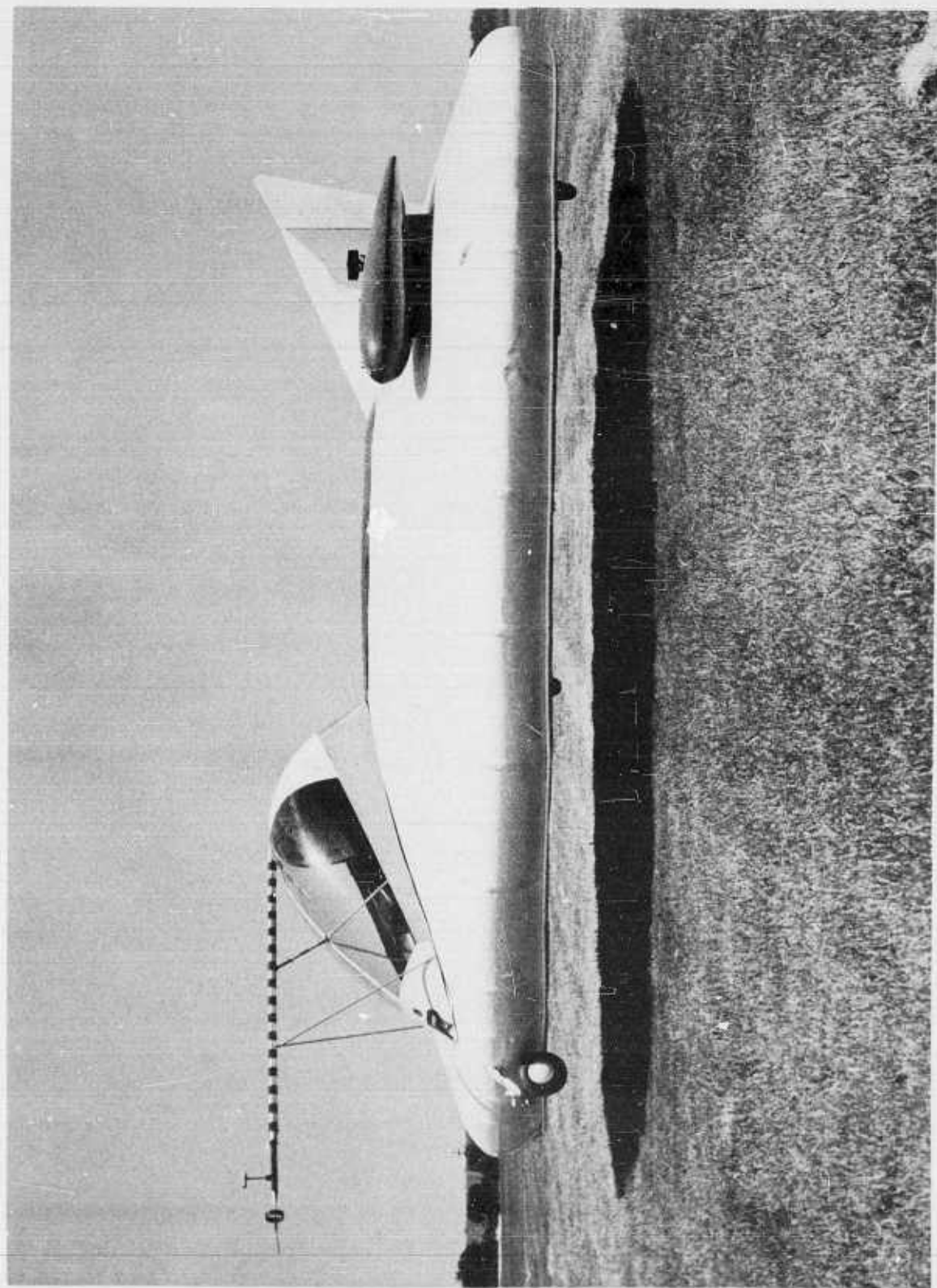


FIGURE 1: THE PRINCETON UNIVERSITY 20-FOOT DIAMETER GROUND EFFECT MACHINE

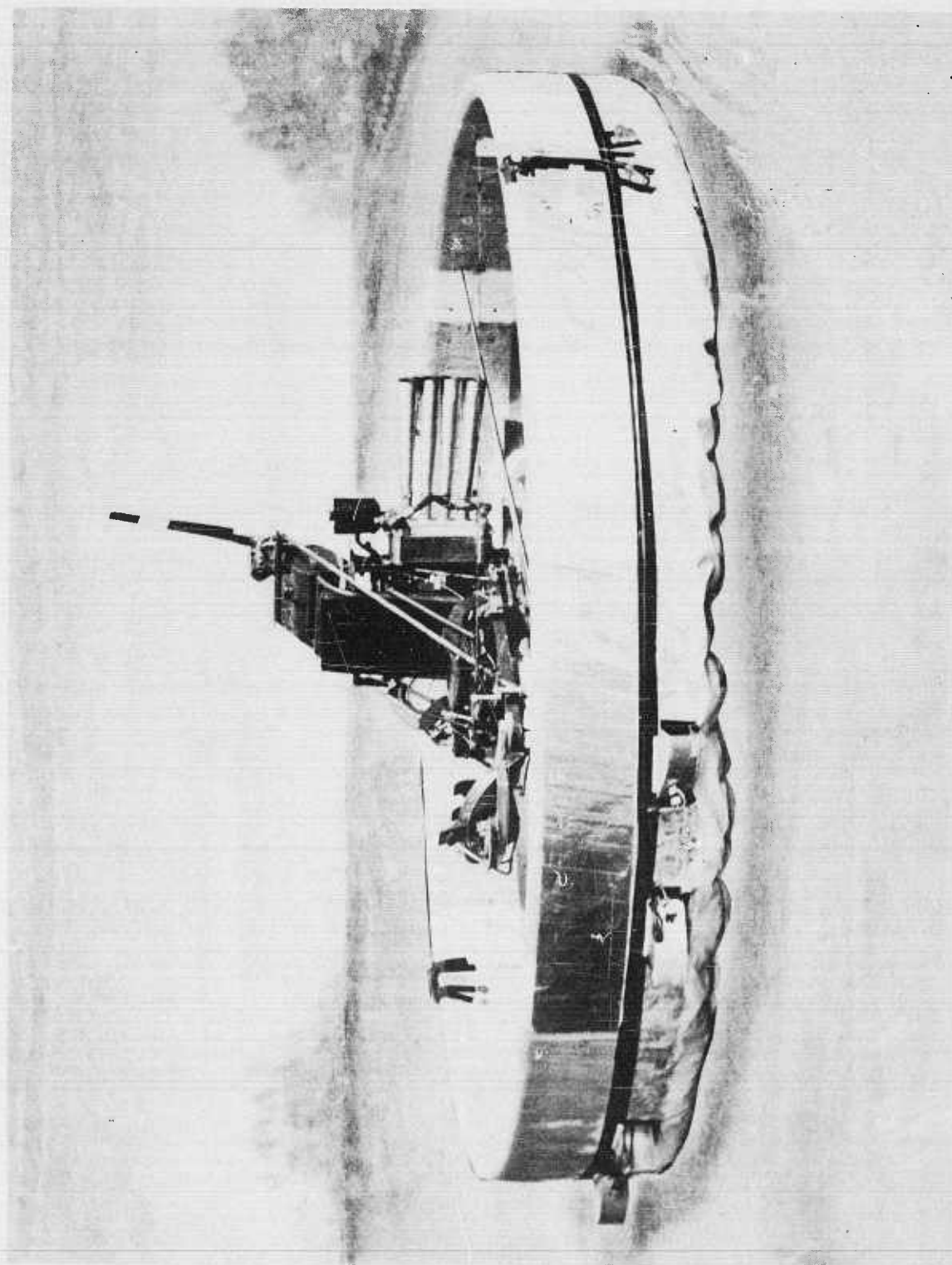


FIGURE 2: THE TRECOT "HULA HOOP"

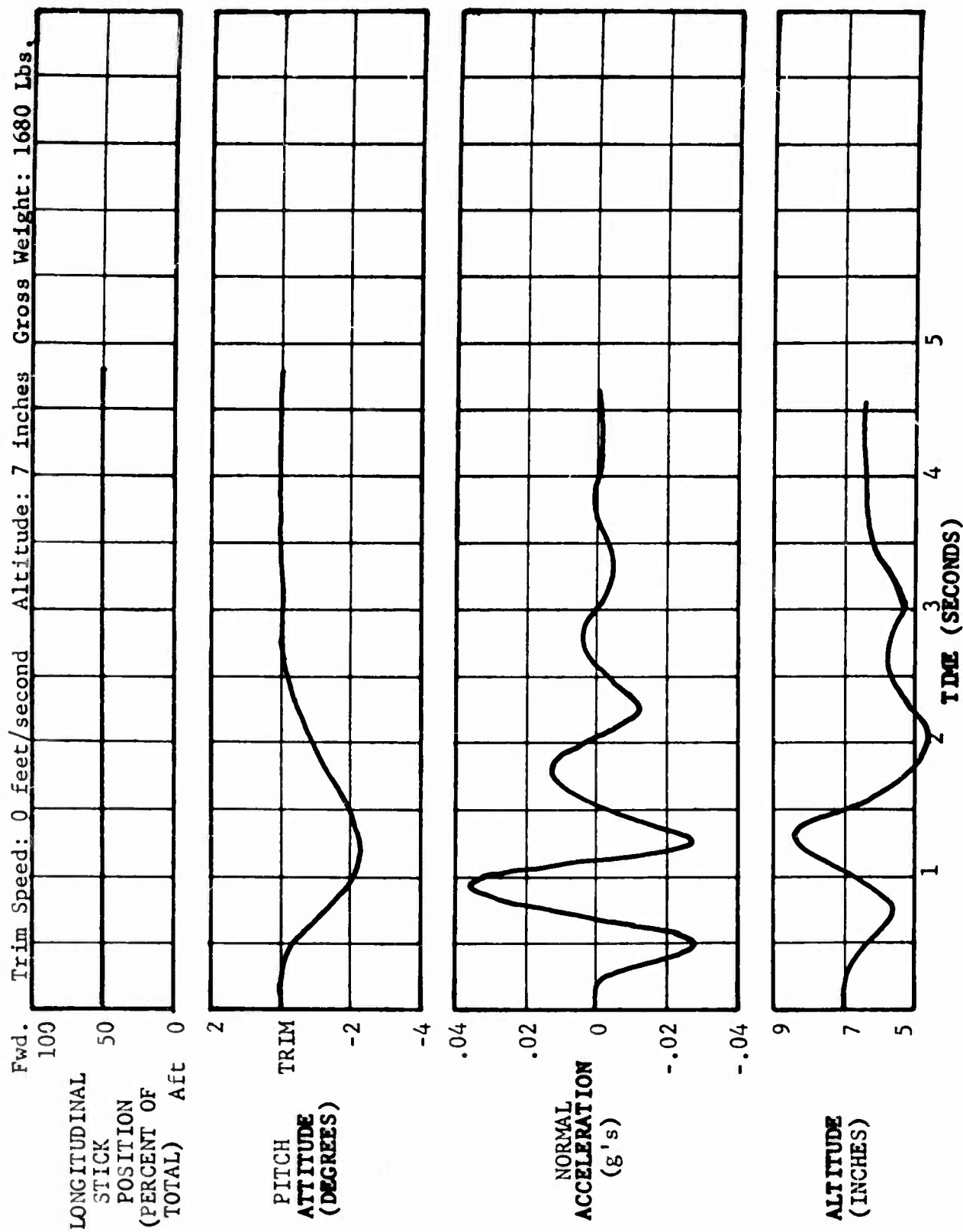


FIGURE 3: P-GEM LOW ALTITUDE RESPONSE TO A LONGITUDINAL DISTURBANCE
 (EXTERNAL PUSH-DOWN)

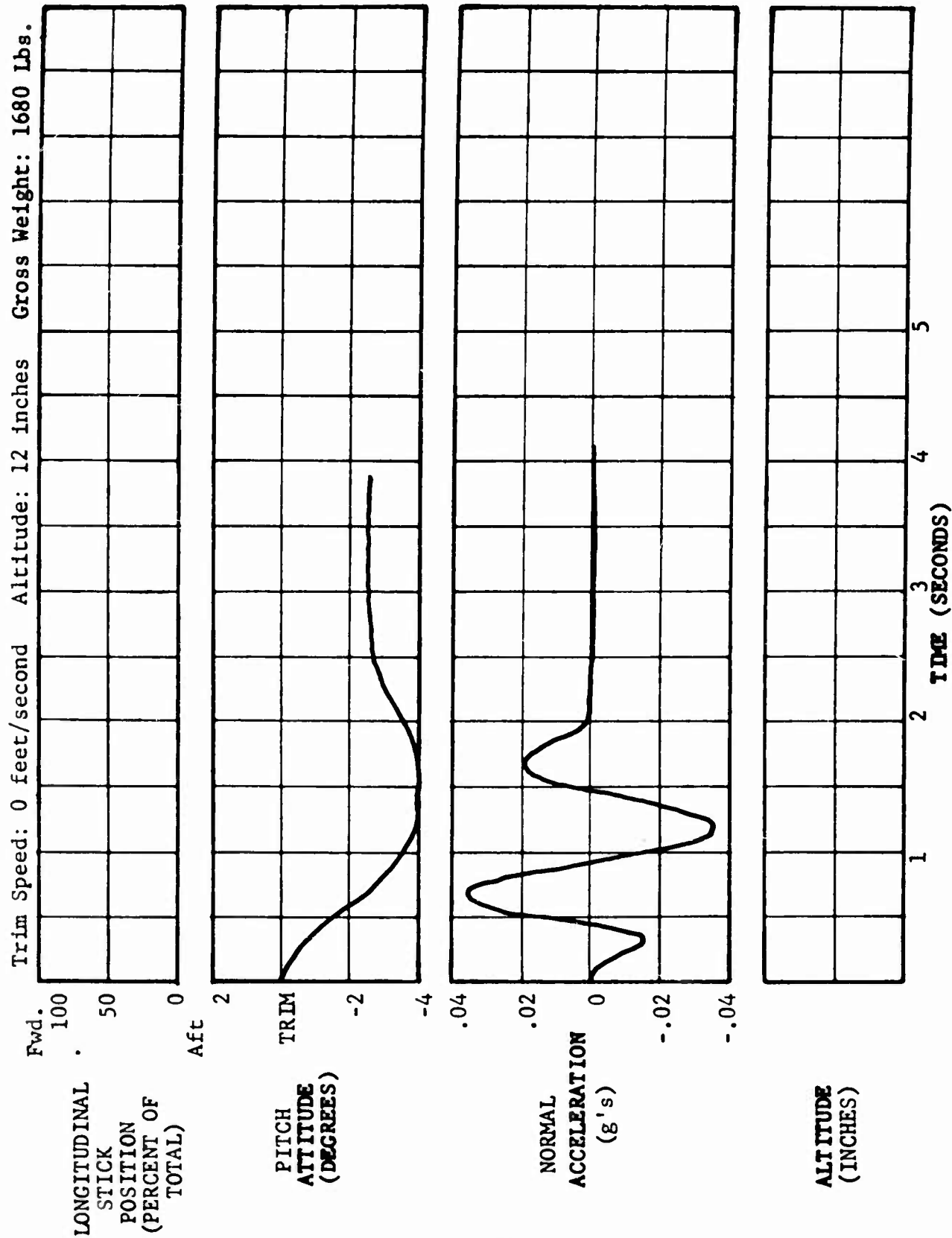


FIGURE 4: P-GEM RESPONSE TO A LONGITUDINAL DISTURBANCE (EXTERNAL PUSH-DOWN) AT A HEIGHT OF 12 INCHES

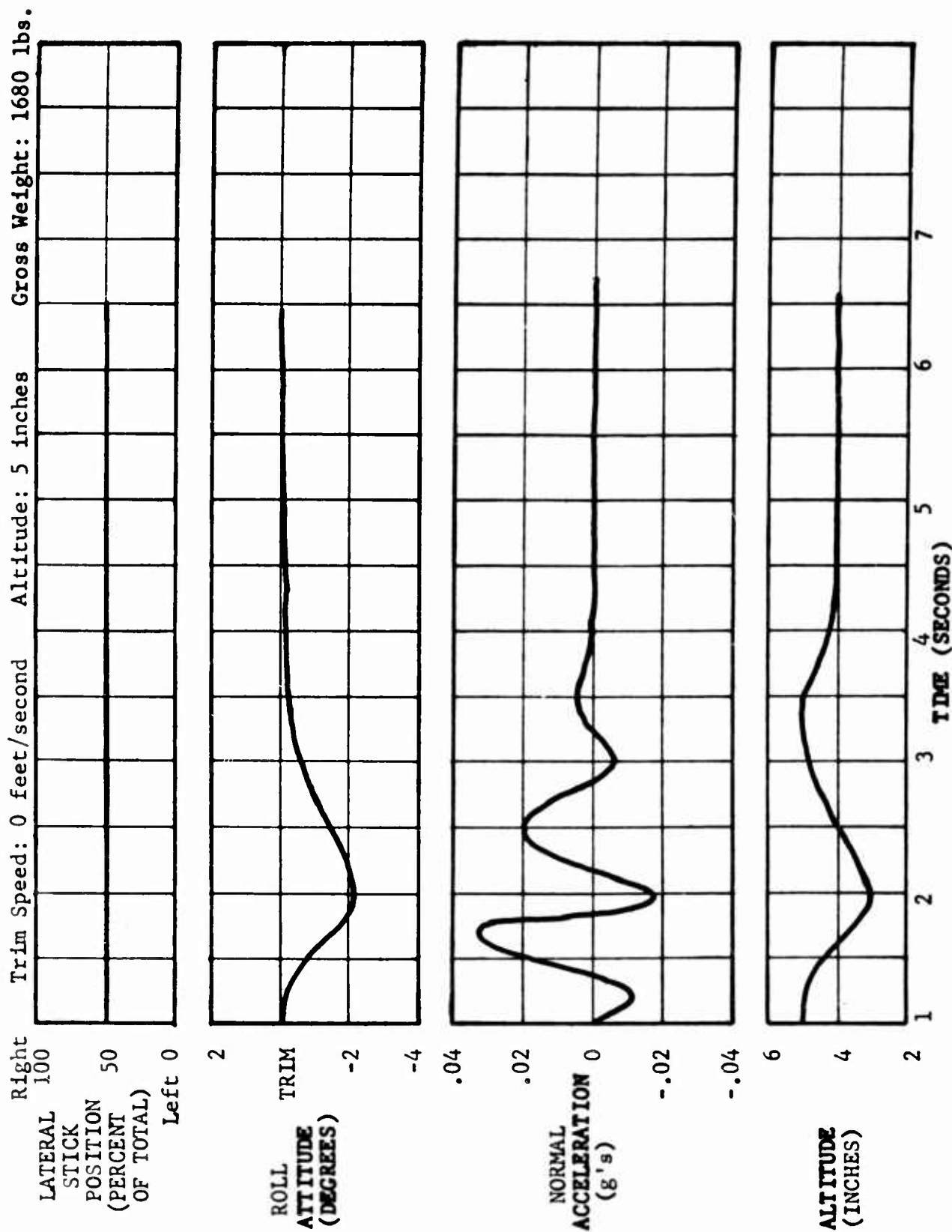


FIGURE 5: P-GEM LOW ALTITUDE RESPONSE TO A LATERAL DISTURBANCE (EXTERNAL PUSH-DOWN)

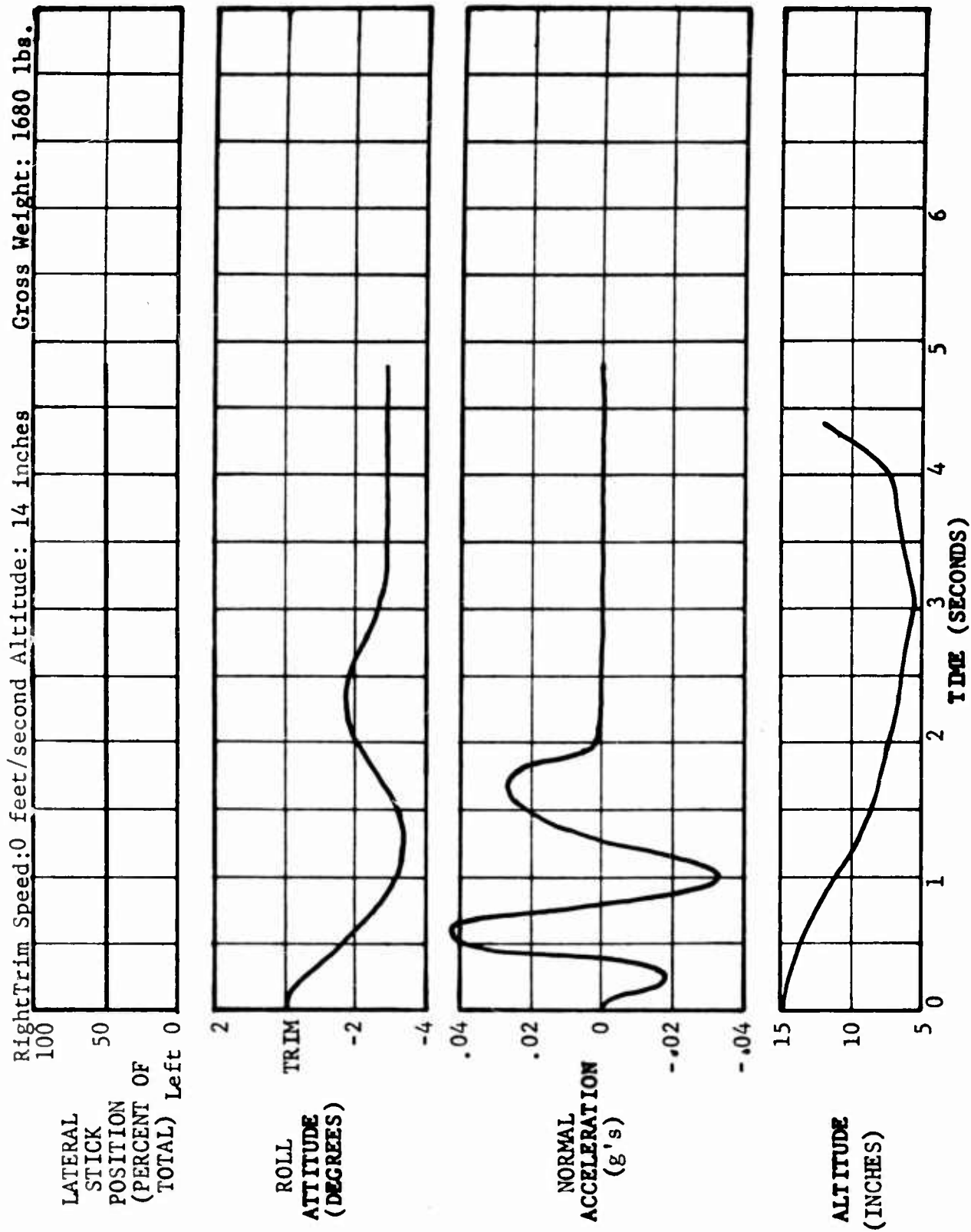


FIGURE 6: P-GEM RESPONSE TO A LATERAL DISTURBANCE (EXTERNAL PUSH-DOWN) AT A HEIGHT OF 14 INCHES

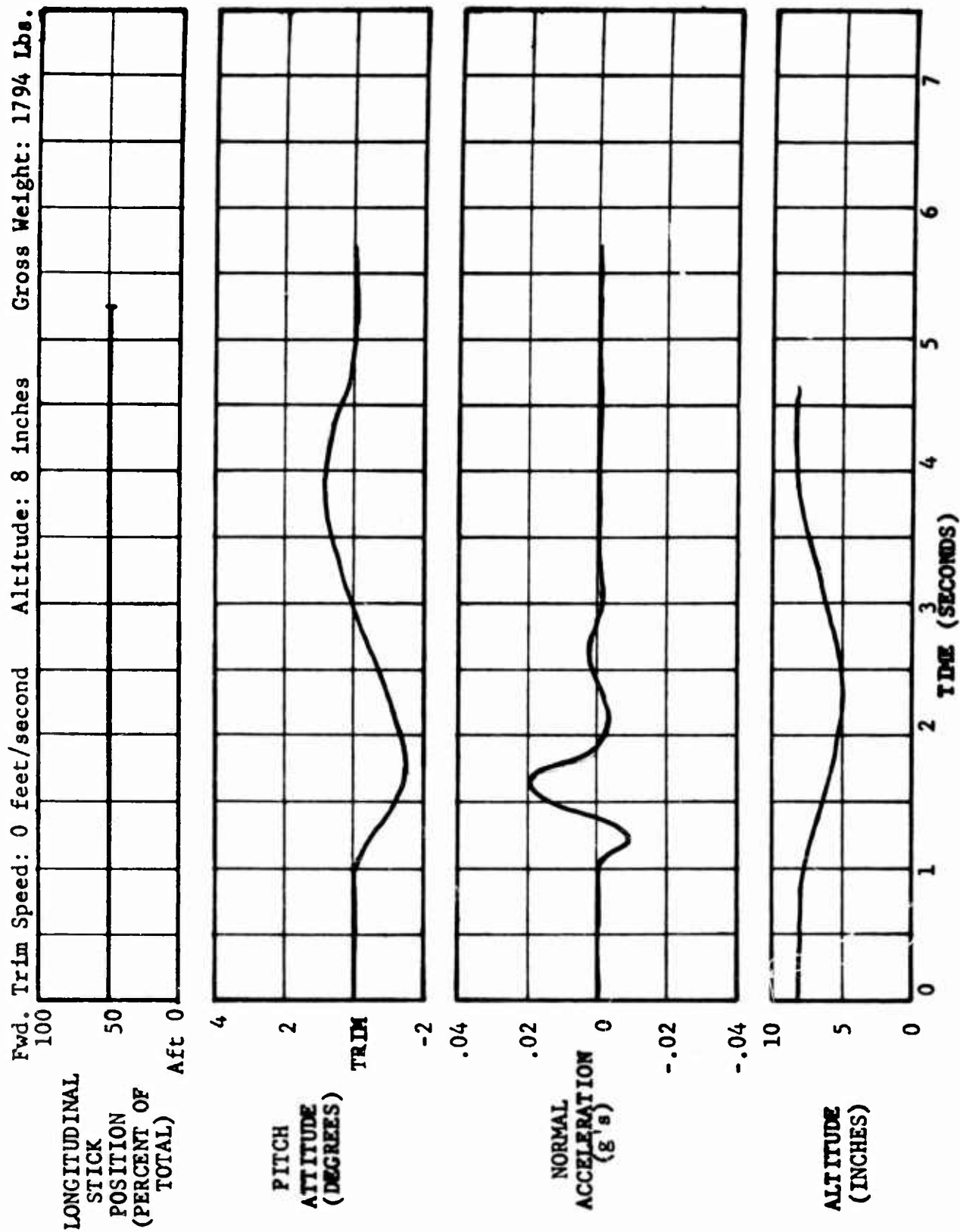


FIGURE 7: EFFECT OF INCREASED MOMENT OF INERTIA ON THE LONGITUDINAL RESPONSE CHARACTERISTICS OF THE P-GEN

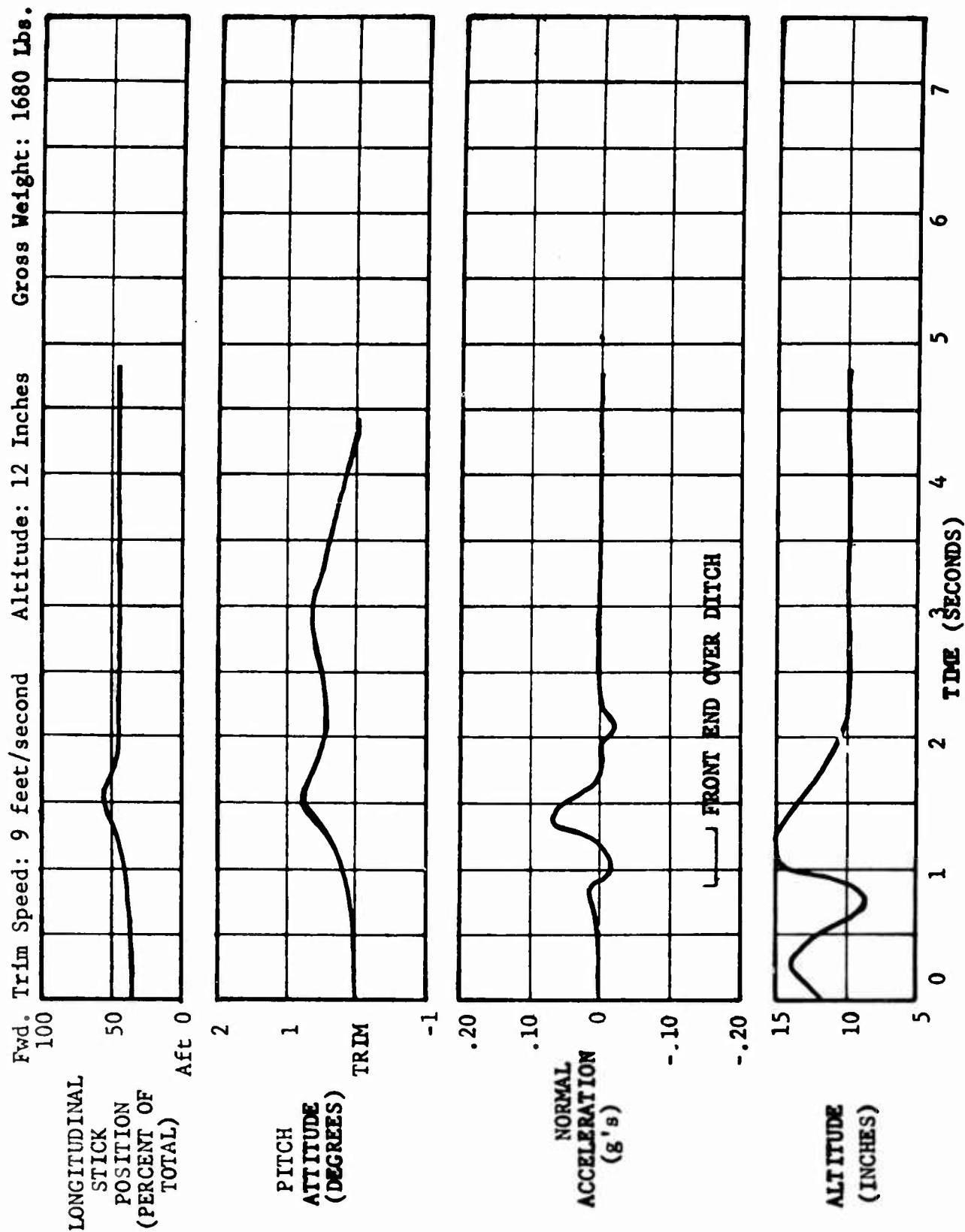


FIGURE 8: P-GEM LOW SPEED RESPONSE TO A LONGITUDINAL DISTURBANCE

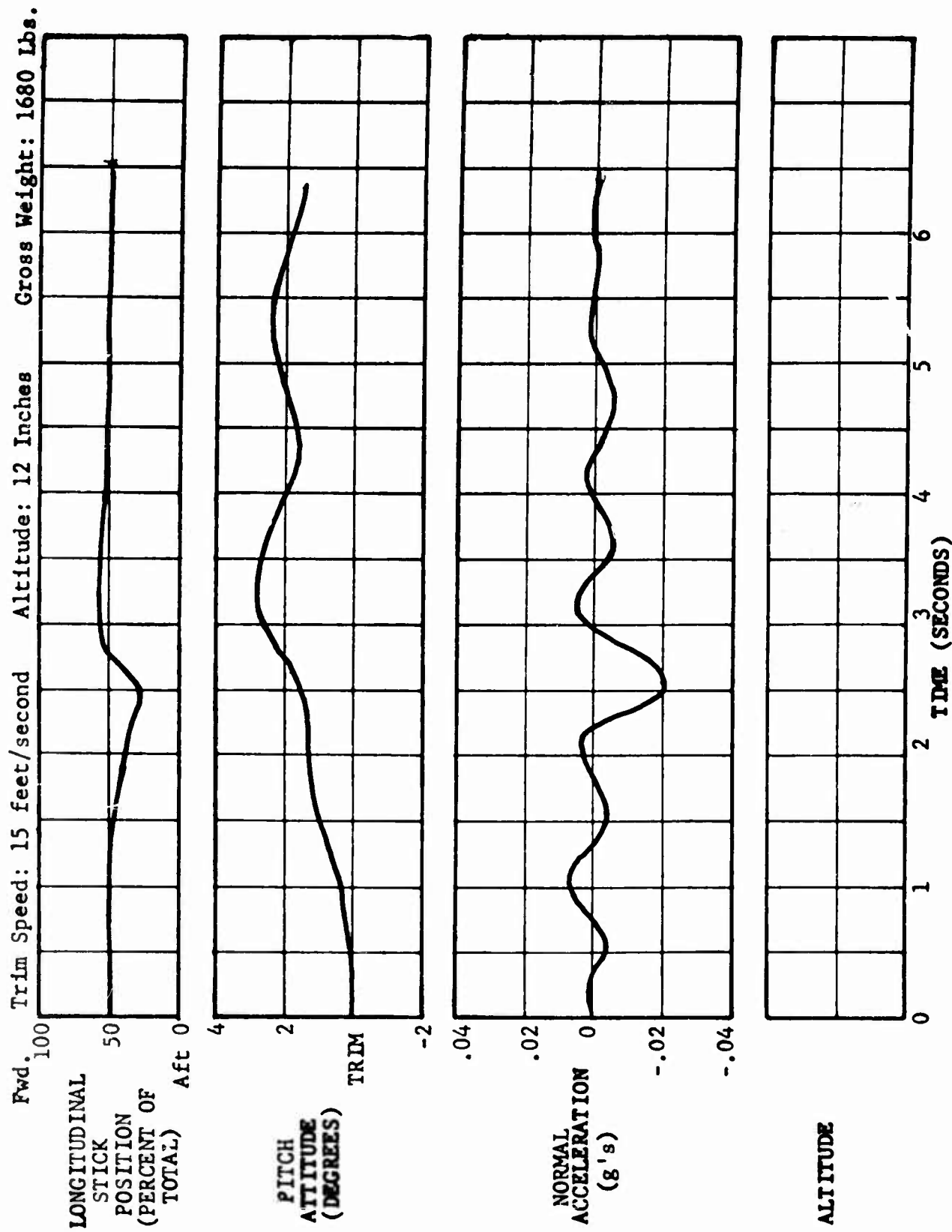


FIGURE 9: P-GEM MEDIUM SPEED RESPONSE TO A LONGITUDINAL CONTROL PULSE

Trim Speed: 22 feet/second Altitude: 8 inches Gross Weight: 1680 Lbs.

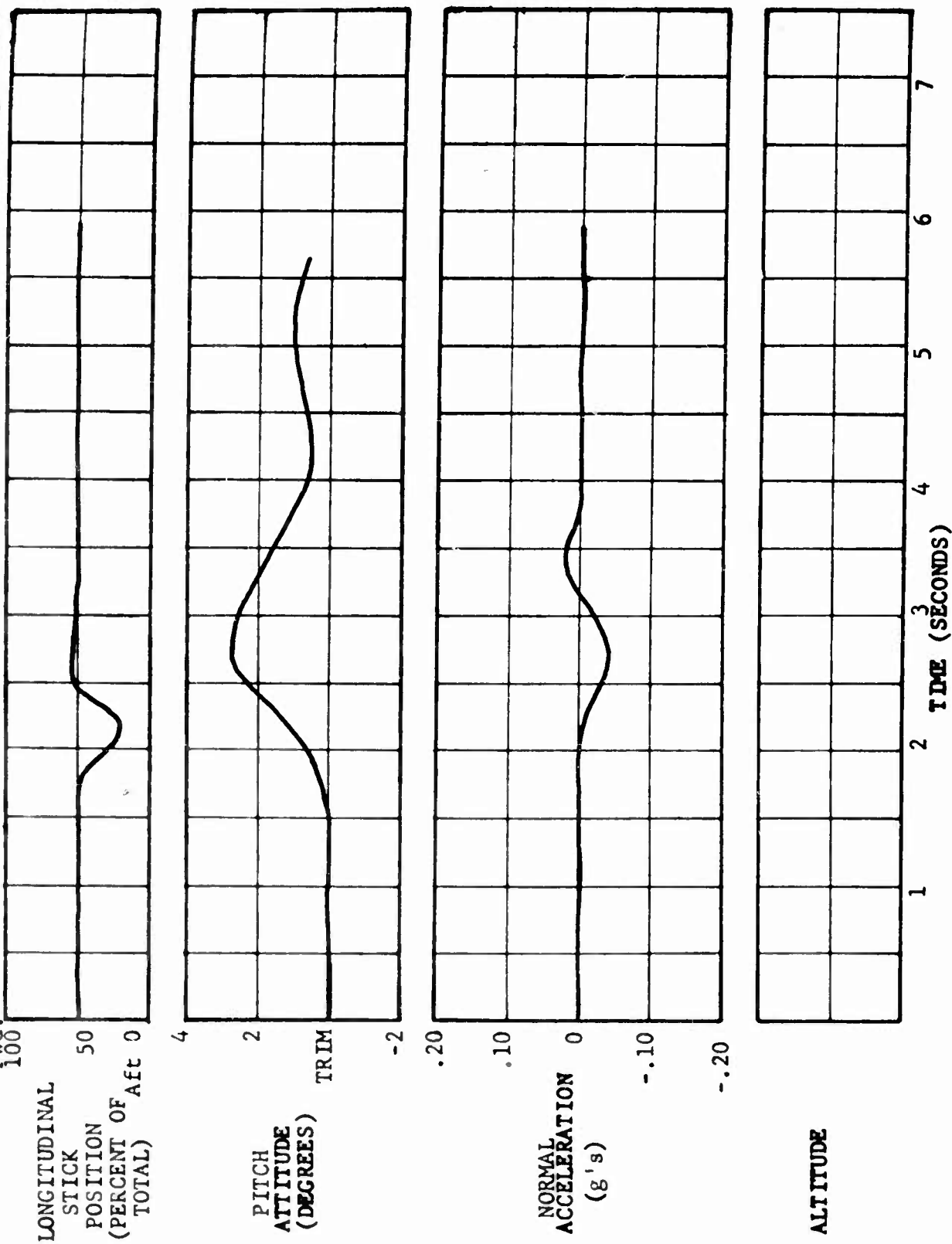


FIGURE 10: P-GEM HIGH SPEED RESPONSE TO A LONGITUDINAL STICK PULSE

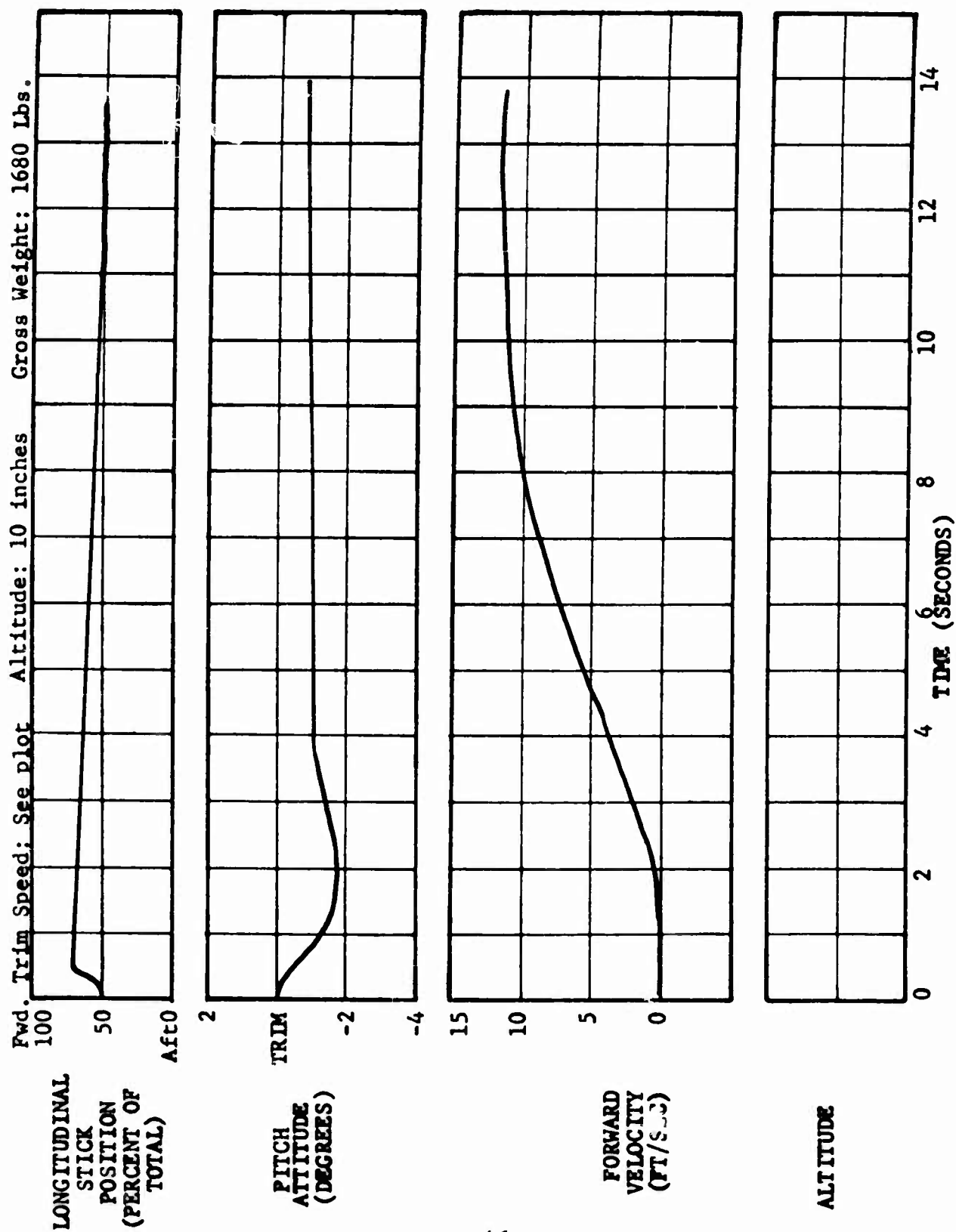


FIGURE 11: P-GEM RESPONSE TO A FORWARD CONTROL STEP INPUT

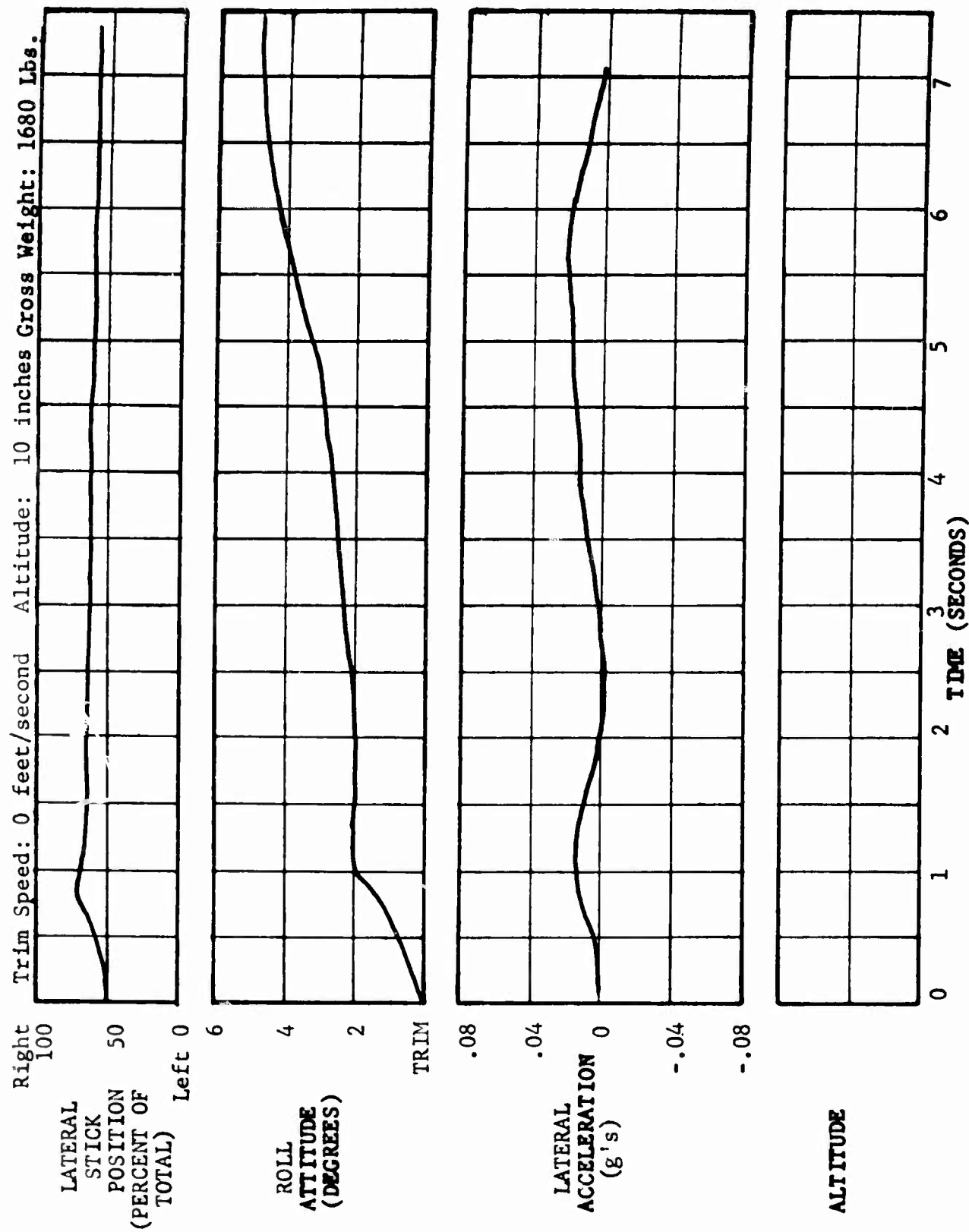


FIGURE 12: P-GEM RESPONSE TO A LATERAL CONTROL STEP INPUT

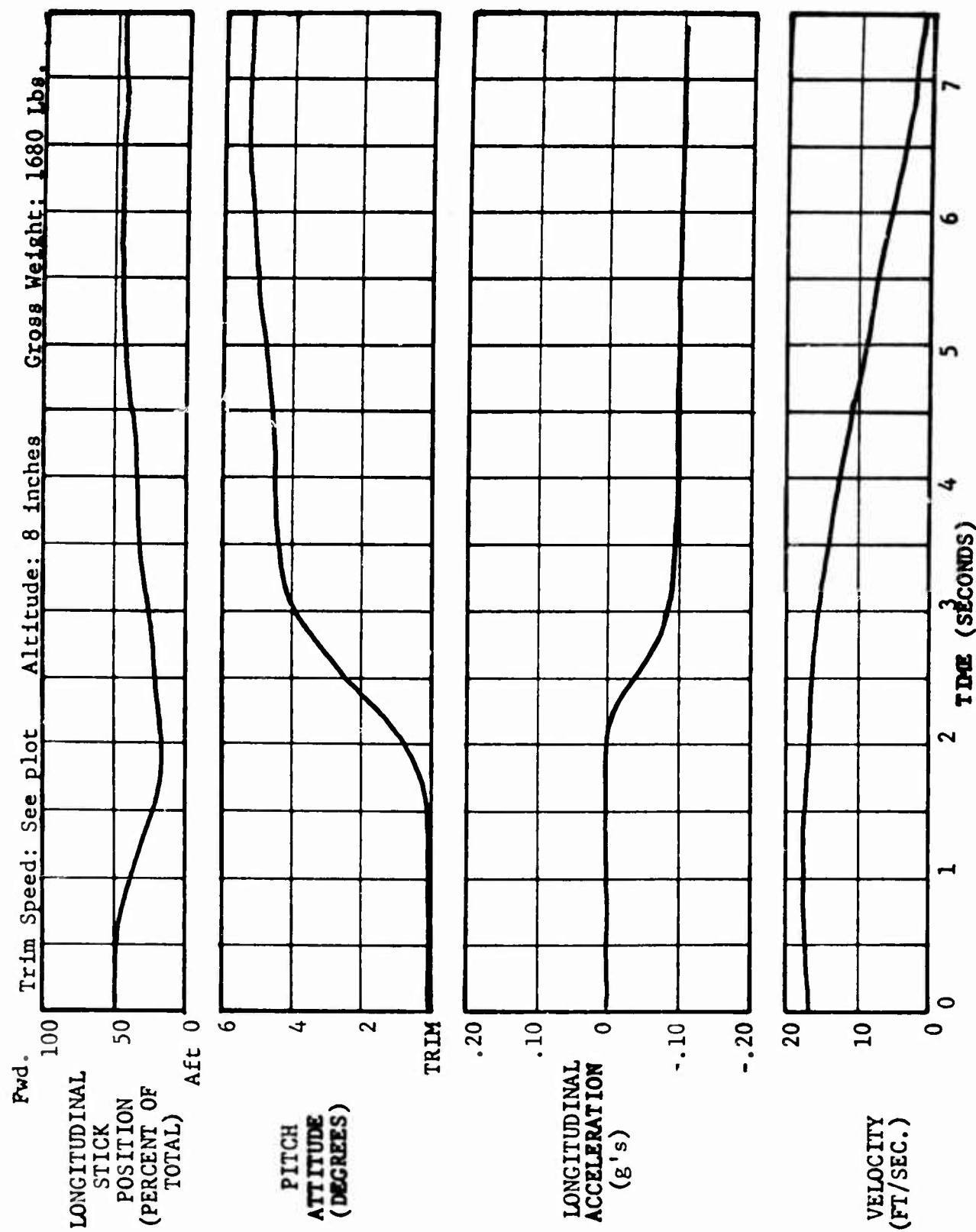


FIGURE 13: P-GEM RESPONSE TO AN AFT CONTROL INPUT

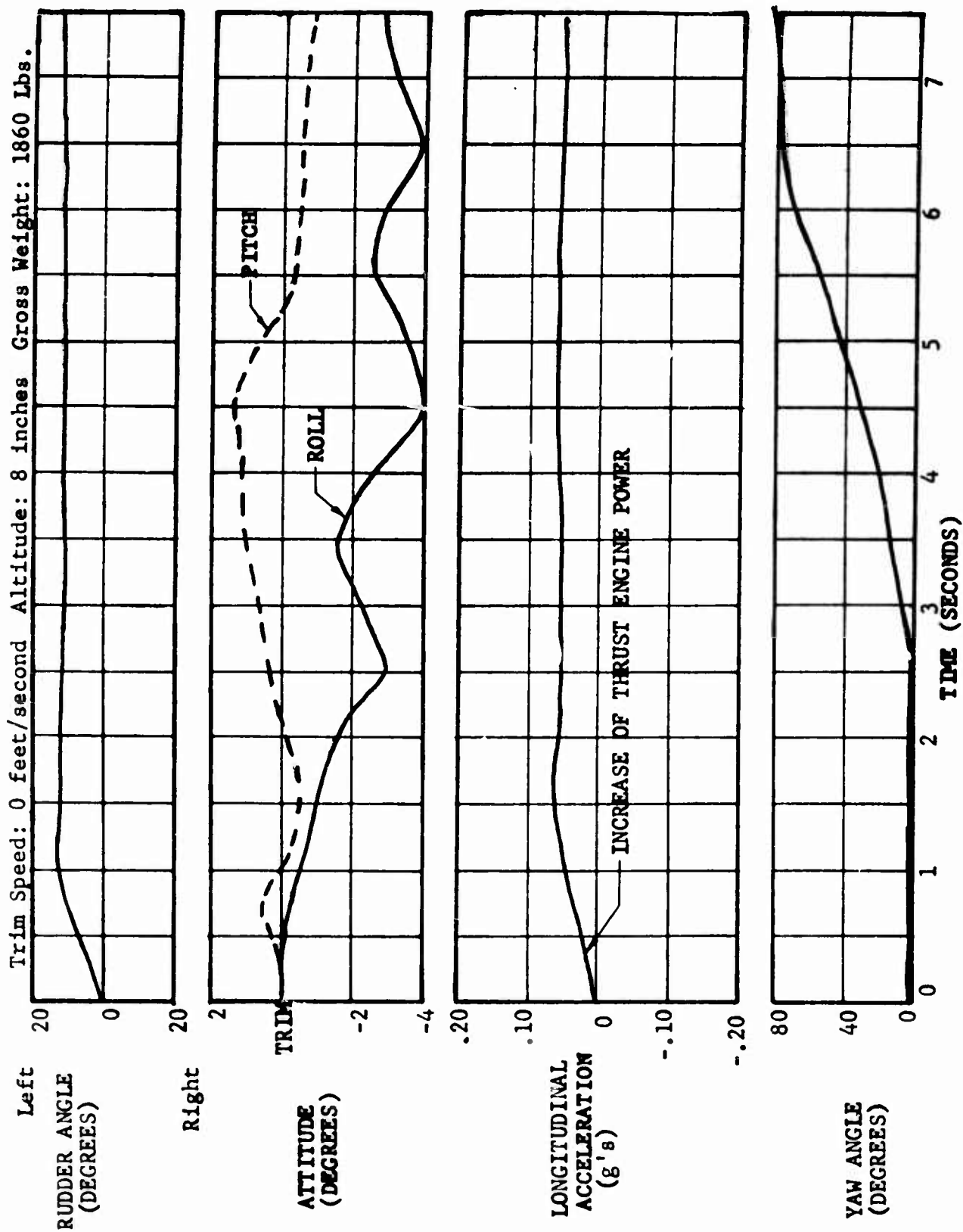


FIGURE 14: P-GEM RESPONSE TO A YAW CONTROL STEP INPUT FROM ZERO FORWARD SPEED

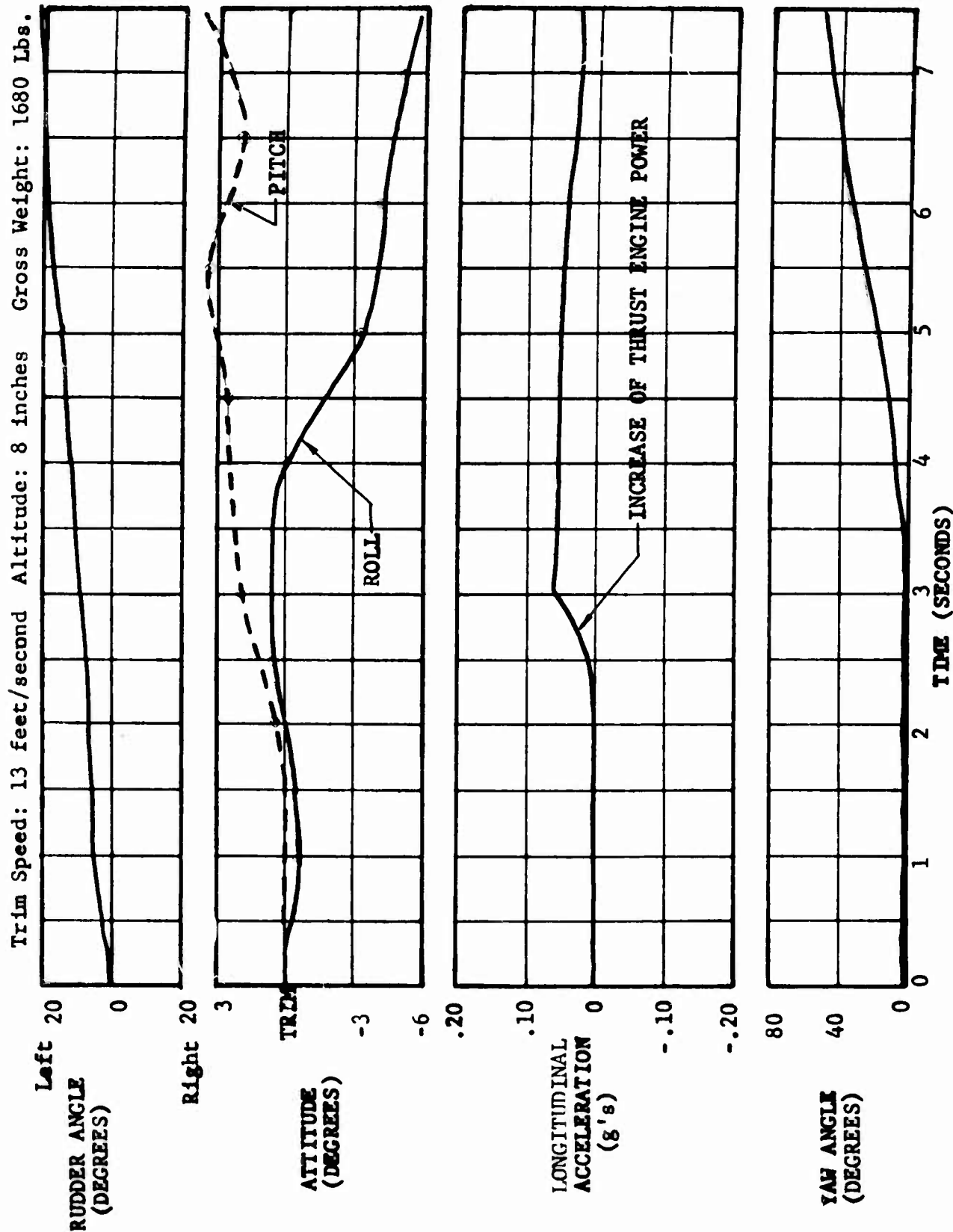


FIGURE 15: P-GEM LOW SPEED RESPONSE TO A YAW CONTROL INPUT

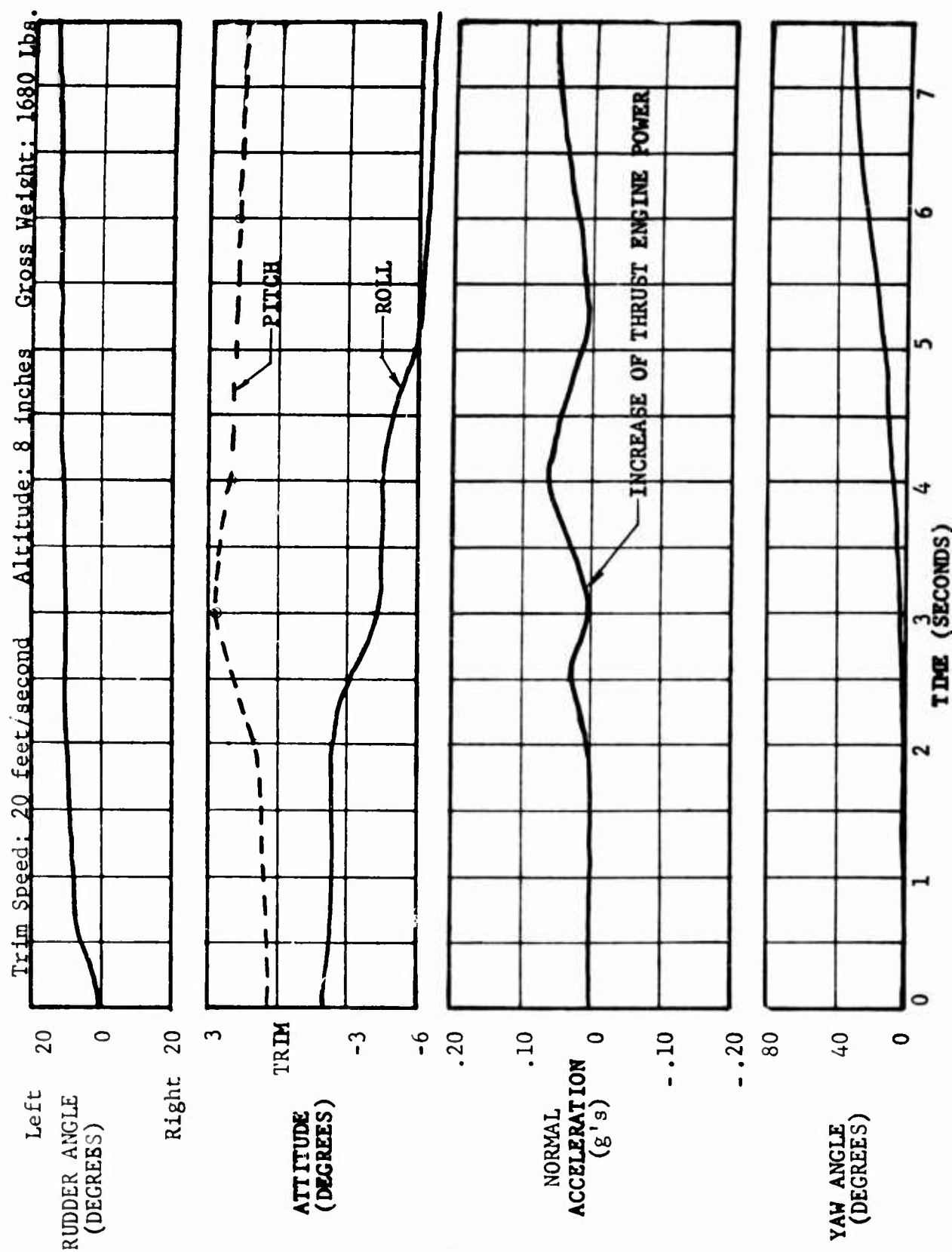


FIGURE 16: P-GEM MEDIUM SPEED RESPONSE TO A YAW CONTROL INPUT

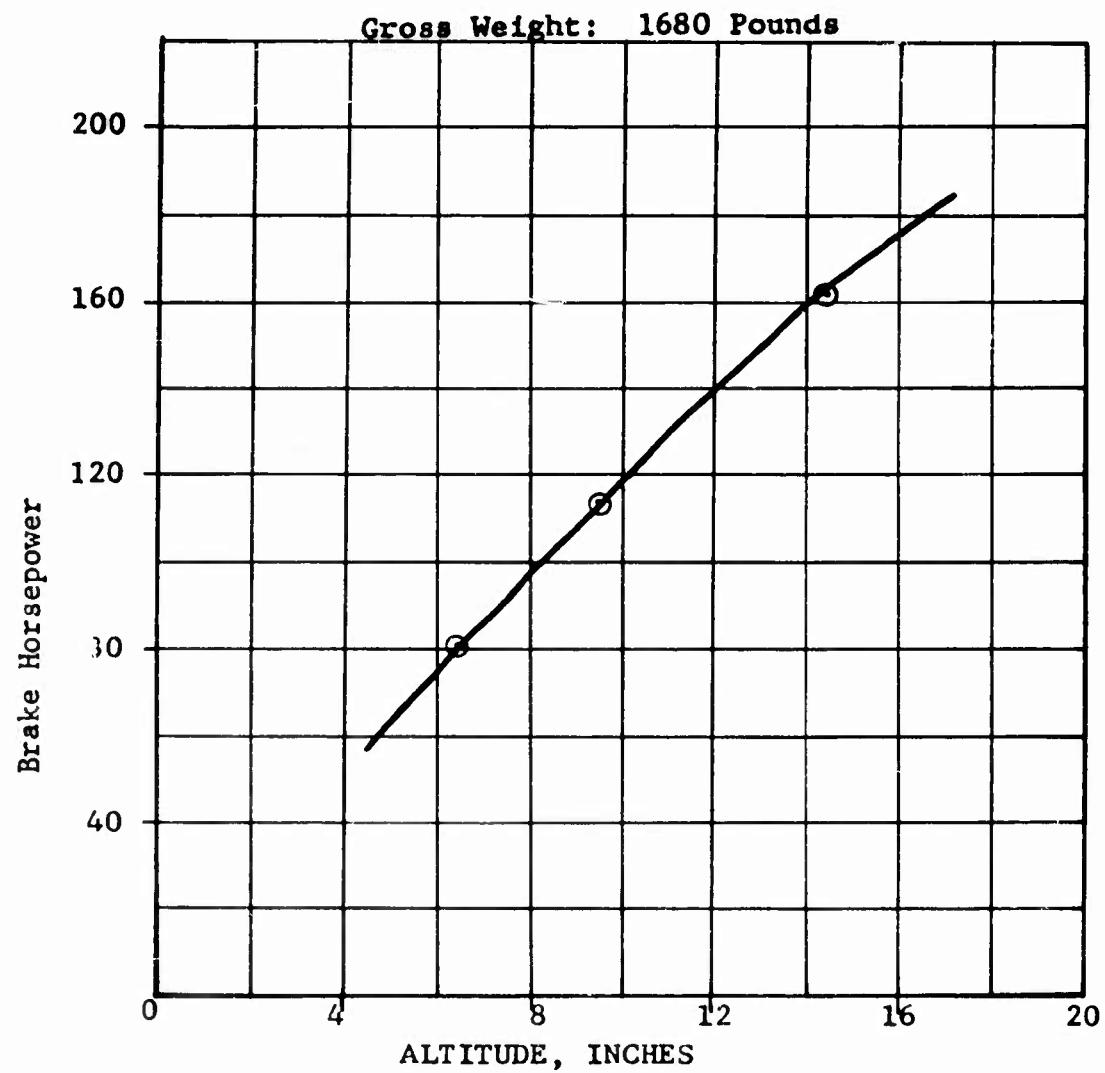


FIGURE 17: VARIATION OF P-GEM ALTITUDE WITH BRAKE HORSEPOWER

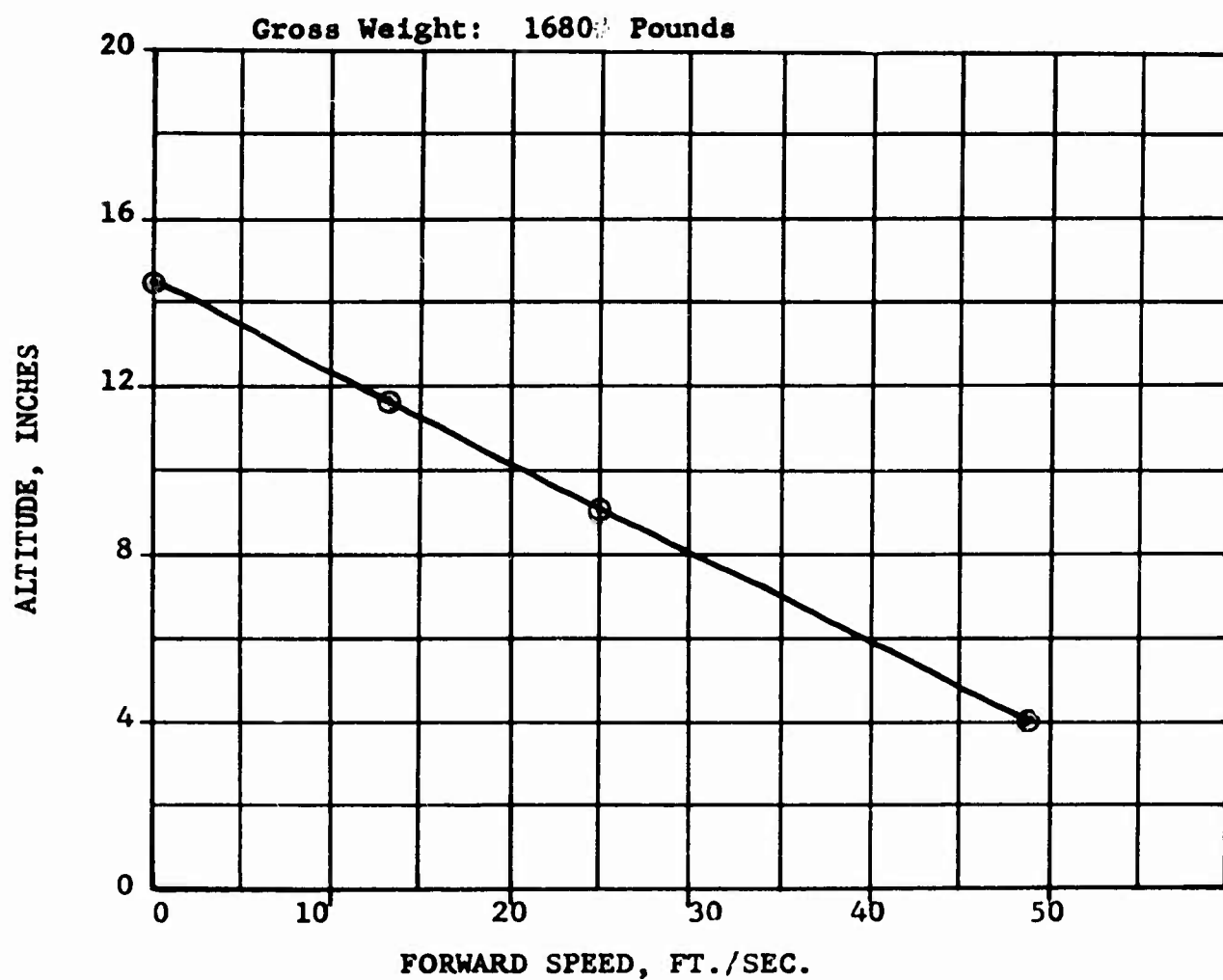


FIGURE 18: OPERATING ALTITUDE OF THE P-GEM AS A FUNCTION OF FORWARD SPEED AT A CONSTANT POWER OF ABOUT 160 HP

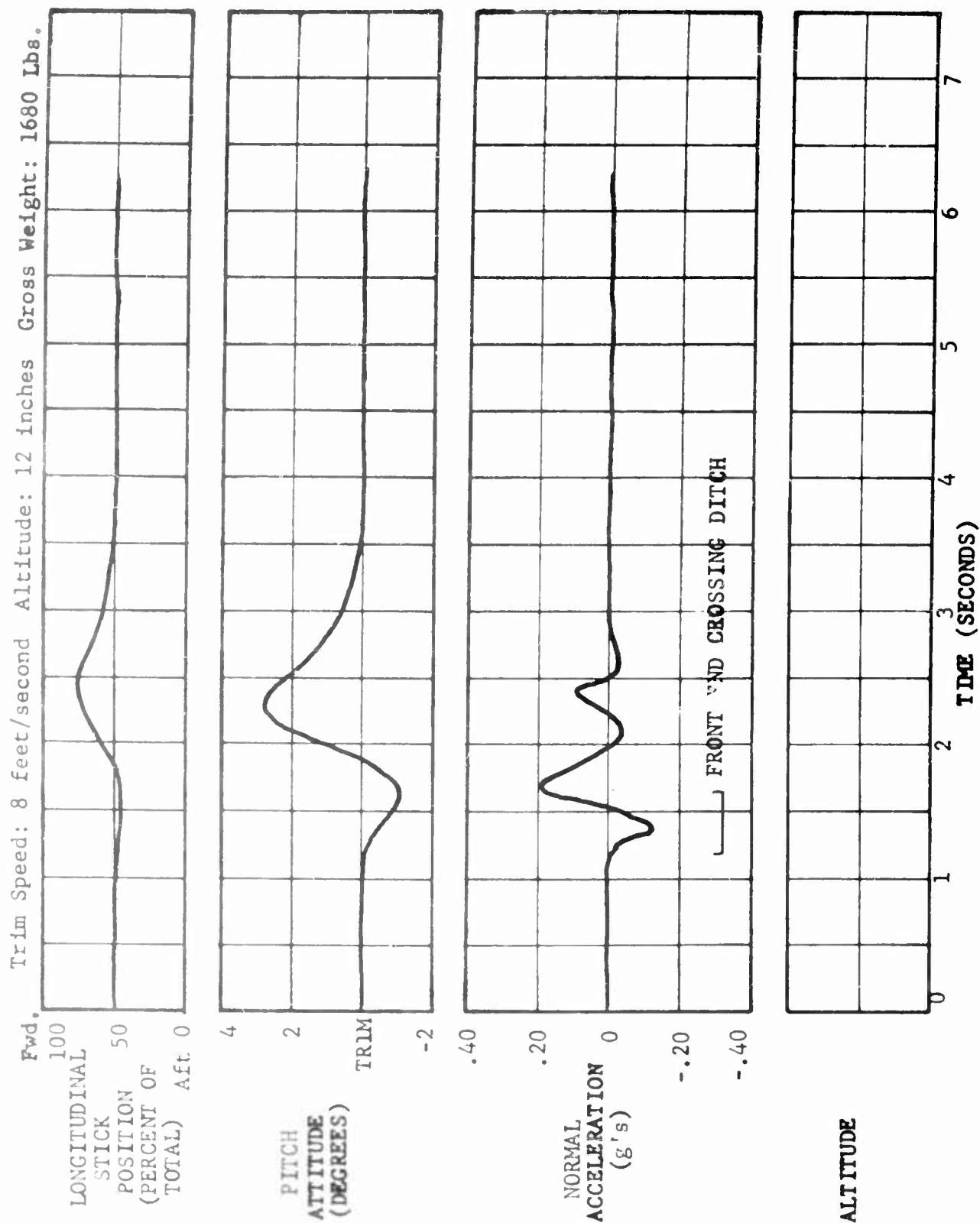


FIGURE 19: RESPONSE OF THE P-GEM CROSSING A 4-FOOT WIDE X 2-FOOT DEEP DITCH

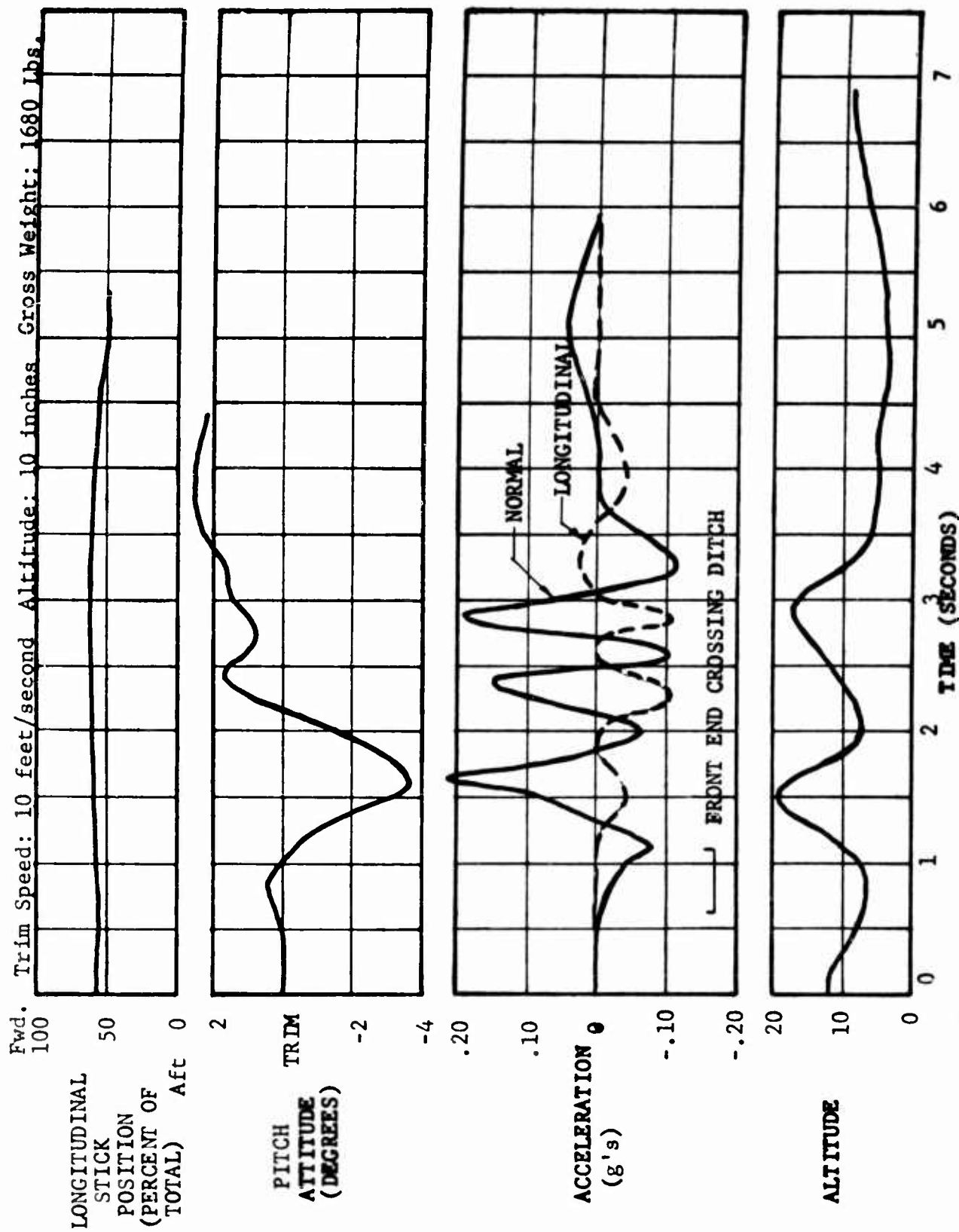


FIGURE 20: LOW SPEED CROSSING OF THE P-GEM OVER A 4-FOOT WIDE X 4-FOOT DEEP DITCH

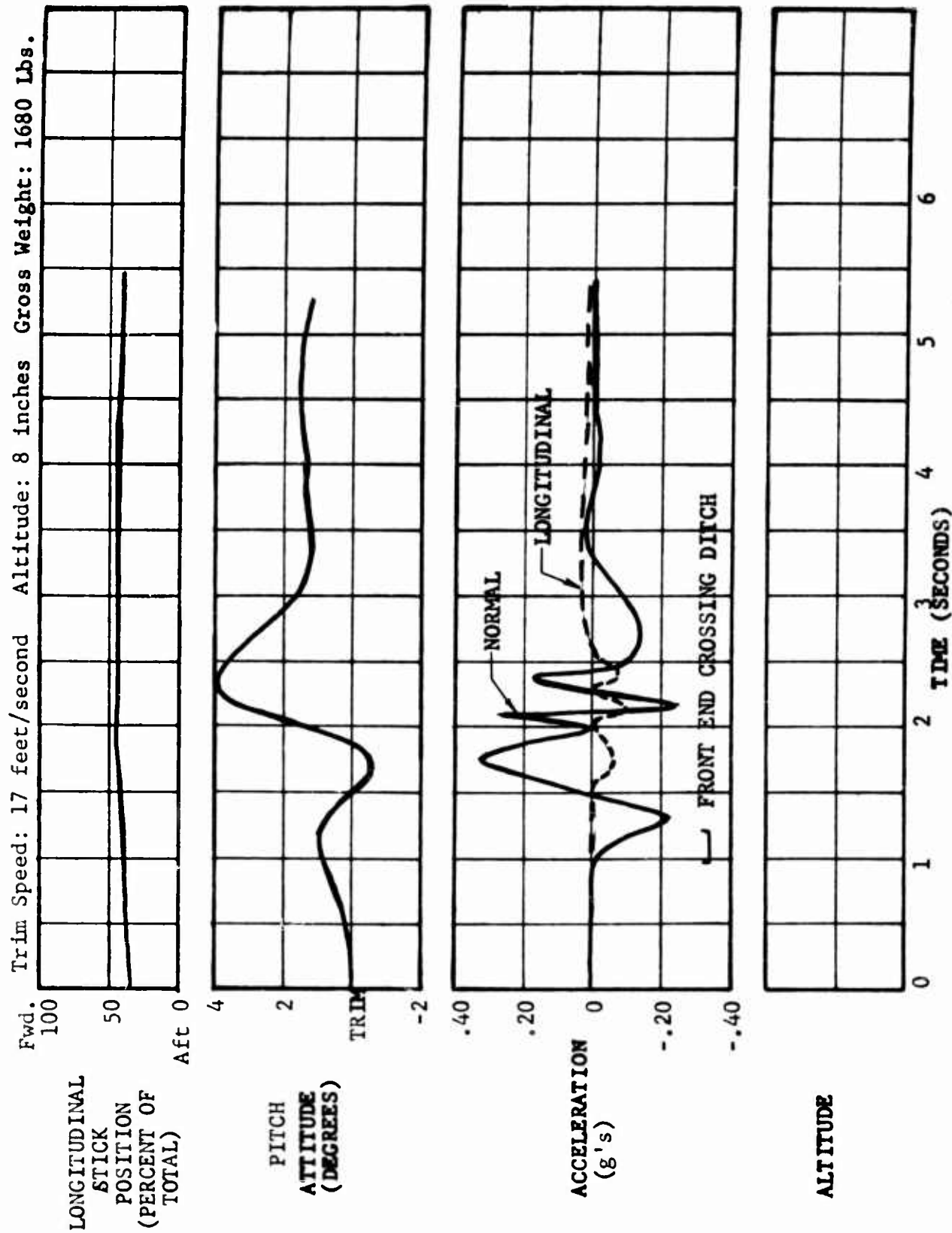


FIGURE 21: MEDIUM SPEED CROSSING OF THE P-GEM OVER A 4-FOOT WIDE X 4-FOOT DEEP DITCH

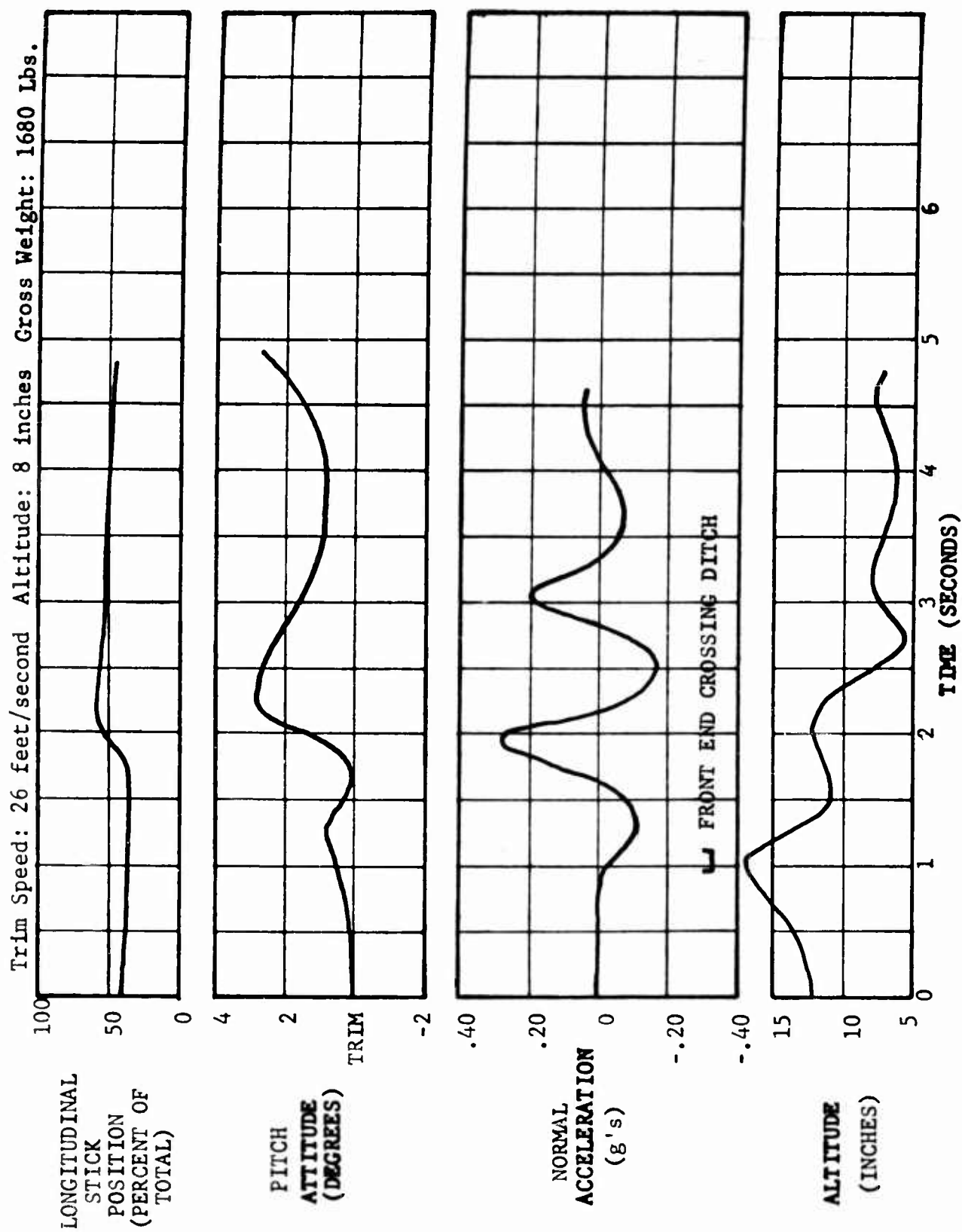


FIGURE 22: HIGH SPEED CROSSING OF THE P-GEM OVER A 4-FOOT WIDE X 4-FOOT DEEP DITCH

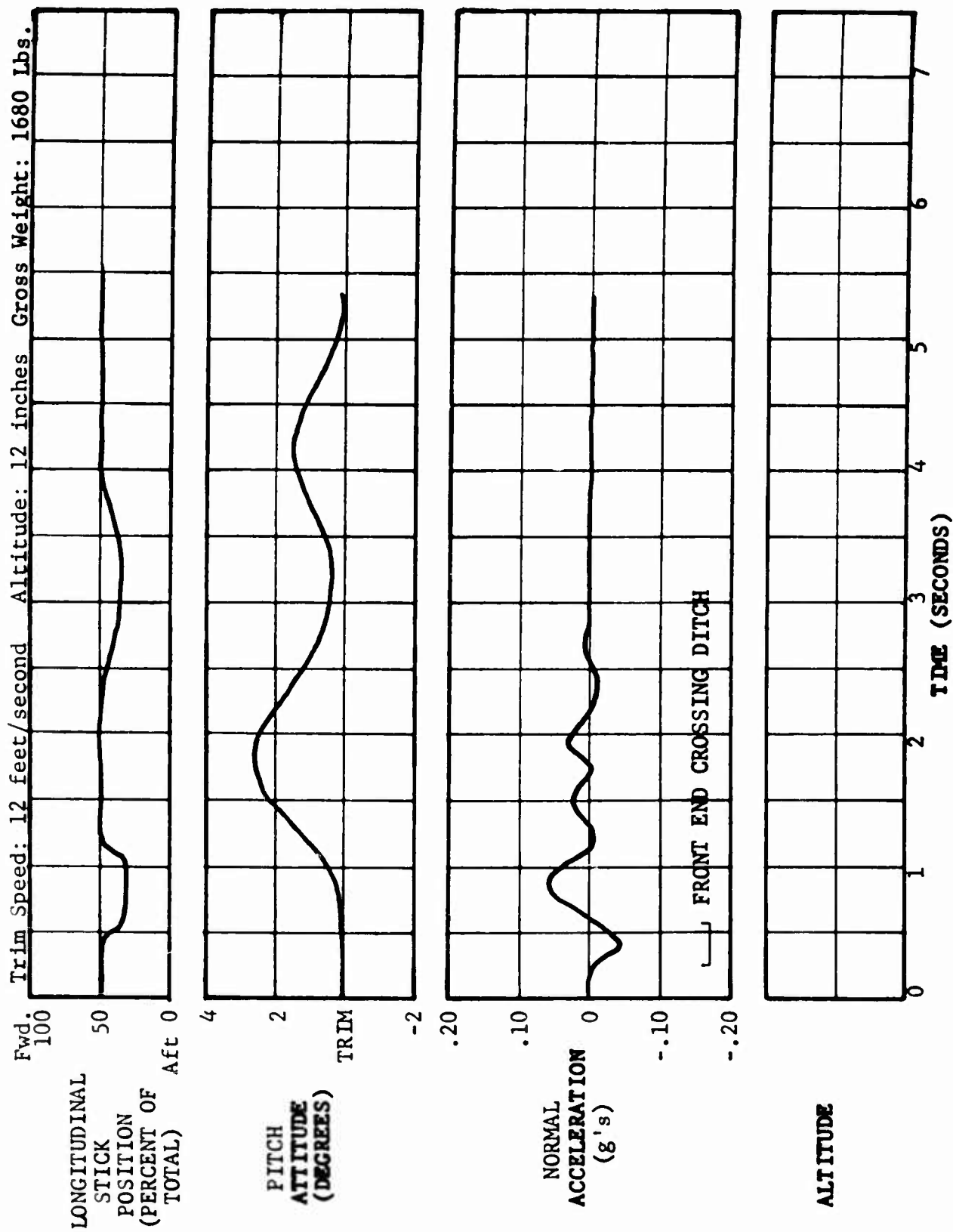


FIGURE 23: RESPONSE OF THE P-GEM CROSSING A 2-FOOT WIDE X 2-FOOT DEEP DITCH

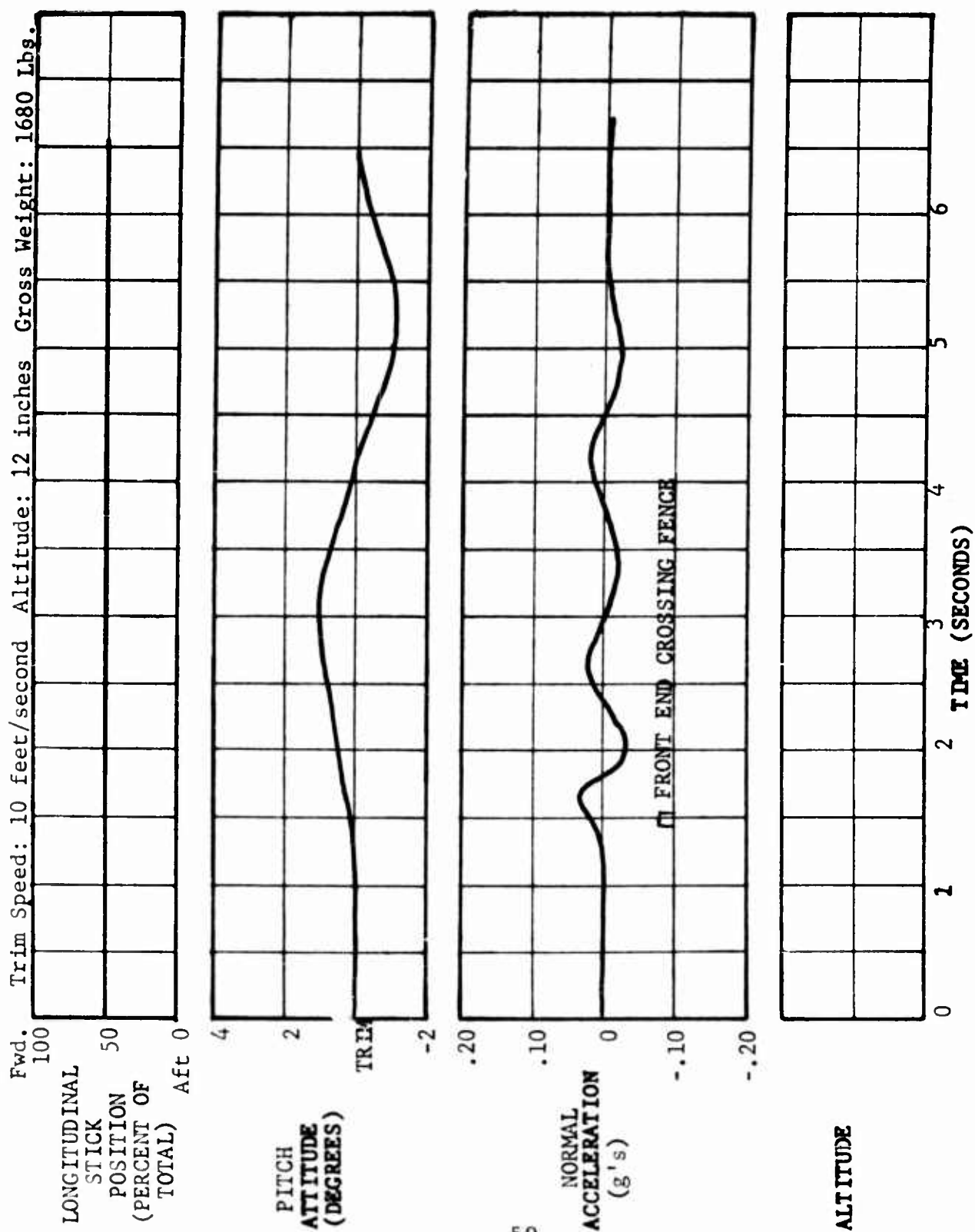


FIGURE 24: LOW SPEED CROSSING OF THE P-GEM OVER A 3-INCH THICK X 6-INCH HIGH FENC

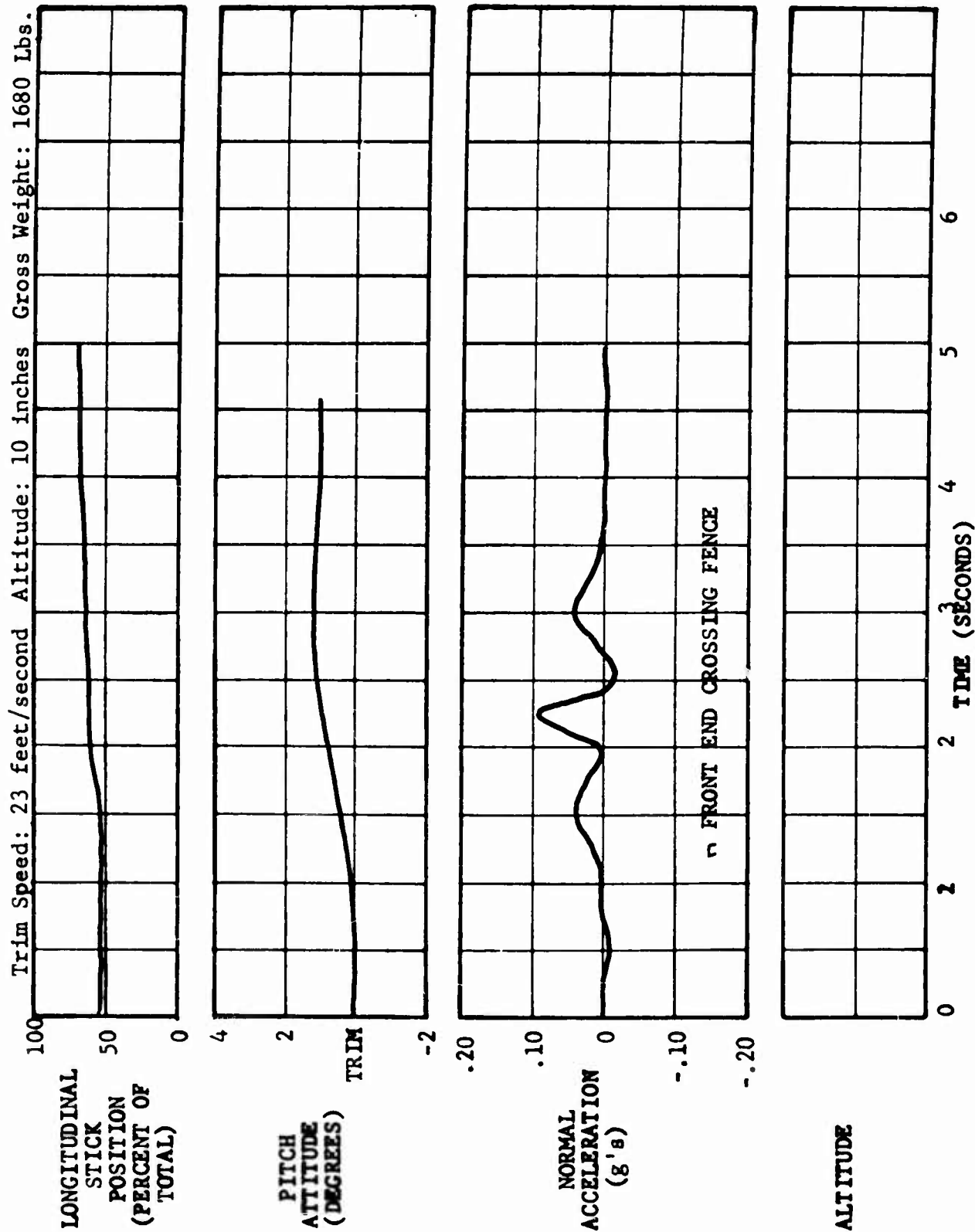


FIGURE 25: HIGH SPEED CROSSING OF THE P-GEM OVER A 3-INCH THICK X 6-INCH HIGH FENCE

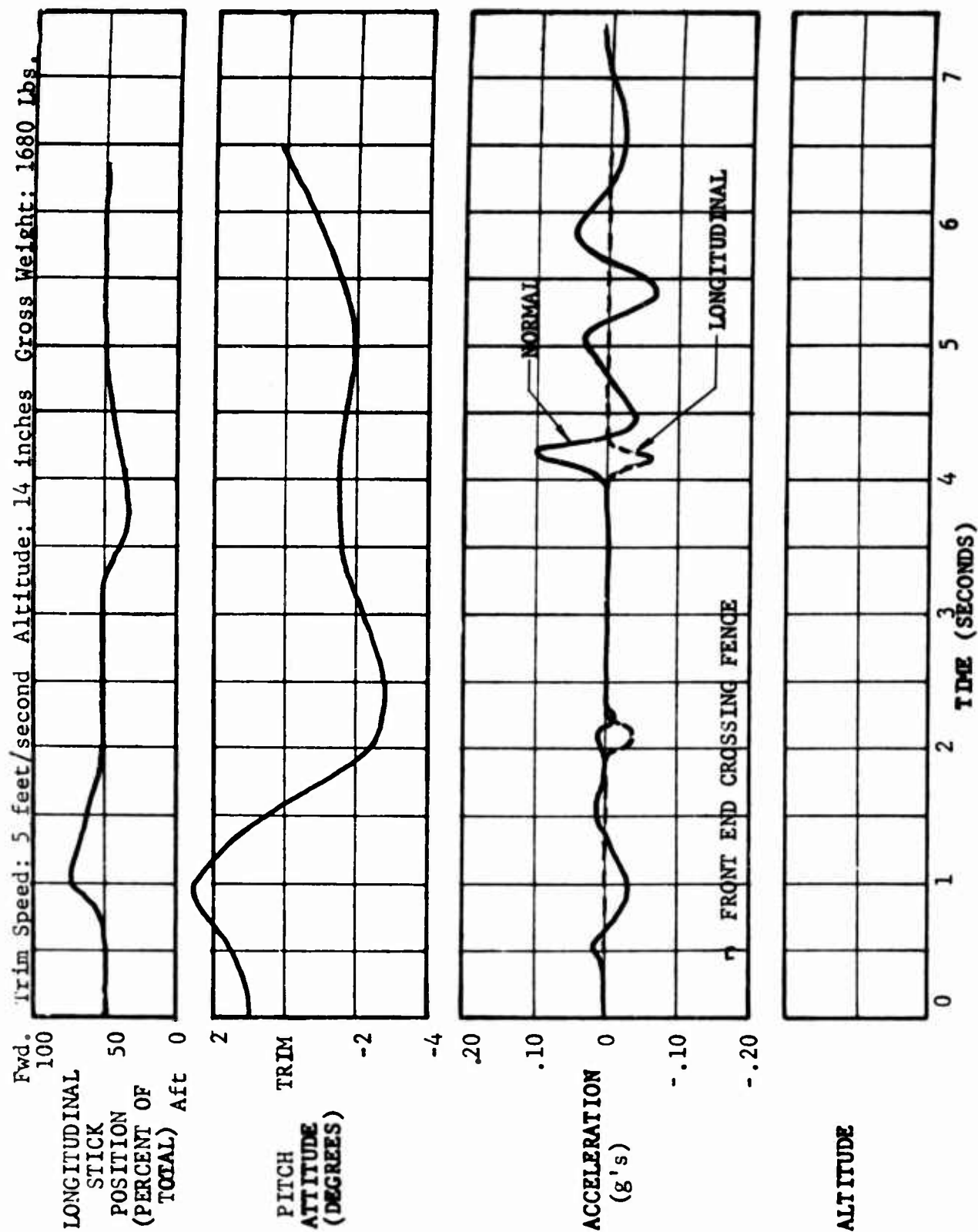


FIGURE 26: LOW SPEED CROSSING OF THE P-GEM OVER A 3-INCH THICK X 12-INCH HIGH FENCE

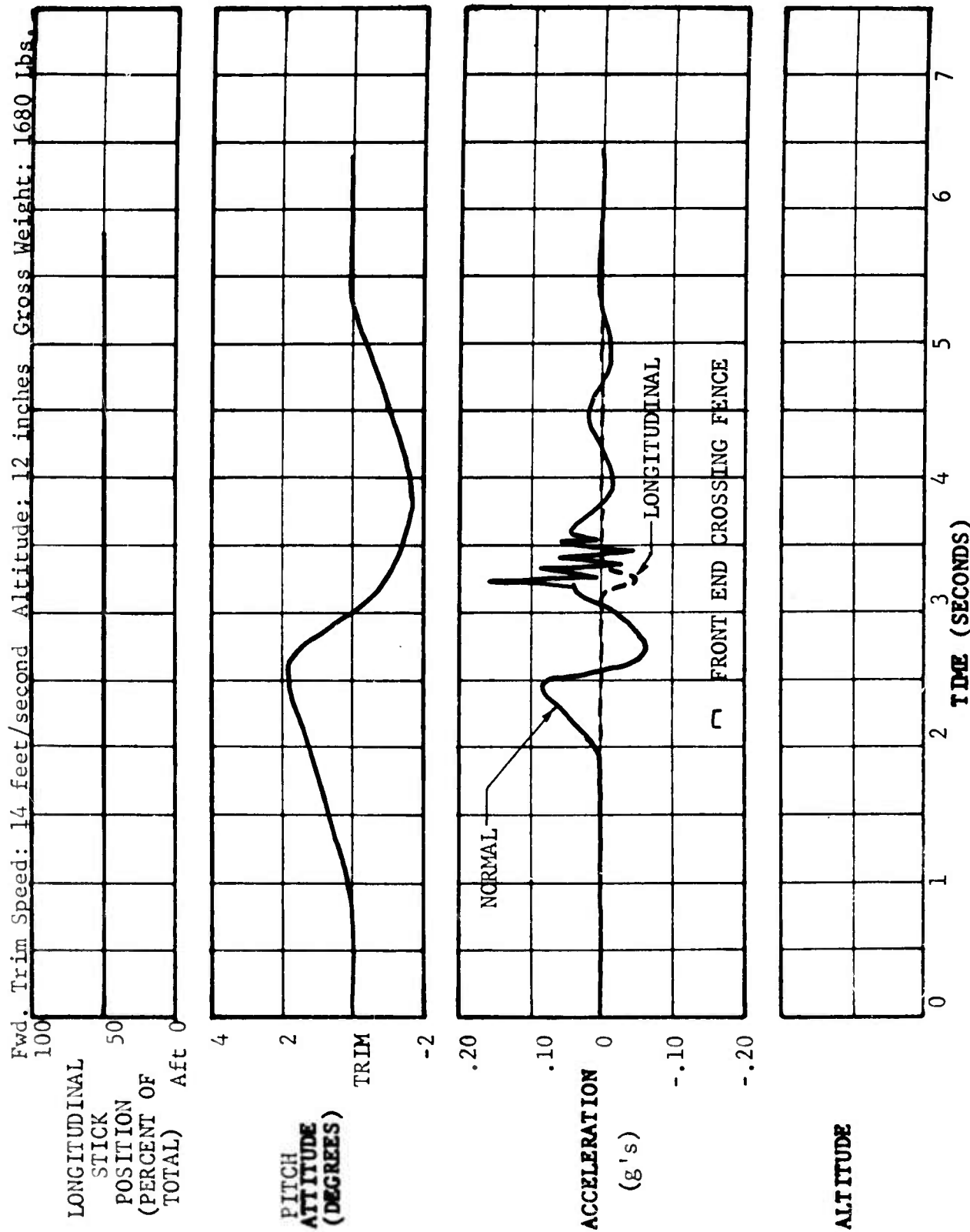


FIGURE 27: HIGH SPEED CROSSING OF THE P-GEM OVER A 3-INCH THICK X 12-INCH HIGH FENCE

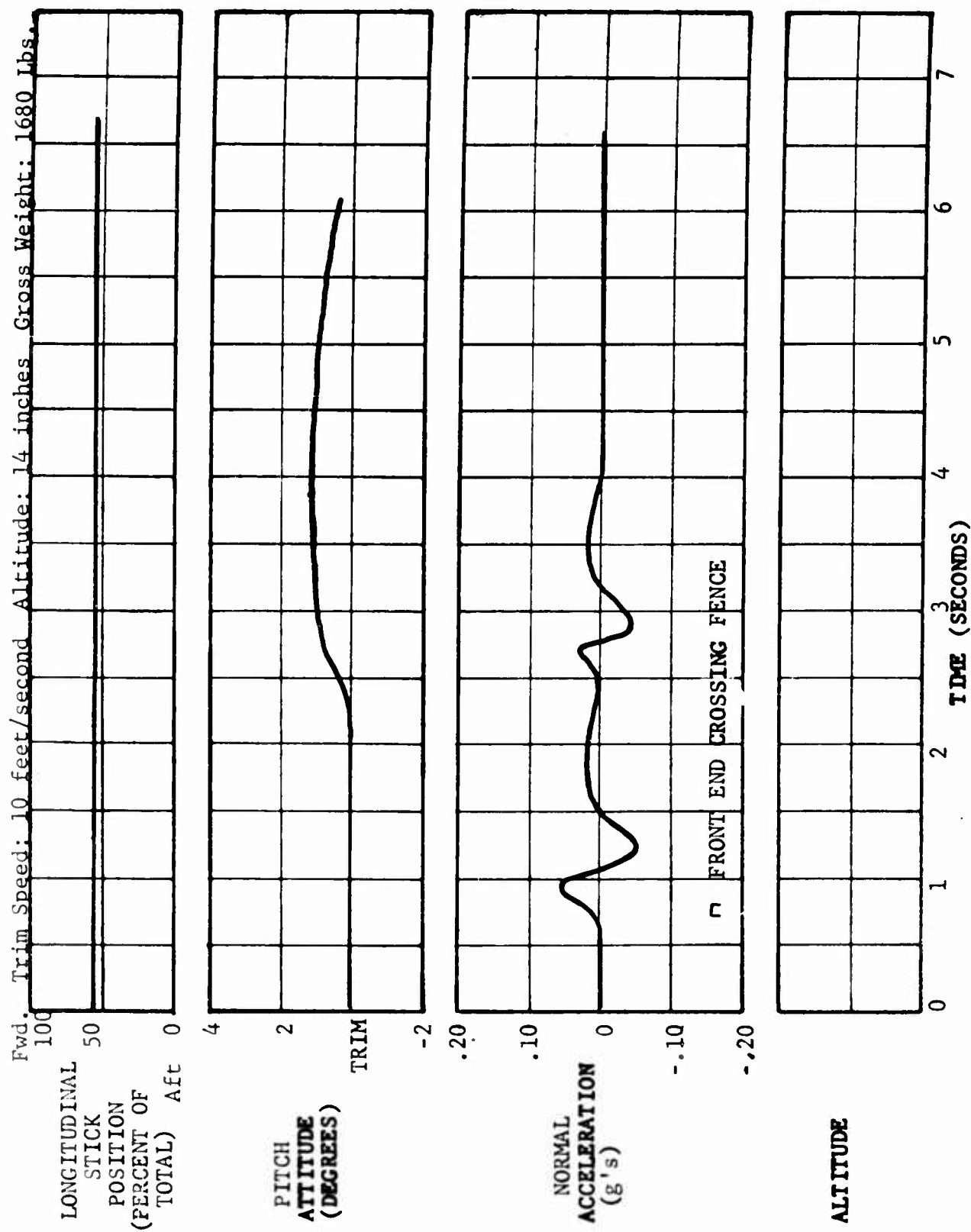


FIGURE 28: LOW SPEED CROSSING OF THE P-GEM OVER A 24-INCH THICK X 6-INCH HIGH FENCE

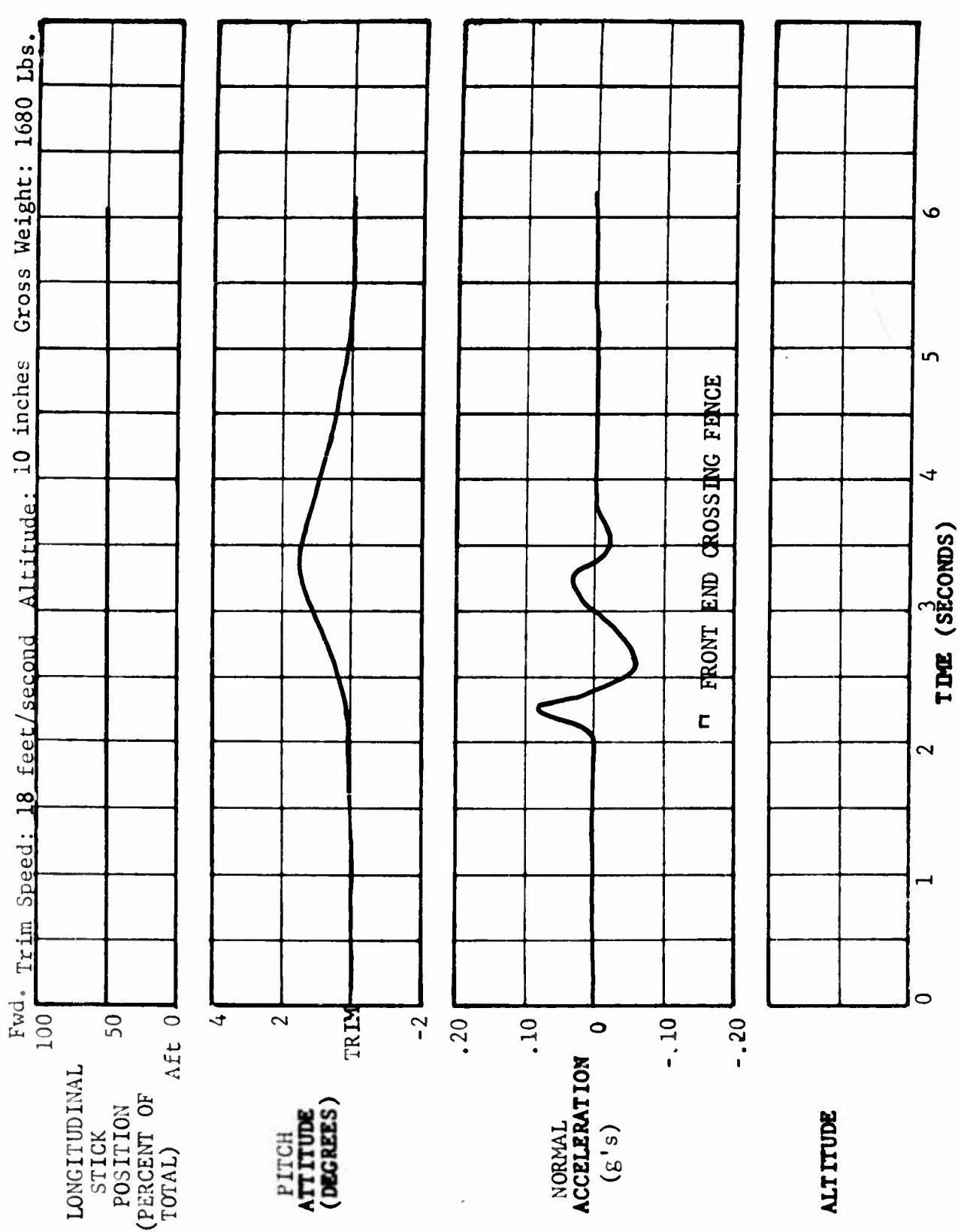


FIGURE 29: MEDIUM SPEED CROSSING OF THE P-GEM OVER A 24-INCH THICK X 6-INCH HIGH FENCE

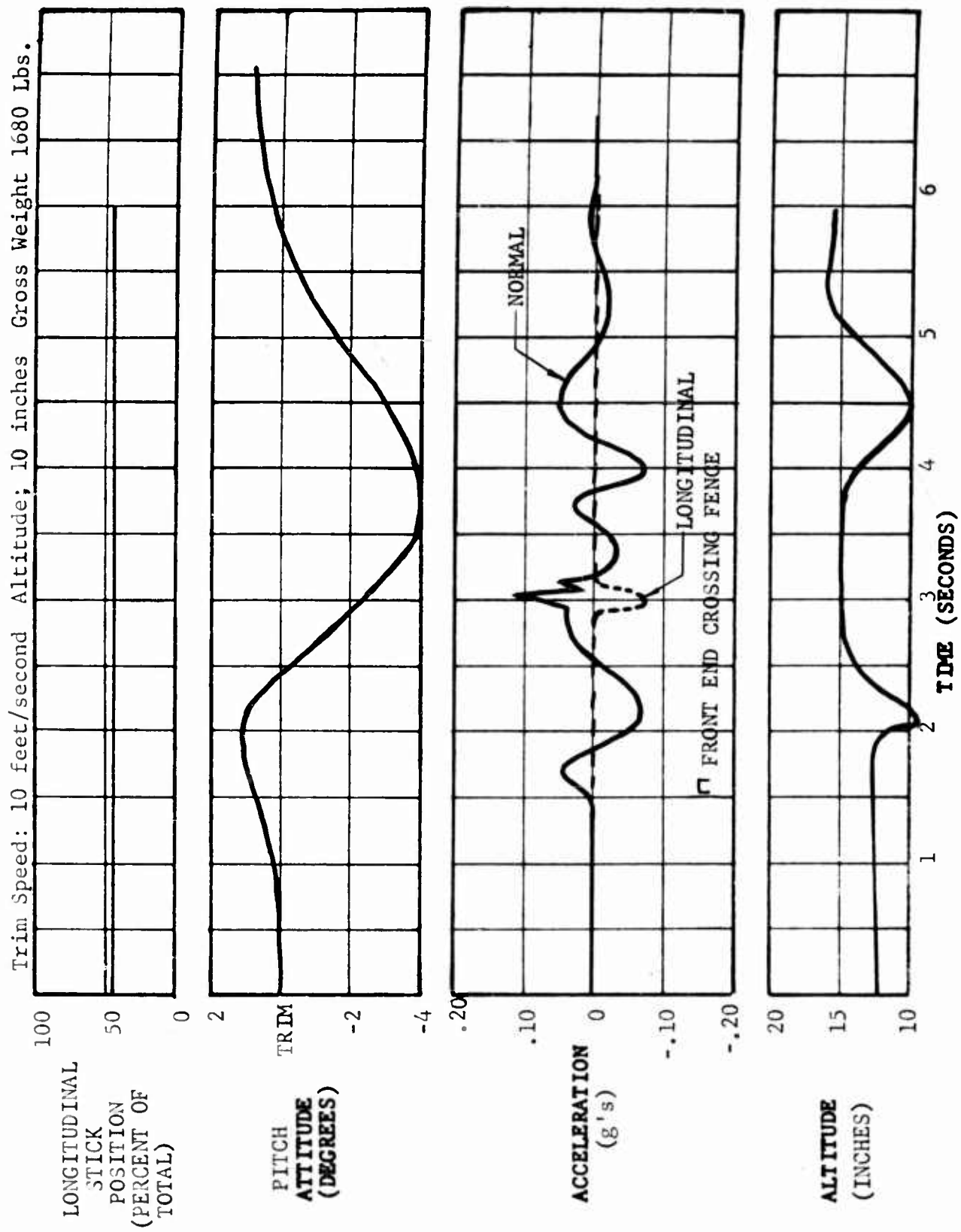


FIGURE 30: LOW SPEED CROSSING OF THE P-GEM OVER A 24-INCH THICK X 12-INCH HIGH FENCE

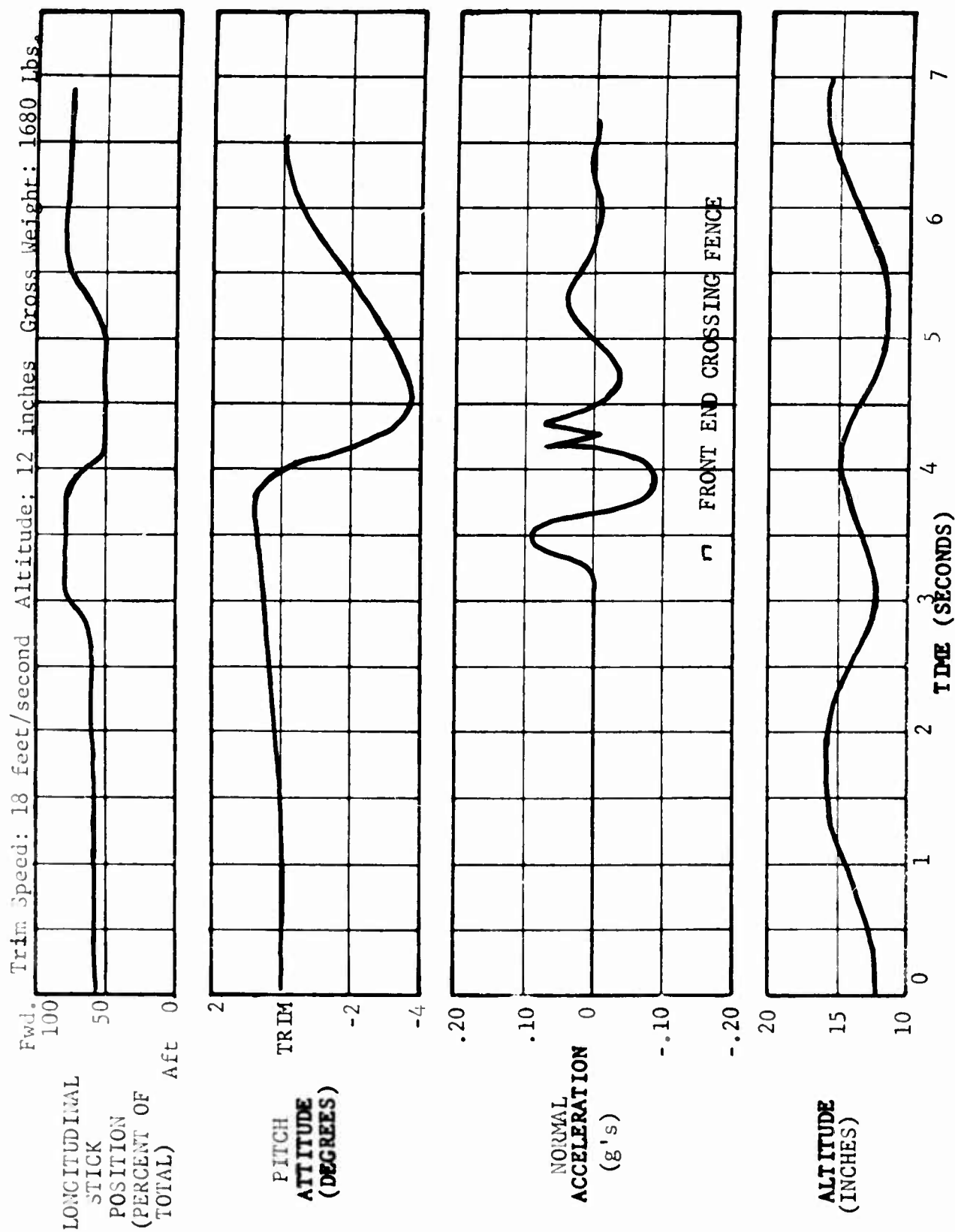


FIGURE 31: MEDIUM SPEED CROSSING OF THE P-GEM OVER A 24-INCH THICK X 12-INCH HIGH FENCE

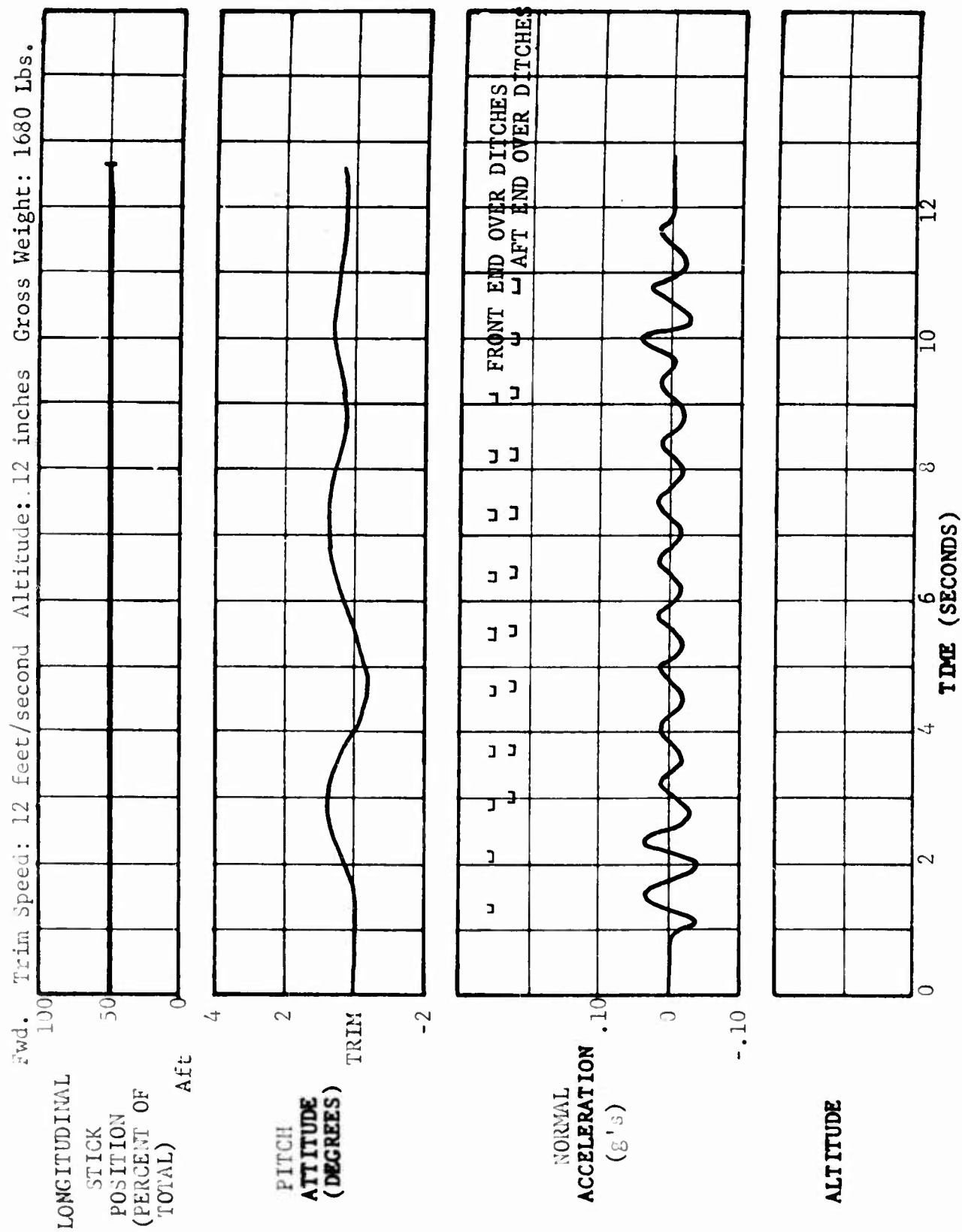


FIGURE 32 : LOW SPEED CROSSING OF THE P-GEM OVER A SERIES OF 2-FOOT WIDE X 1-FOOT DEEP DITCHES

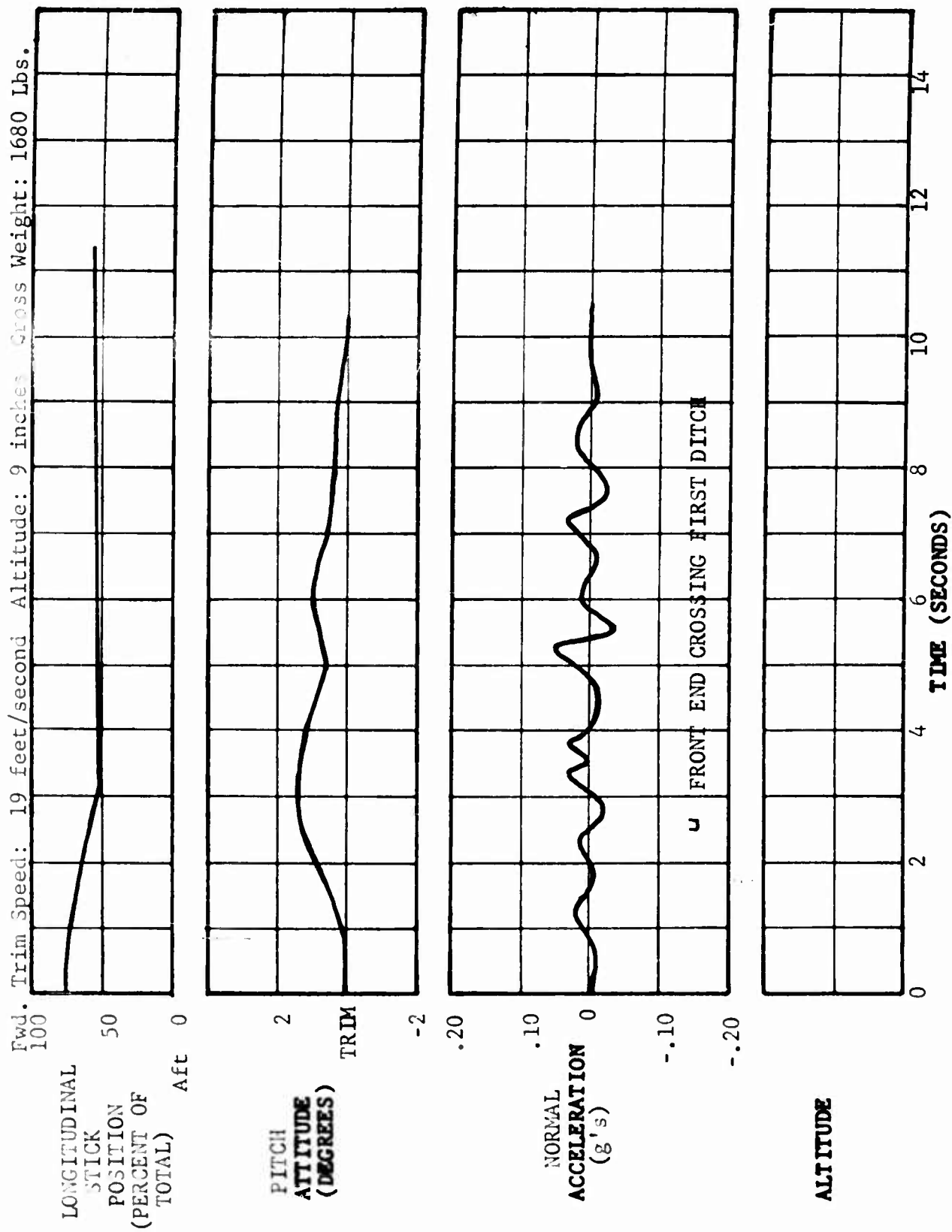


FIGURE 33: MEDIUM SPEED CROSSING OF THE P-GEM OVER A SERIES OF 2-FOOT WIDE X 1-FOOT DEEP DITCHES

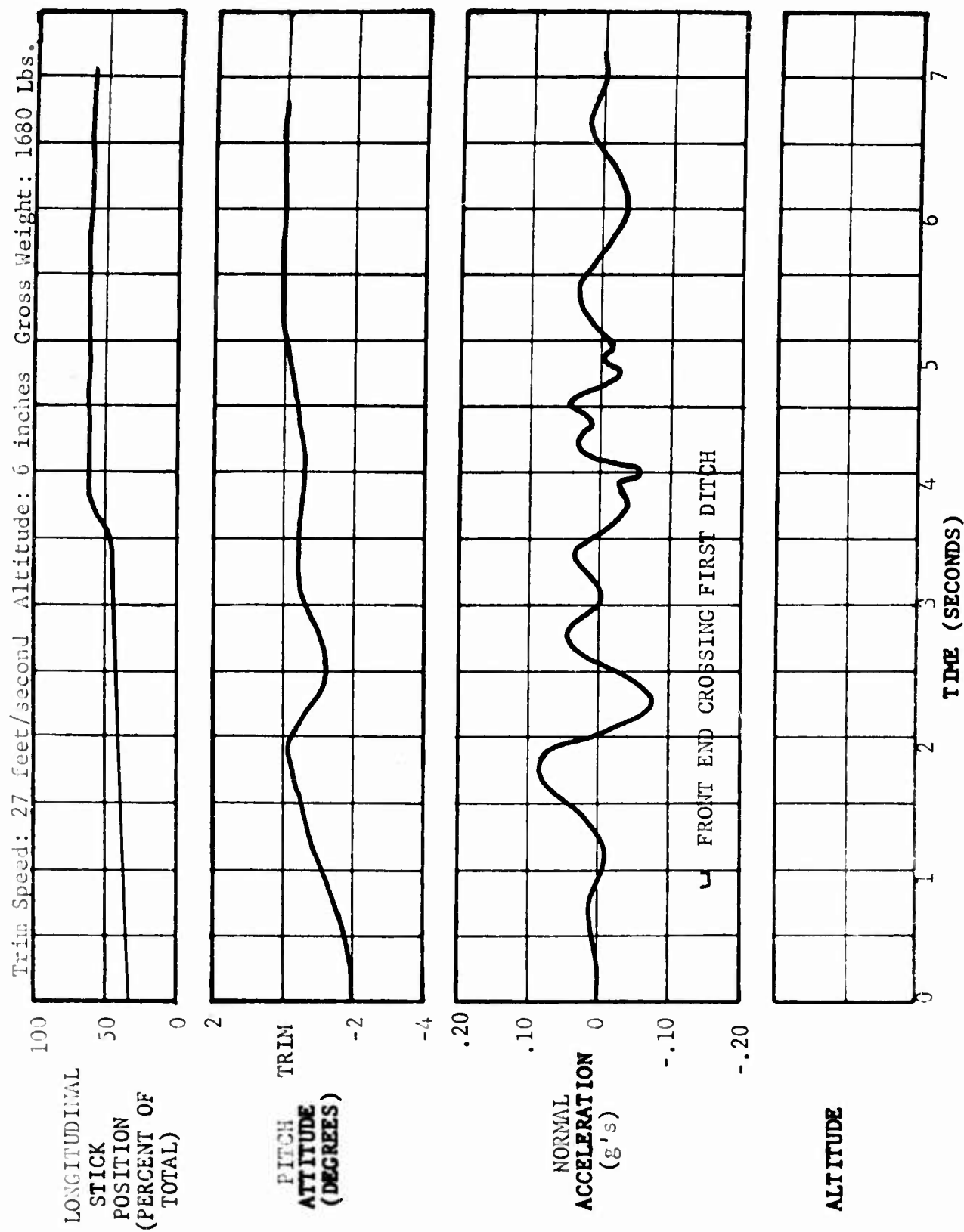


FIGURE 34: HIGH SPEED CROSSING OF THE P-GEM OVER A SERIES OF 2-FOOT WIDE X 1-FOOT DEEP DITCHES

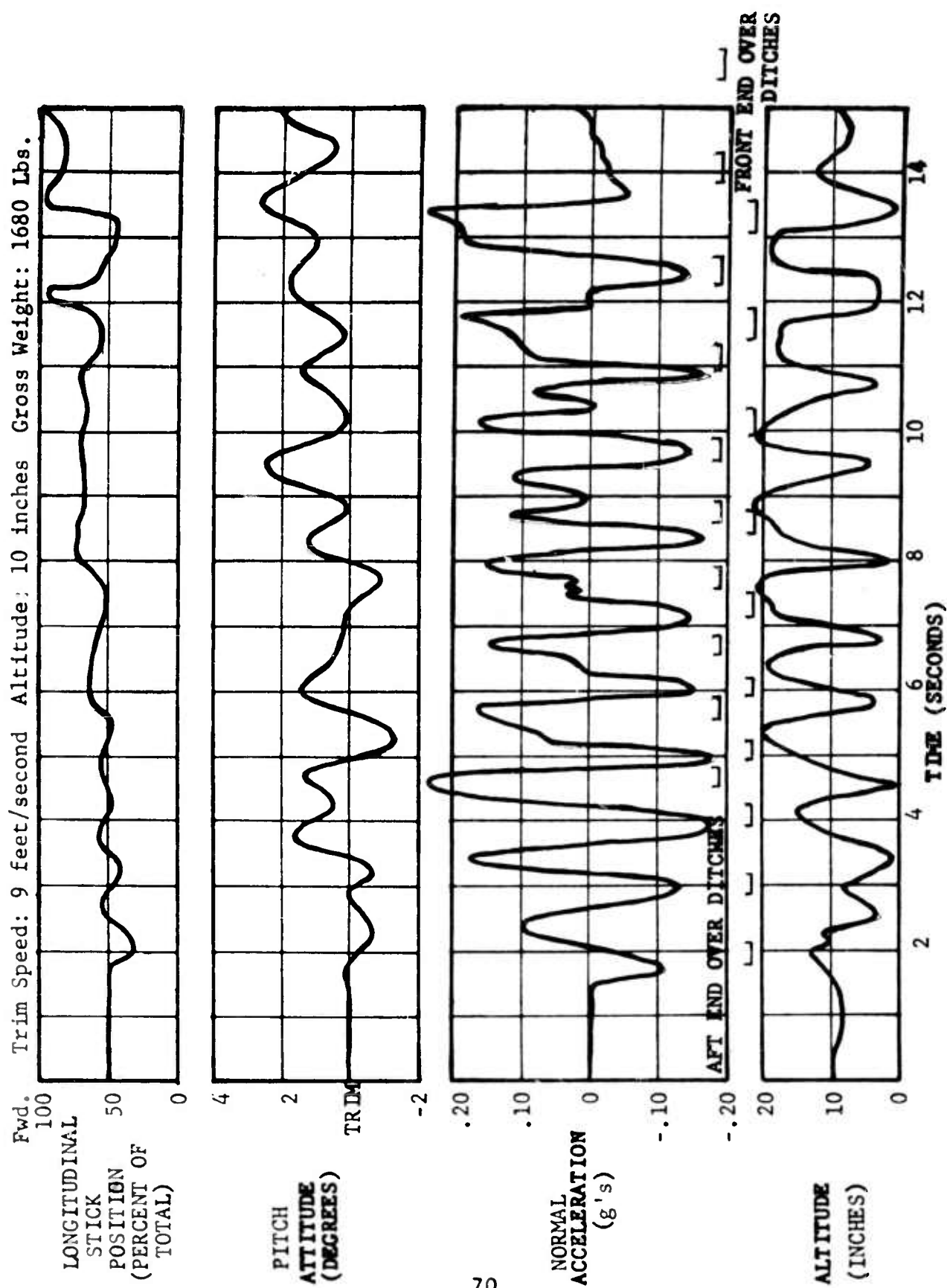


FIGURE 35: LOW SPEED CROSSING OF THE P-GEM OVER A SERIES OF 4-FOOT WIDE X 2-FOOT DEEP DITCHES

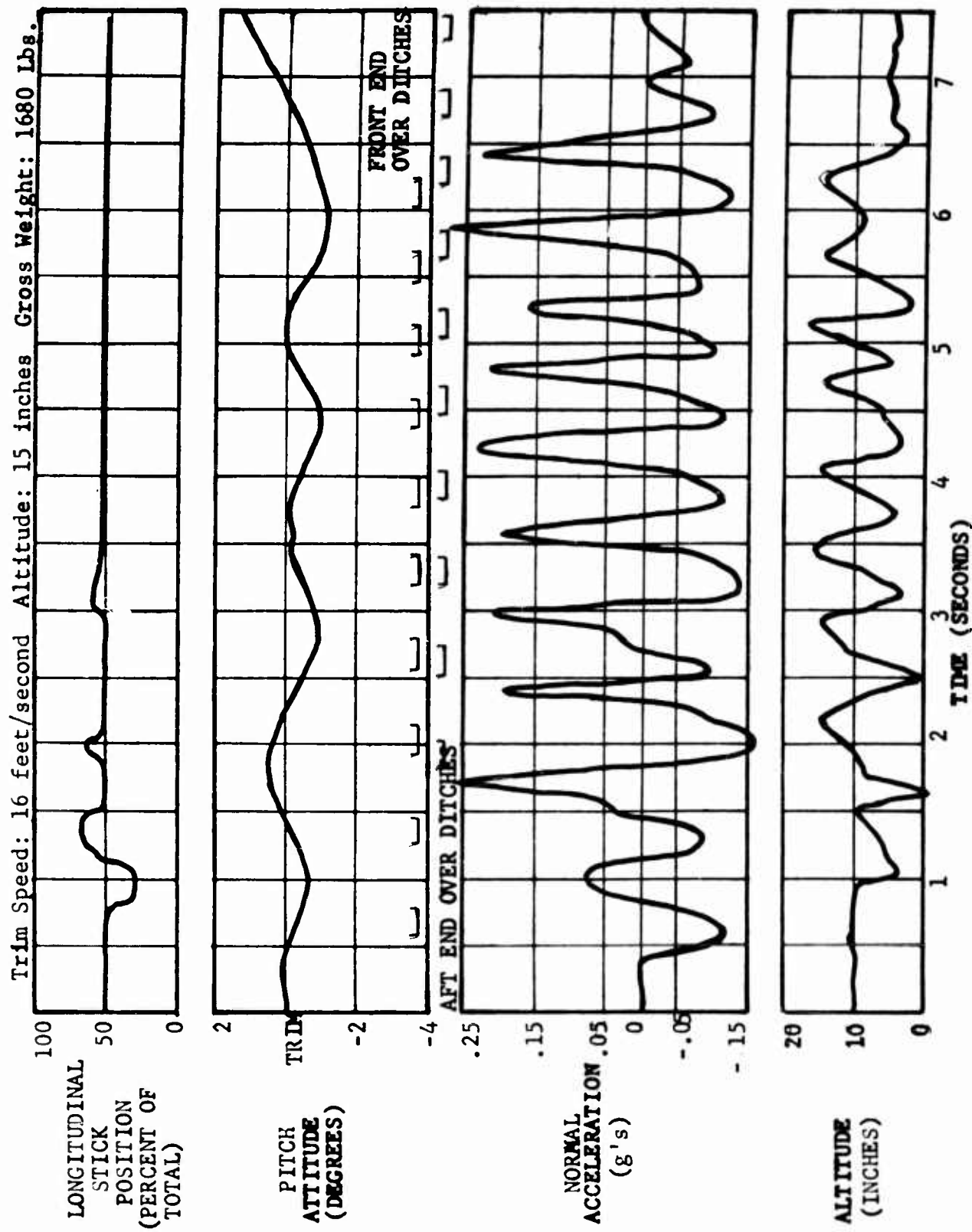


FIGURE 36: MEDIUM SPEED CROSSING OF THE P-GEM OVER A SERIES OF 4-FOOT WIDE X 2-FOOT DEEP DITCHES

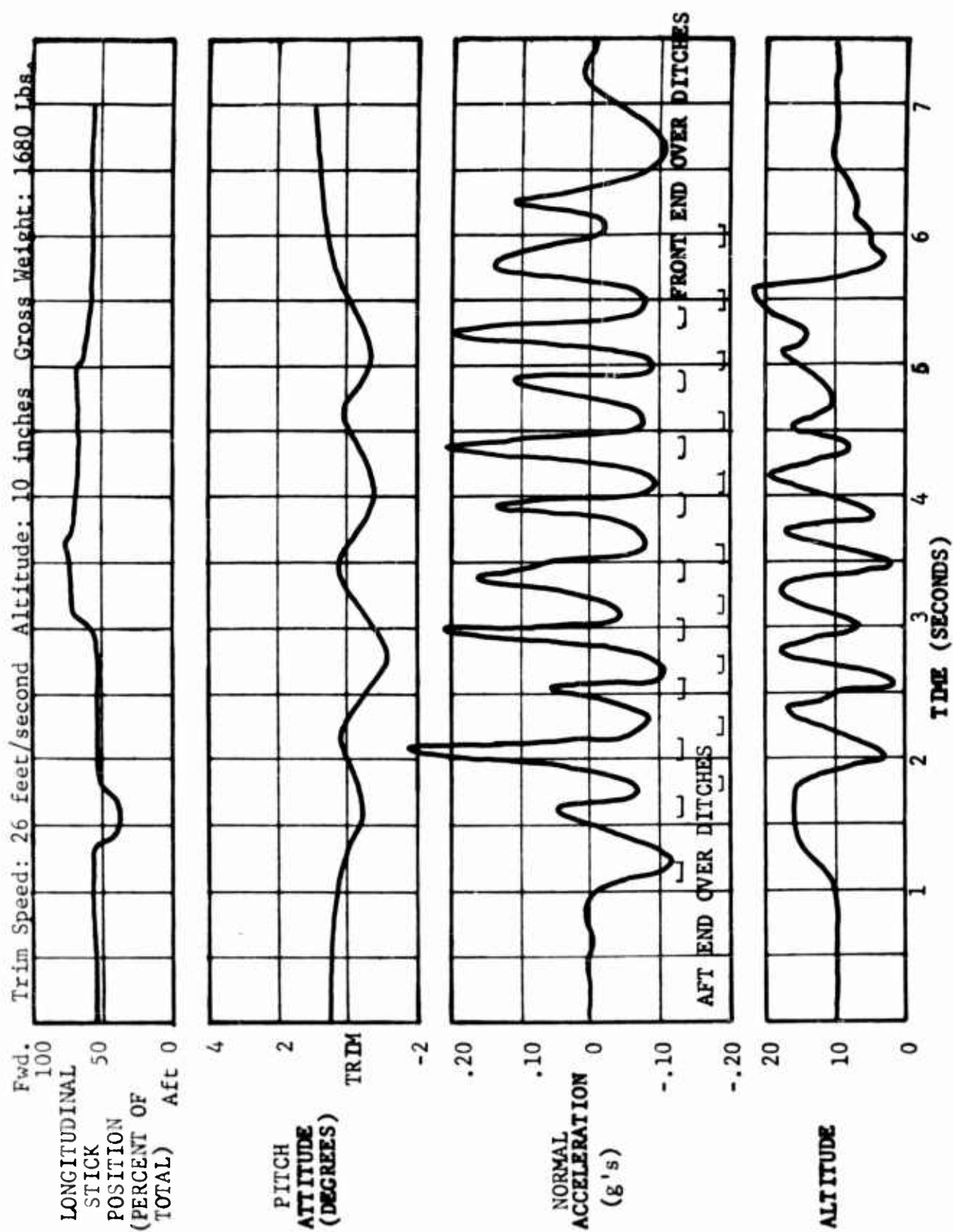


FIGURE 37: HIGH SPEED CROSSING OF THE P-GEM OVER A SERIES OF 4-FOOT WIDE X 2-FOOT DEEP DITCHES

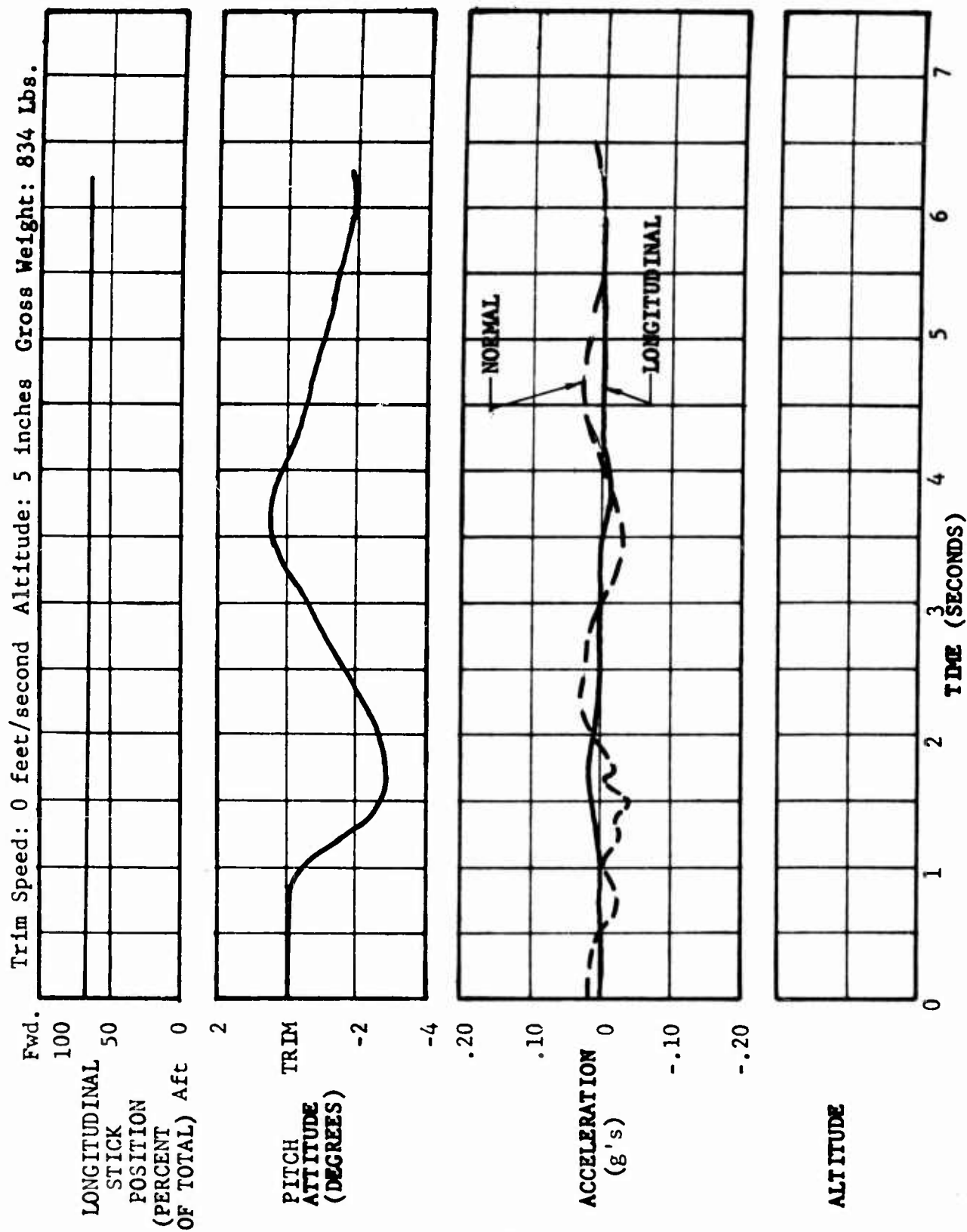


FIGURE 38: "HULA HOOP" RESPONSE TO AN EXTERNAL LONGITUDINAL DISTURBANCE

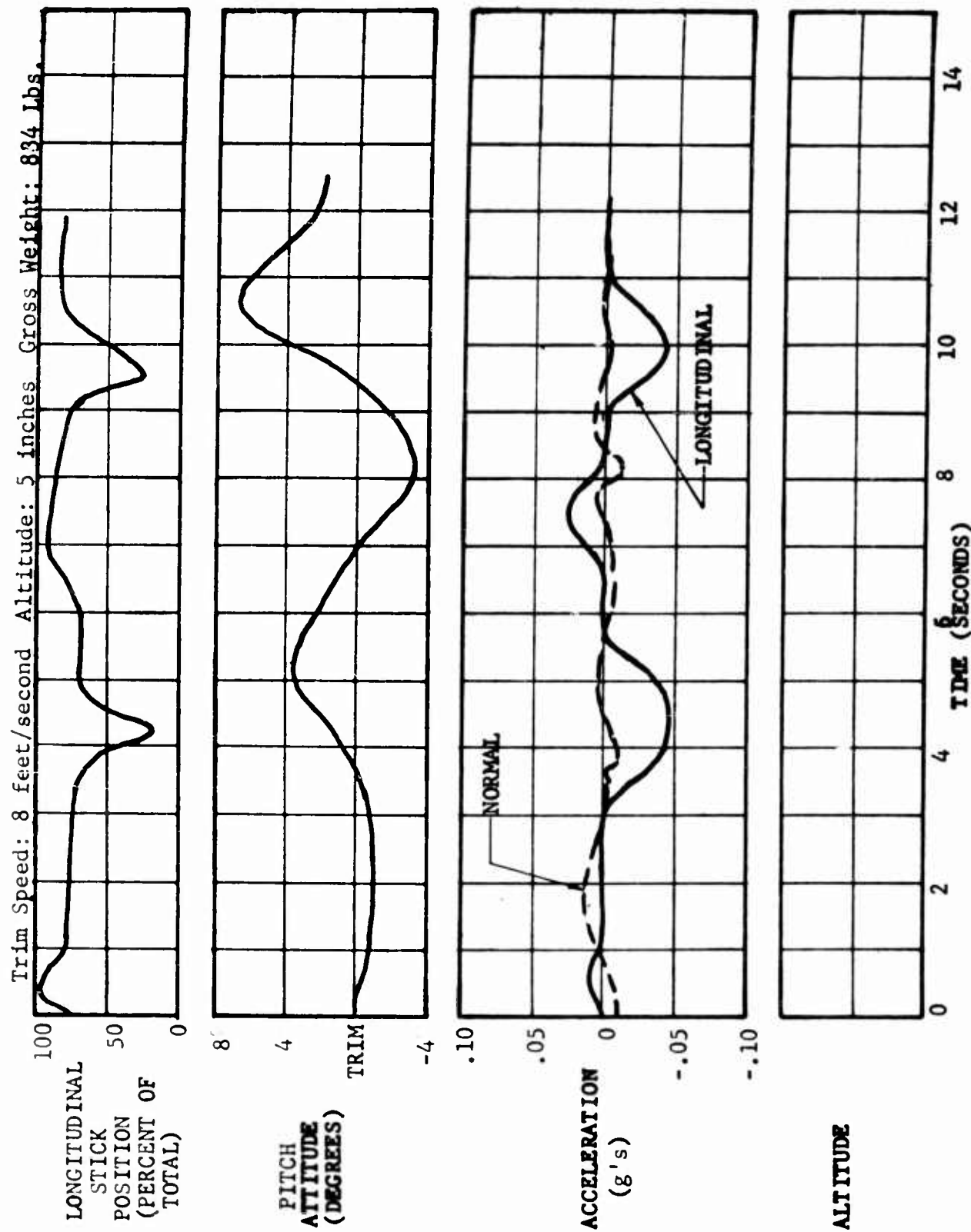


FIGURE 39: 'HULA HOOP' RESPONSE TO LONGITUDINAL CONTROL PULSES AT LOW FORWARD SPEED

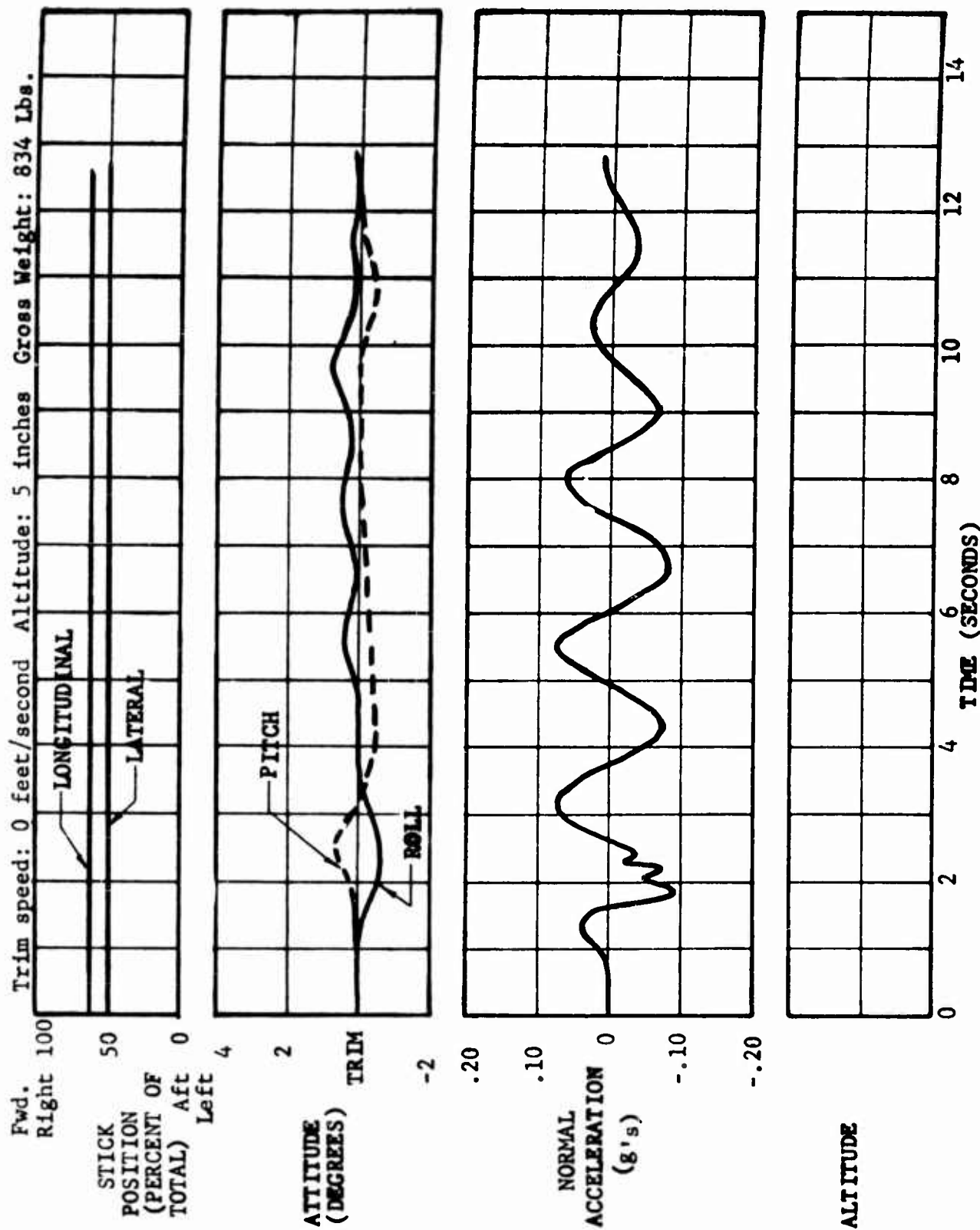


FIGURE 40: "HULA HOOP" RESPONSE TO AN EXTERNAL HEAVE DISTURBANCE

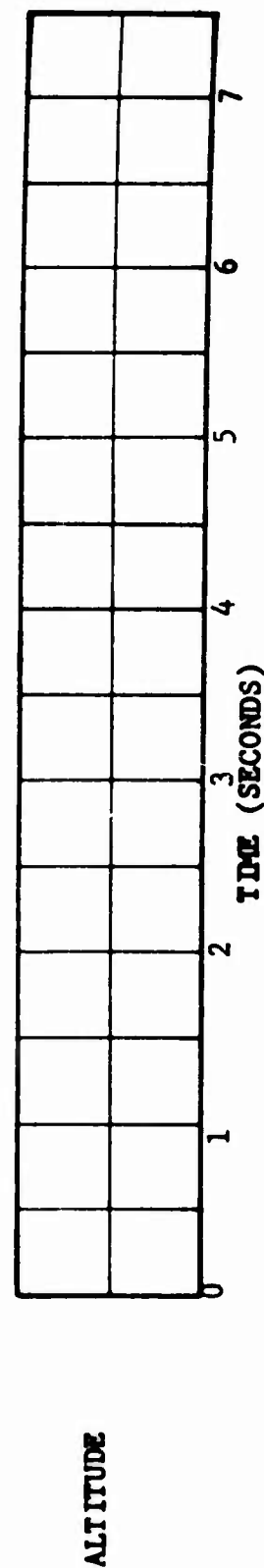
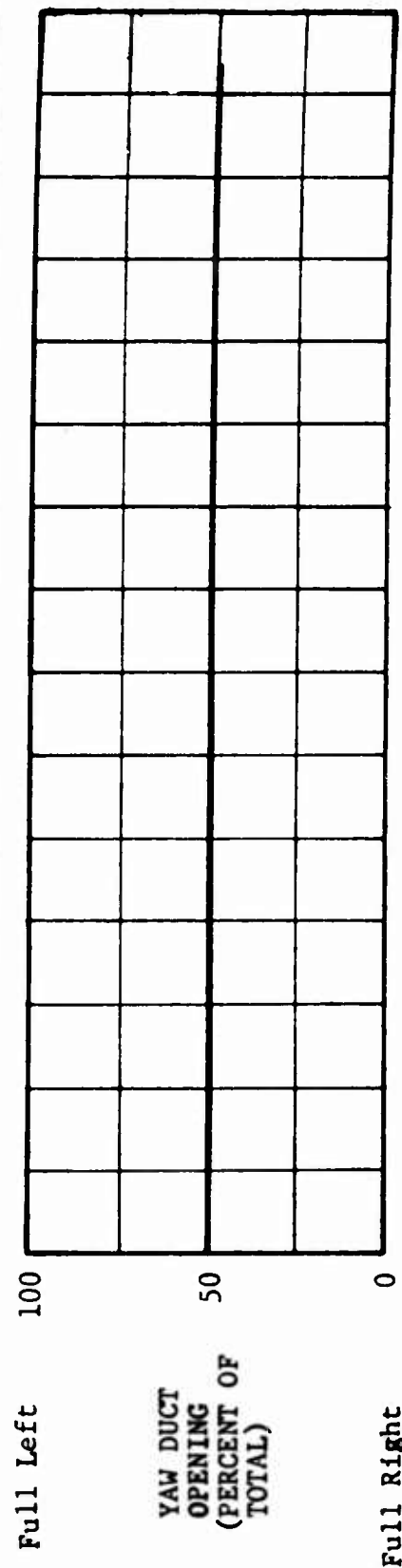
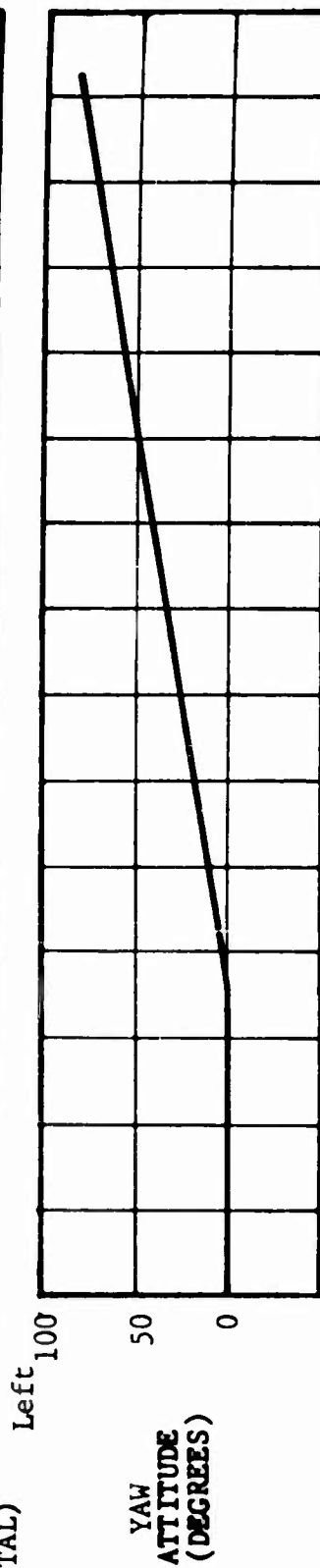
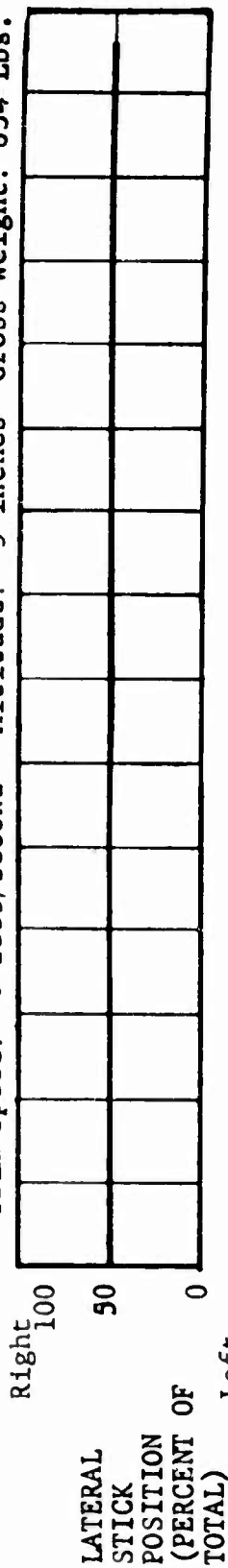


FIGURE 41: "HULA HOOP" RESPONSE TO AN EXTERNAL YAW DISTURBANCE

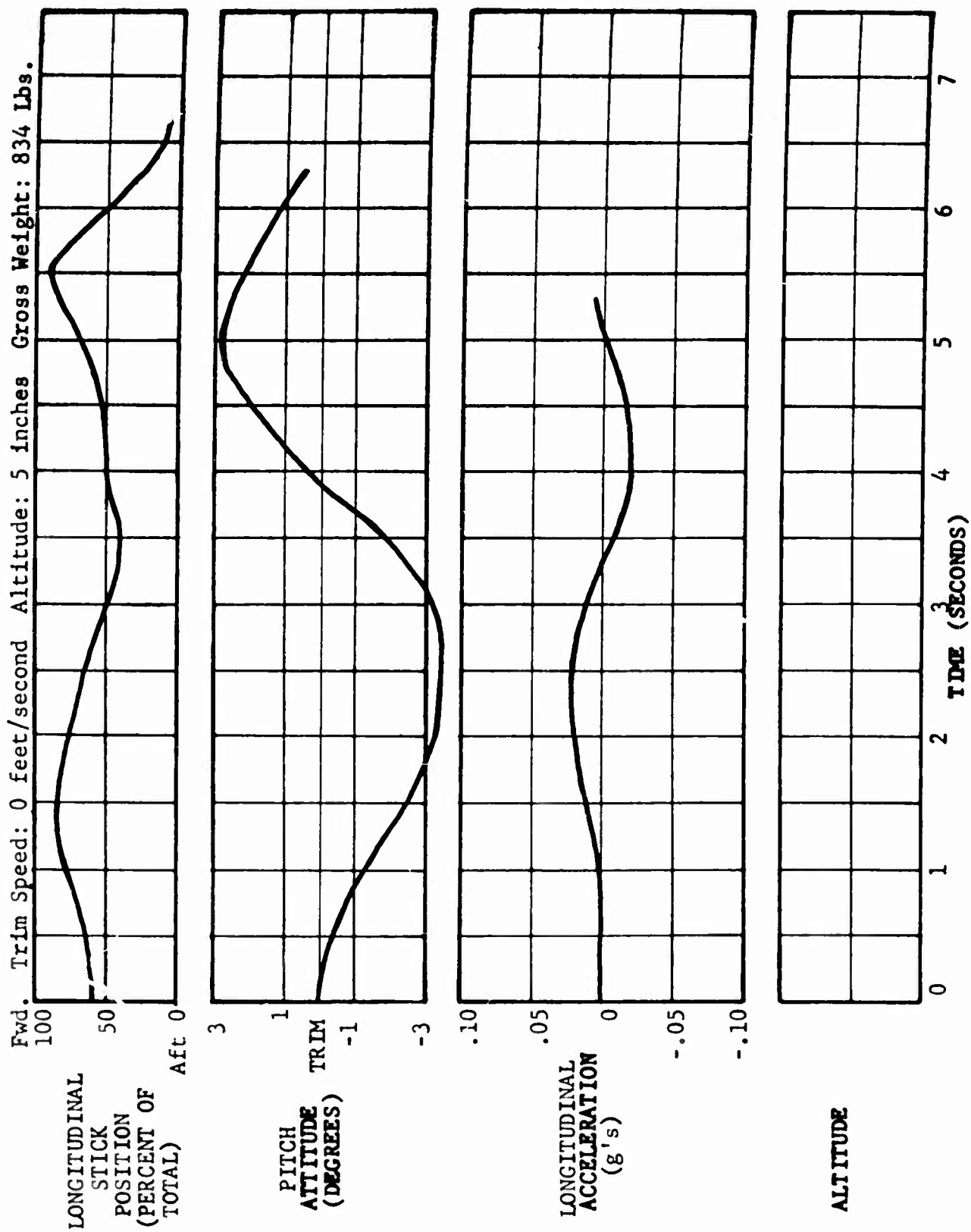


FIGURE 42: "HULA HOOP" RESPONSE TO LONGITUDINAL CONTROL INPUTS

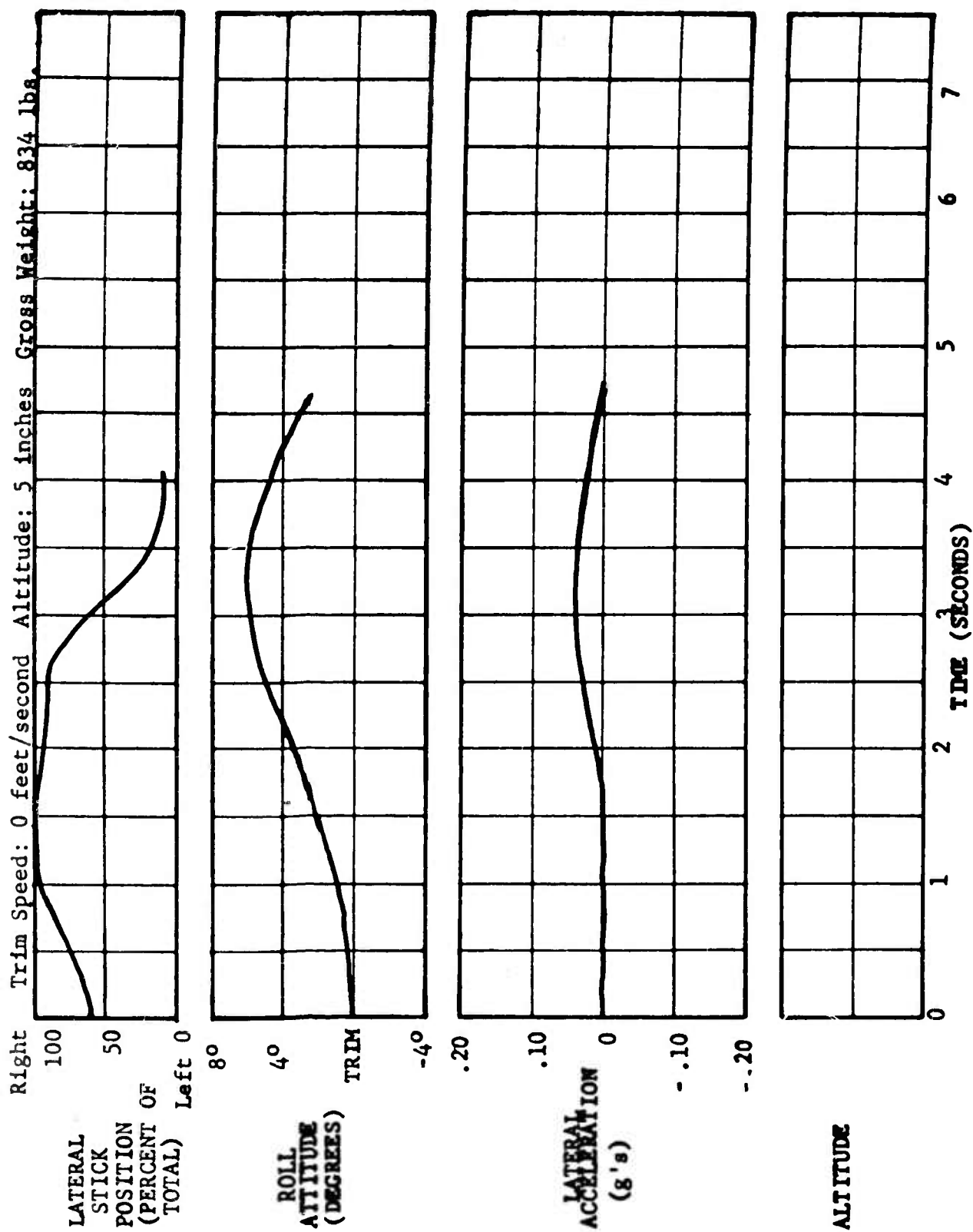


FIGURE 43a: "HULA HOOP" RESPONSE TO LATERAL CONTROL INPUTS

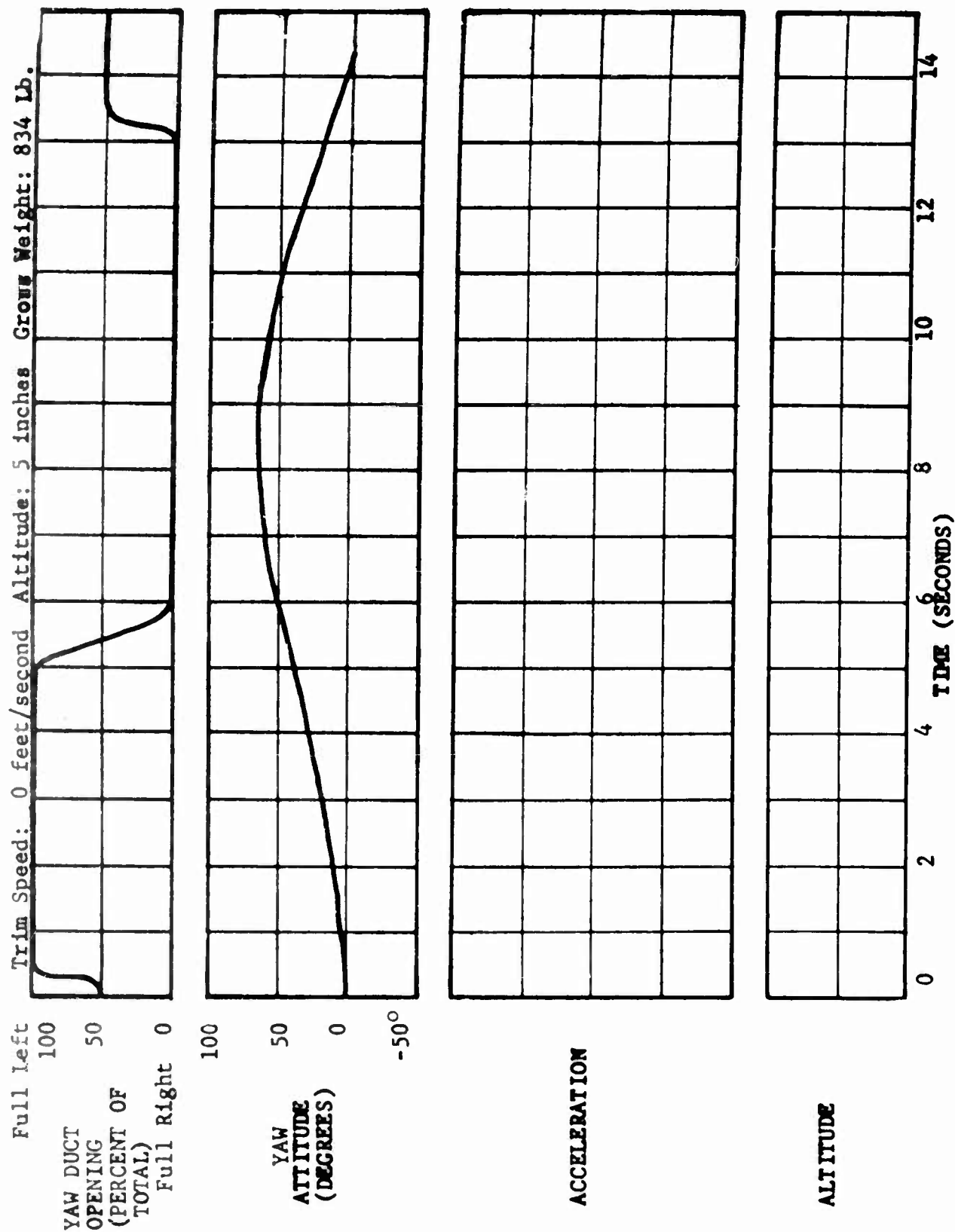


FIGURE 43b: "HULA HOOP" RESPONSE TO A YAW CONTROL INPUT

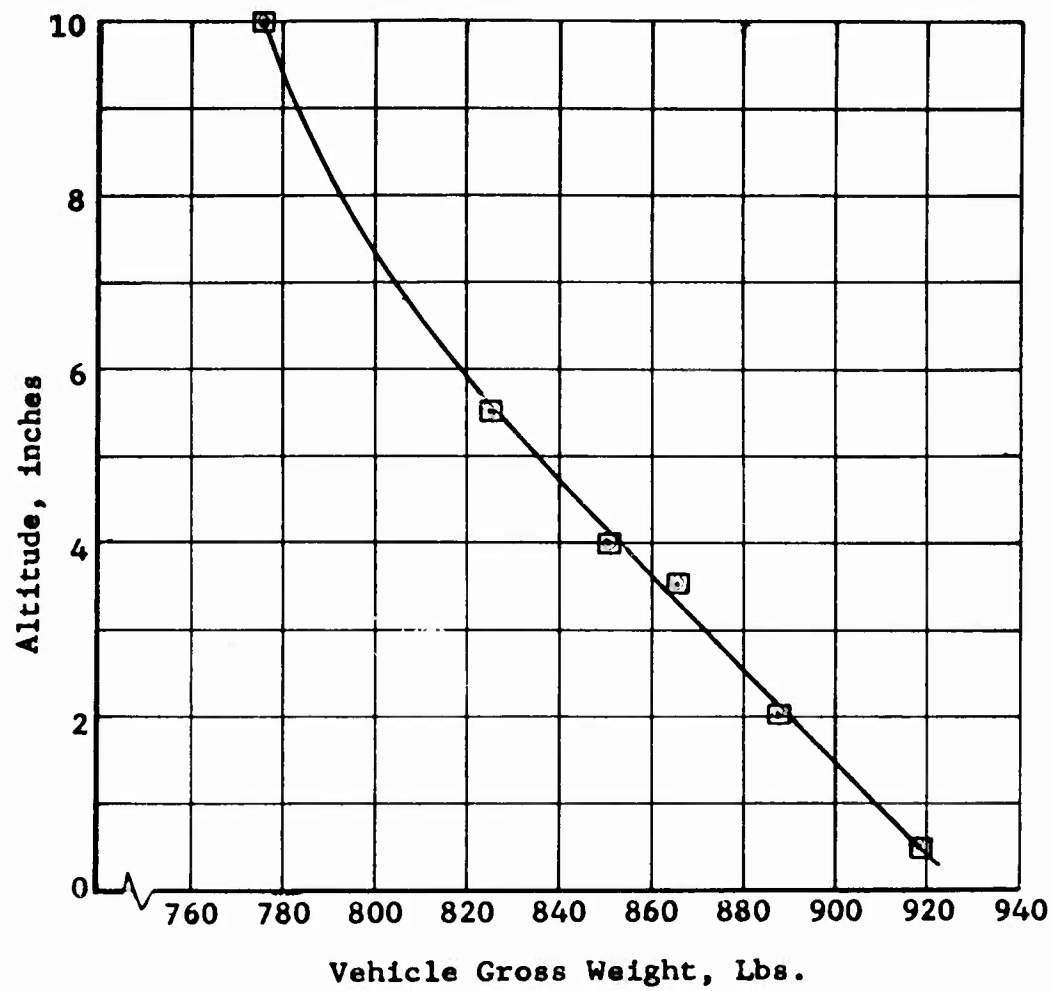


FIGURE 44: EFFECT OF GROSS WEIGHT ON THE HOVERING ALTITUDE OF THE "HULA HOOP" AT 5800 RPM

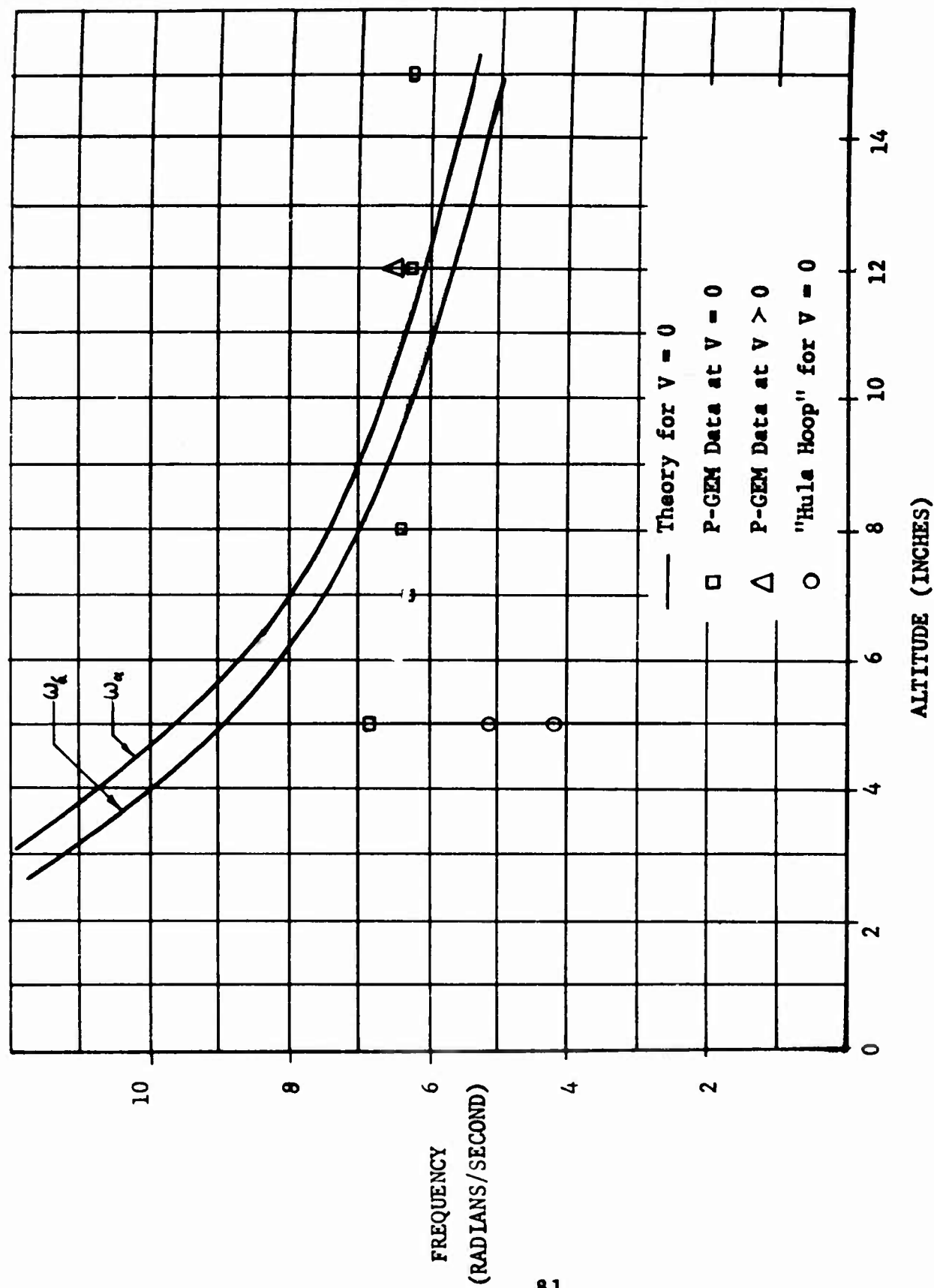


FIGURE 45: COMPARISON OF THEORY WITH TEST DATA OF THE HEAVE FREQUENCY OF THE P-GEM

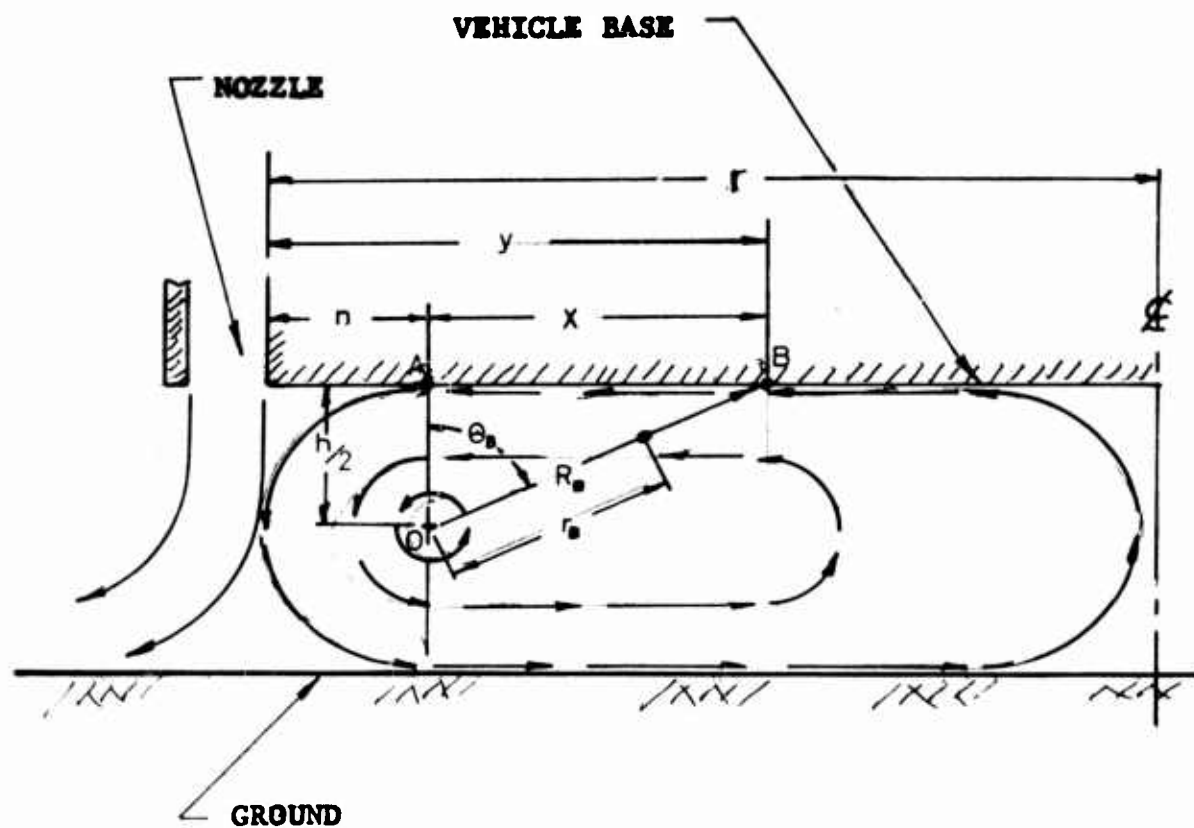


FIGURE 46: THE ROTATIONAL CUSHION FLOW

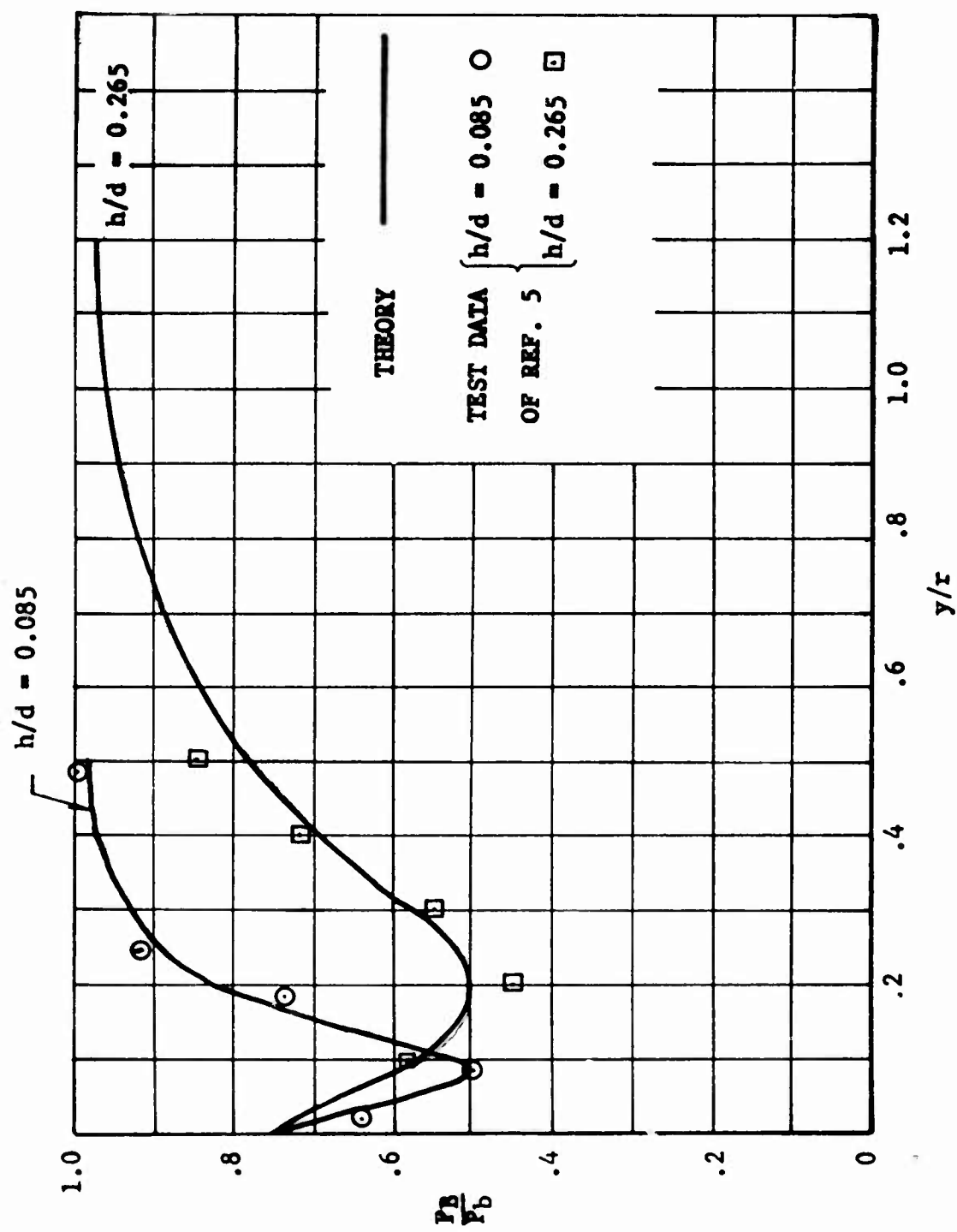
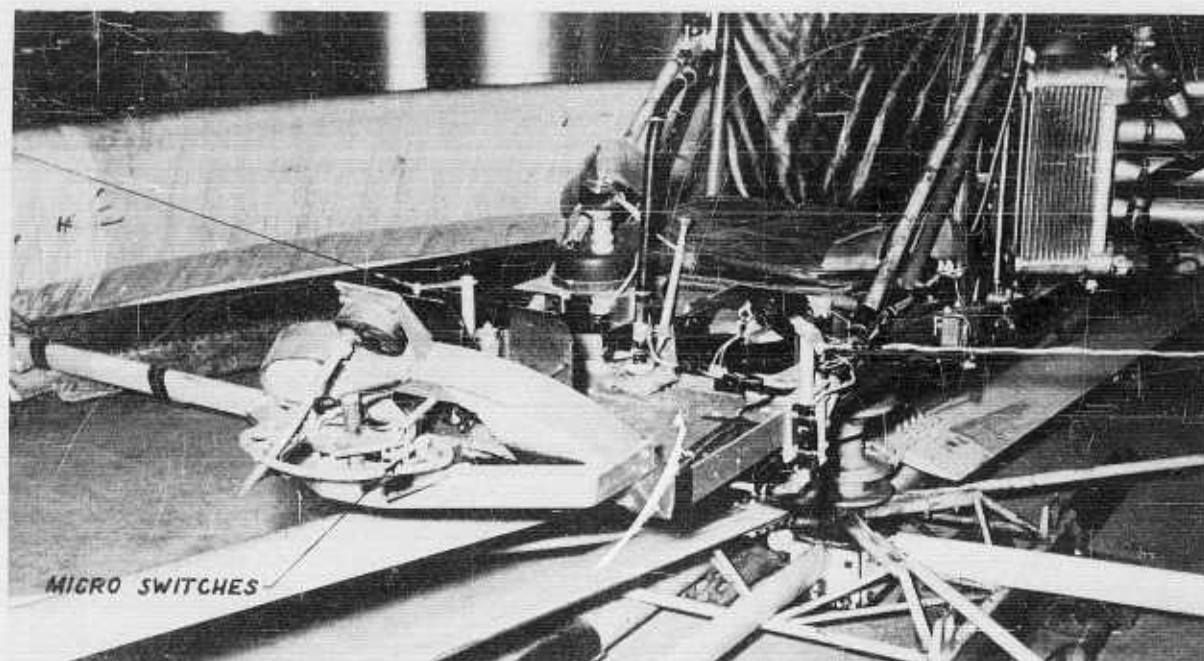
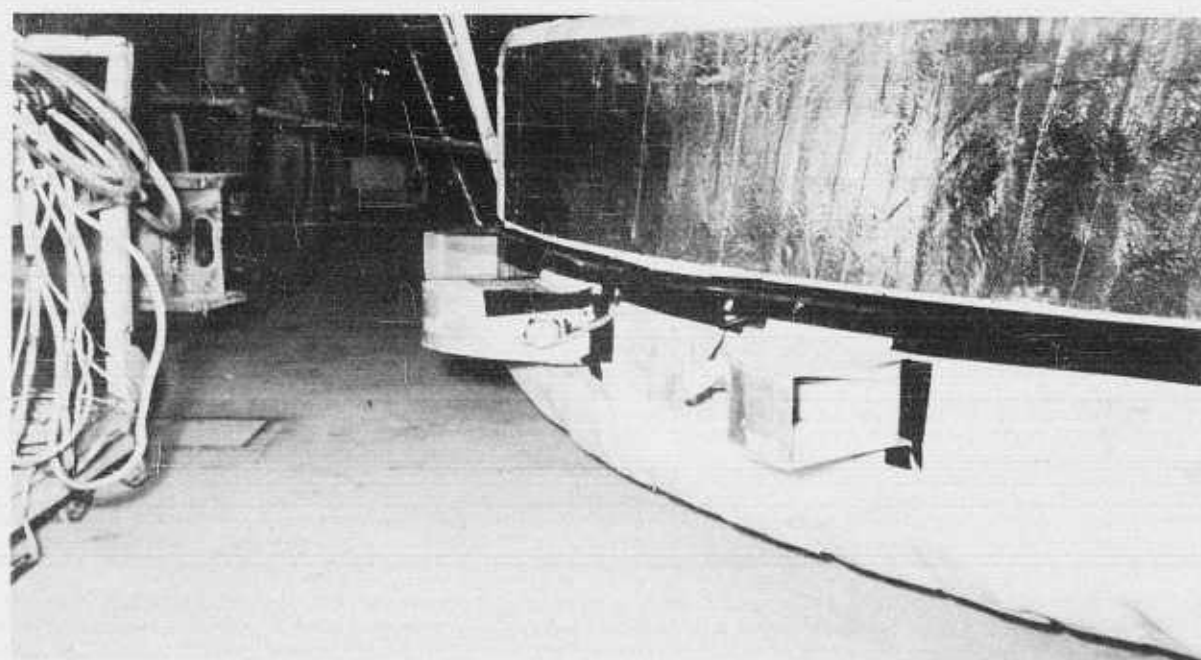


FIGURE 47: VARIATION OF P_B/P_b WITH y/τ



a. INSTALLATION OF MICRO SWITCHES FOR ACTIVATION OF YAW DUCT VANES



b. INSTALLATION OF THE AIR DUCTS

FIGURE 48: YAW CONTROL INSTALLATION

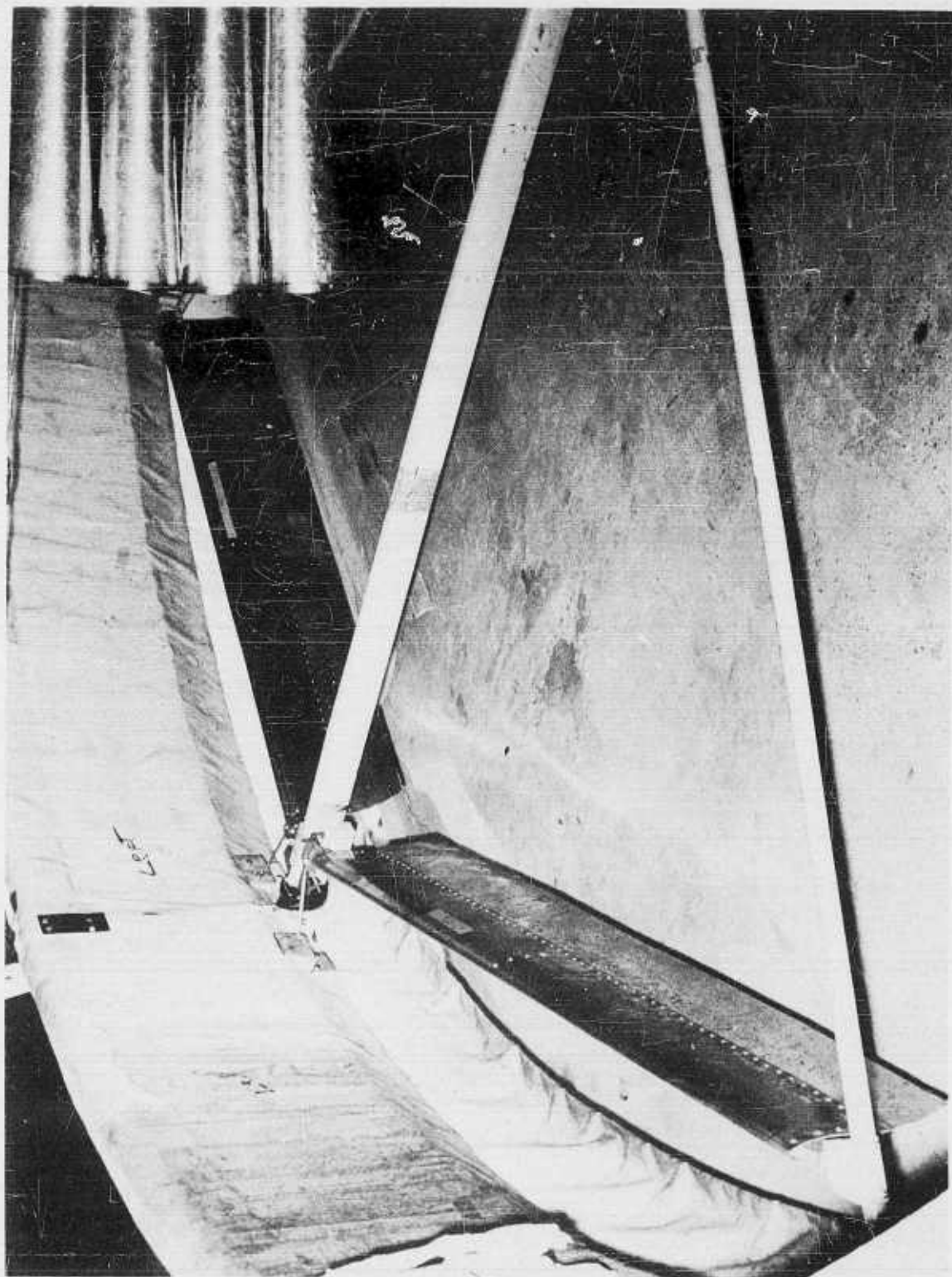


FIGURE 49: "HULA HOOP" ROLL VANE INSTALLATION

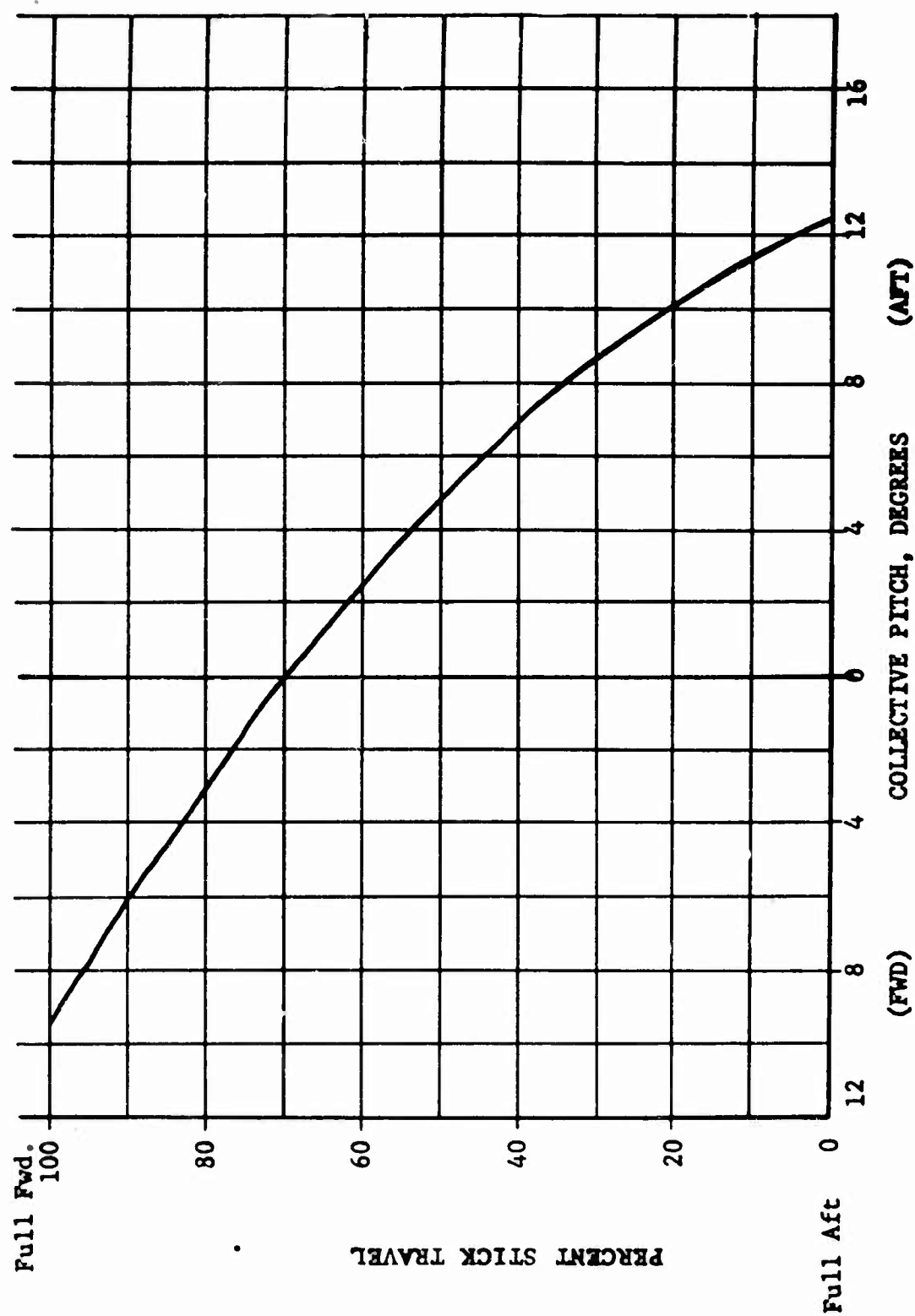


FIGURE 50: PERCENT OF LONGITUDINAL STICK TRAVEL VS. THRUST ROTOR COLLECTIVE PITCH ANGLE, HULA HOOP

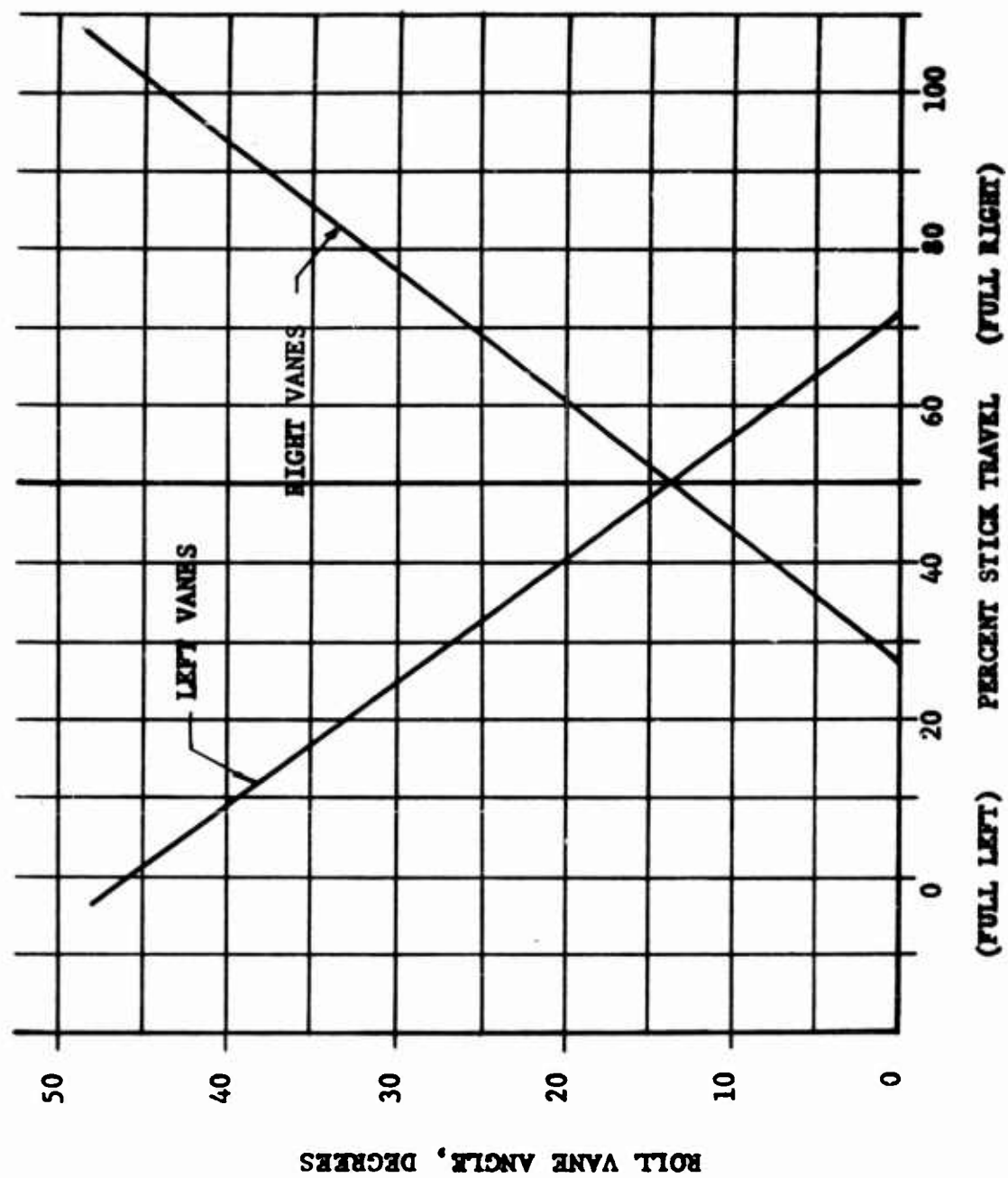


FIGURE 51: PERCENT OF LATERAL STICK TRAVEL VS. ROLL VANE ANGLE, HULA HOOP

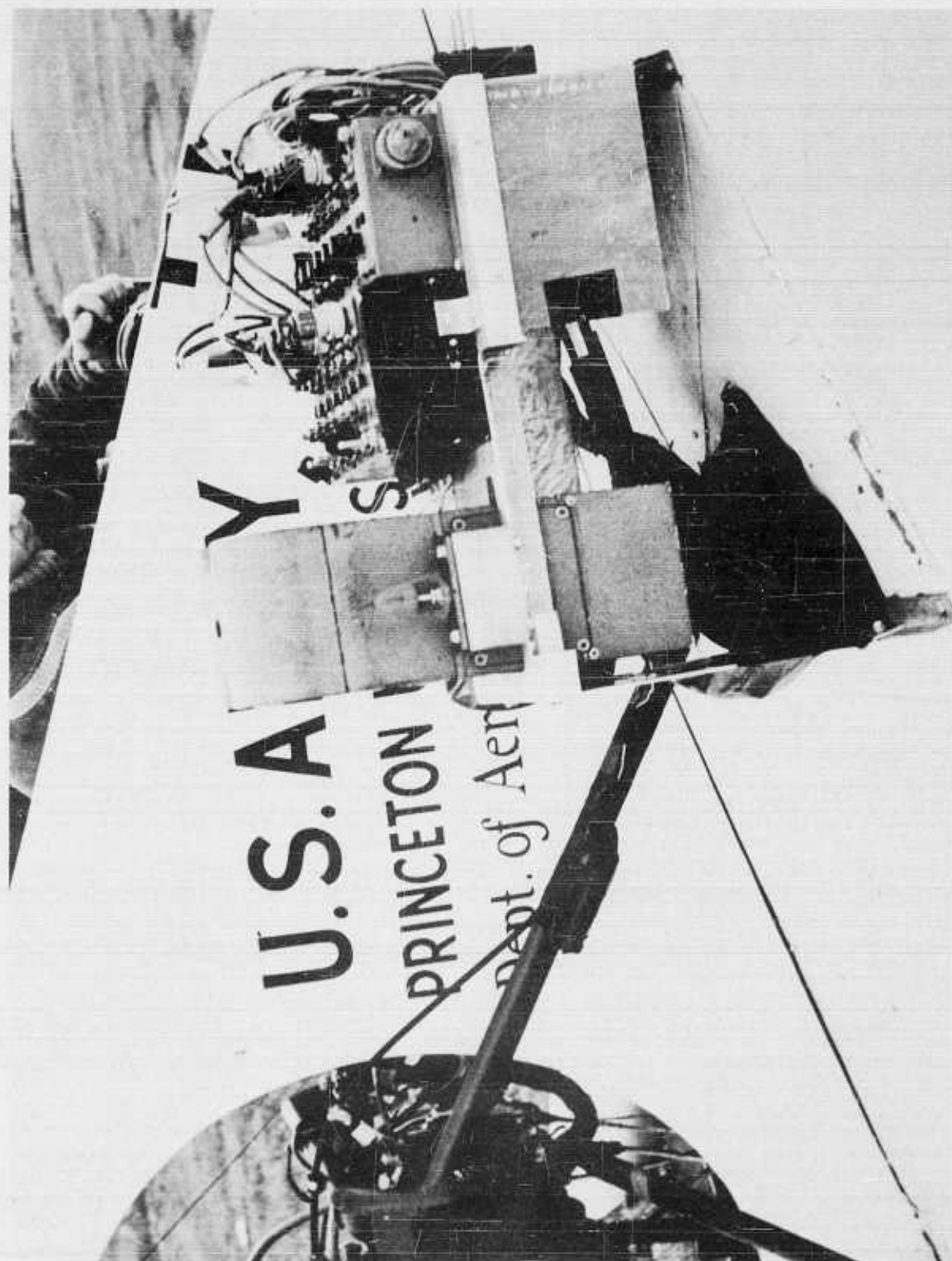


FIGURE 52: OSCILLOGRAPH RECORDER AND BRIDGE BALANCE BOXES INSTALLED ON THE P-GEM

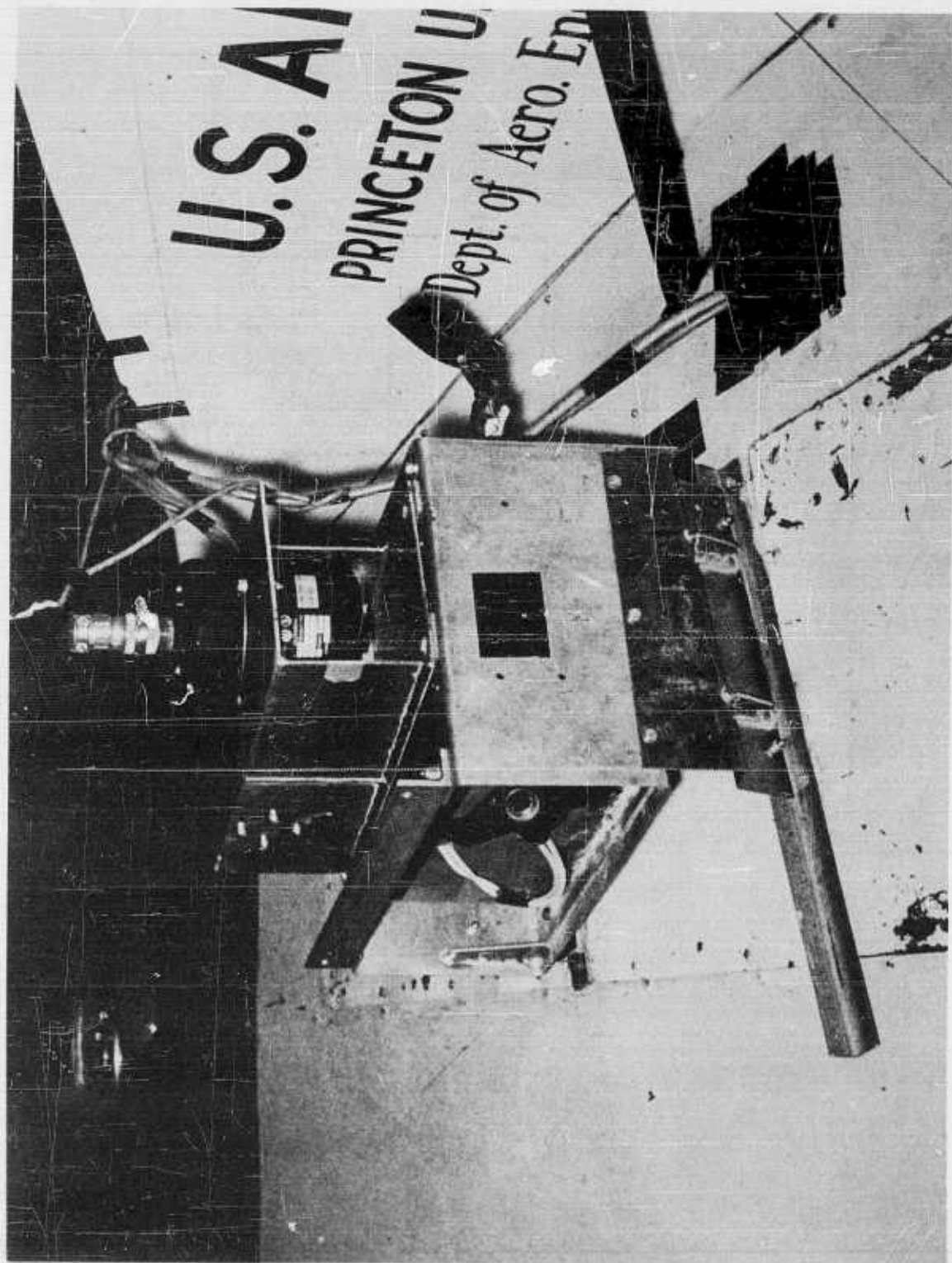
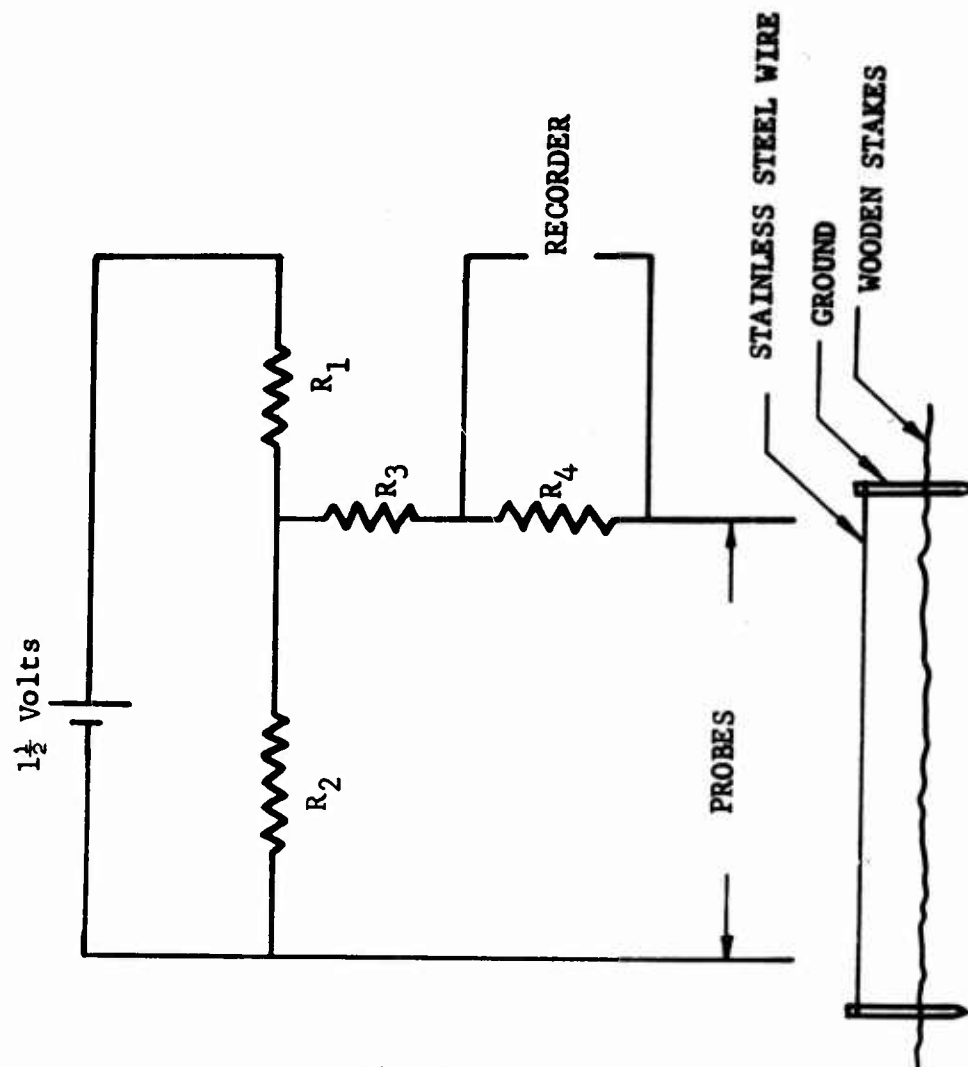


FIGURE 53: VERTICAL AND DIRECTIONAL CYROS INSTALLED ON THE P-GEM



$R_1 = 1000 \text{ ohms}$
 $R_2 = 22 \text{ ohms}$
 $R_3 = 500 \text{ ohms}$
 $R_4 = 33 \text{ ohms}$

FIGURE 54: POSITION INDICATOR WIRING DIAGRAM

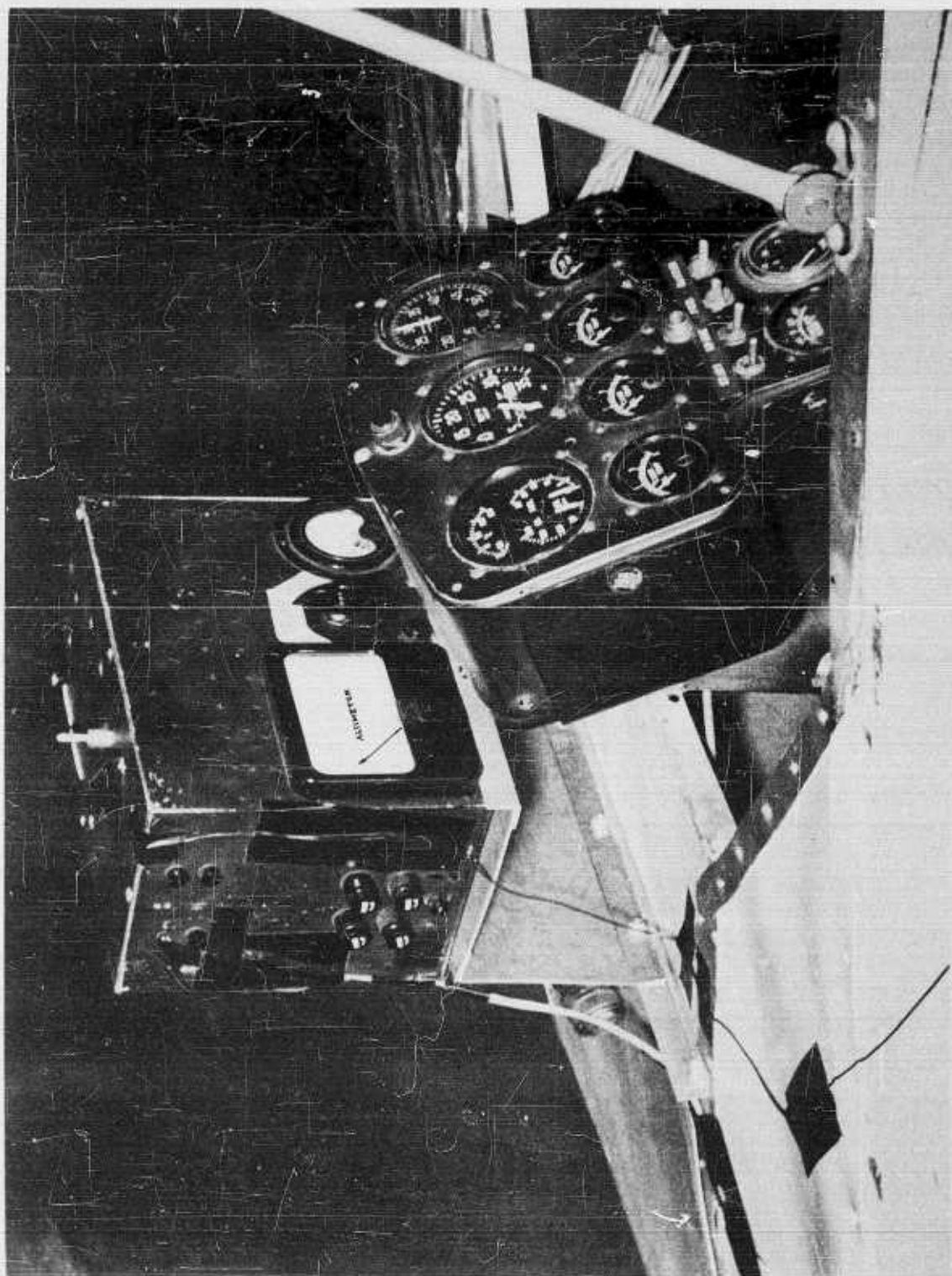


FIGURE 55: INSTALLATION OF CONTROL PANEL ON THE P-GEM

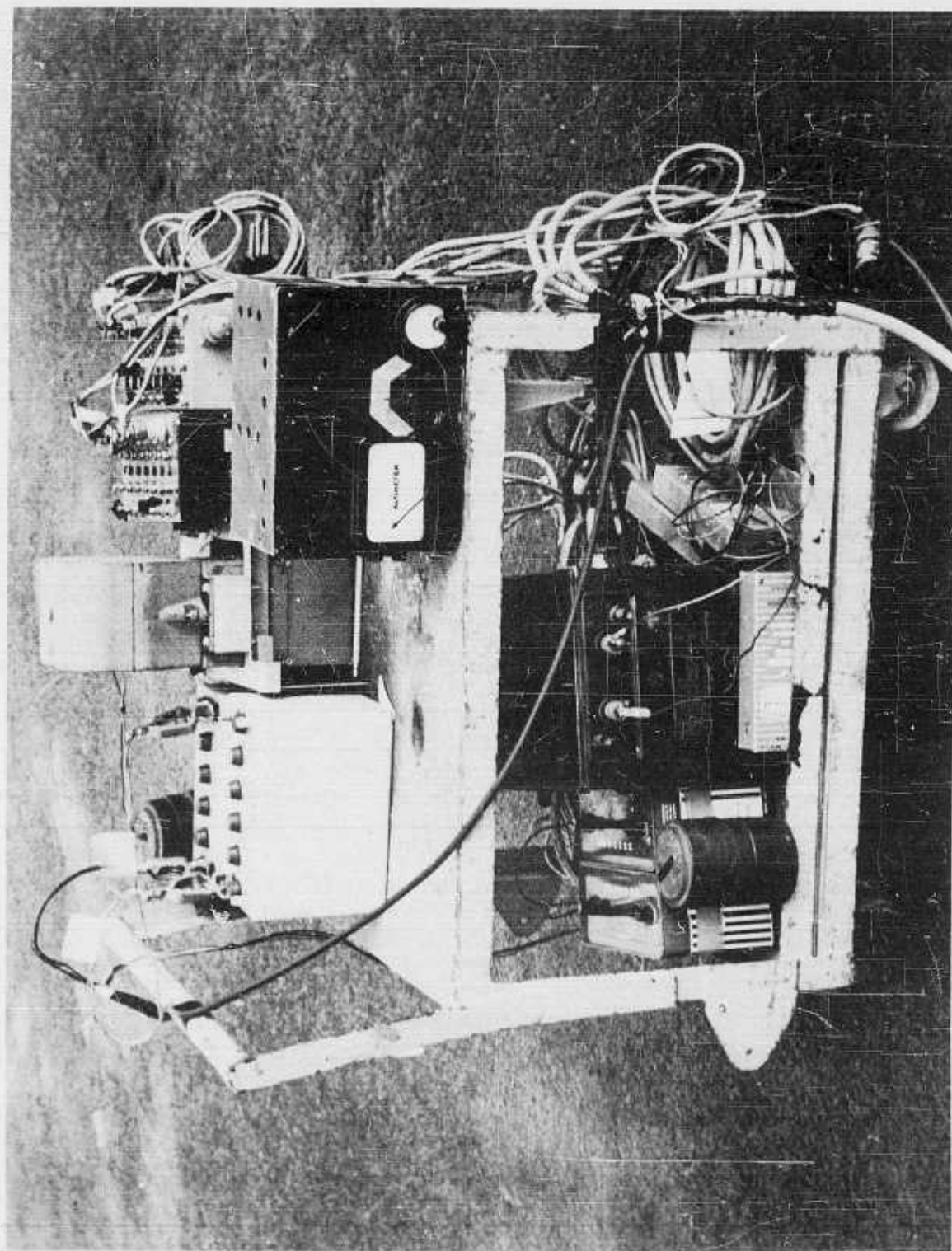


FIGURE 56: INSTRUMENTATION CART UTILIZED IN THE FLIGHT TESTING OF THE "HULA HOOP"

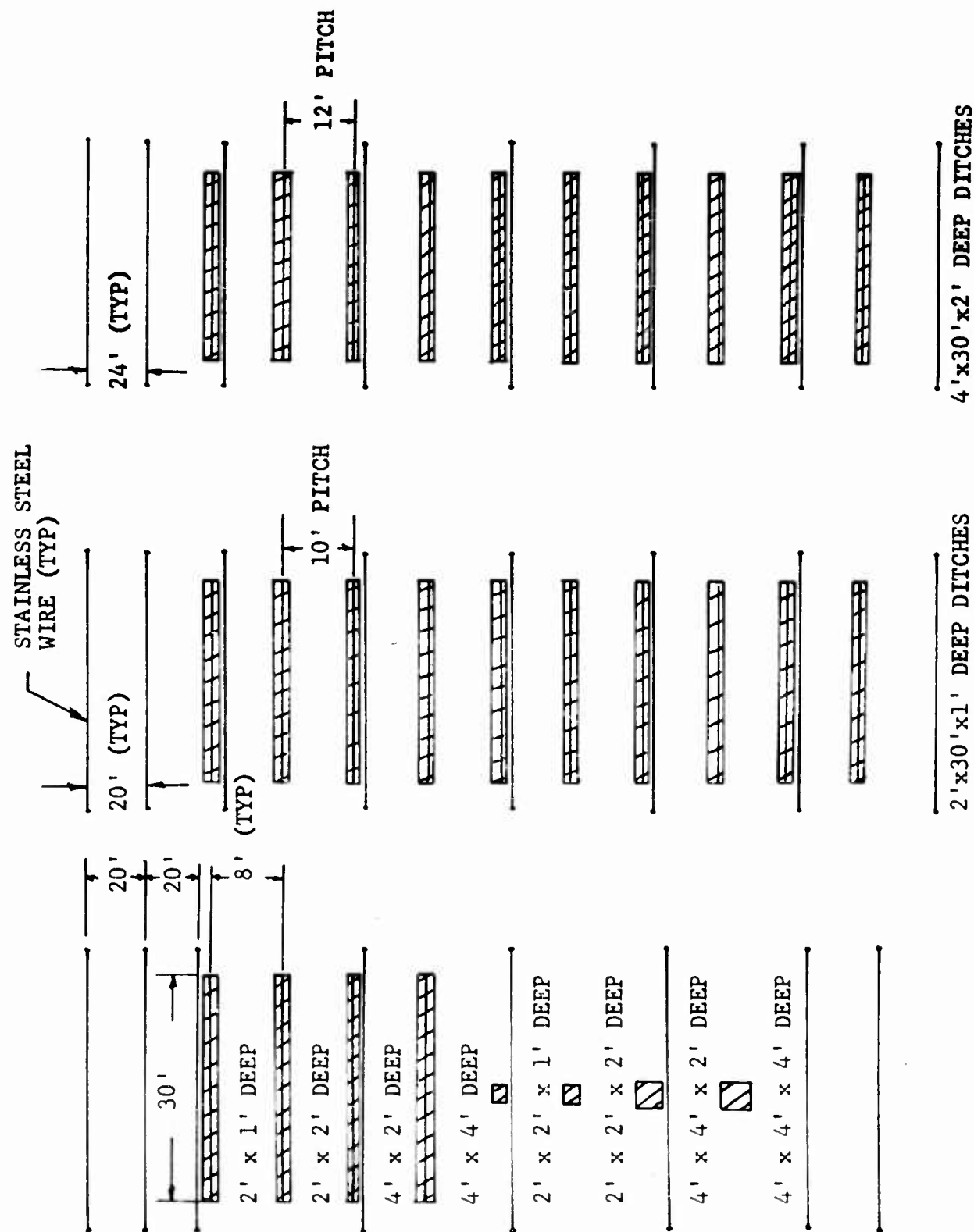


FIGURE 57a: A SCHEMATIC REPRESENTATION OF THE TEST TRACKS UTILIZED IN THE P-GEM TESTS

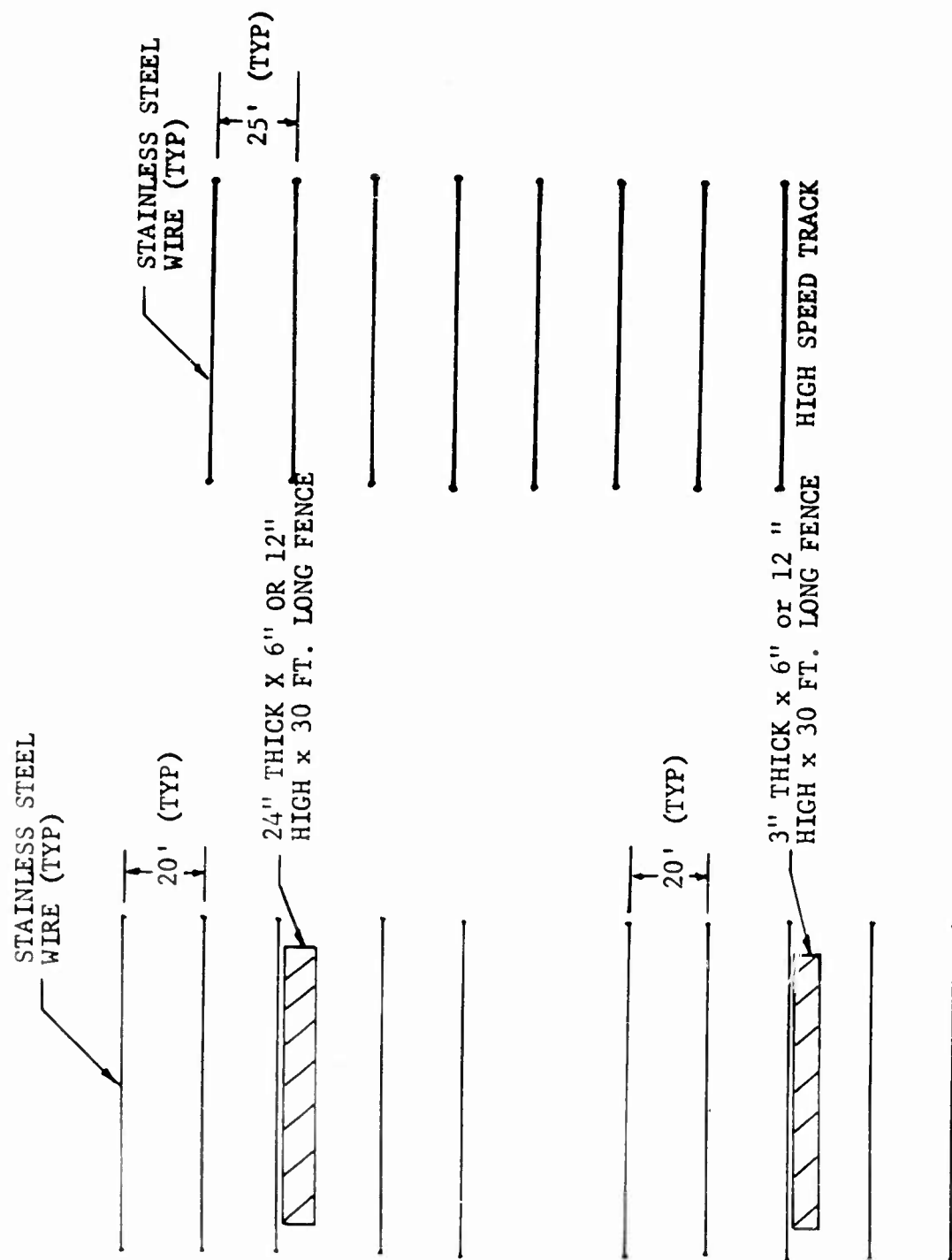
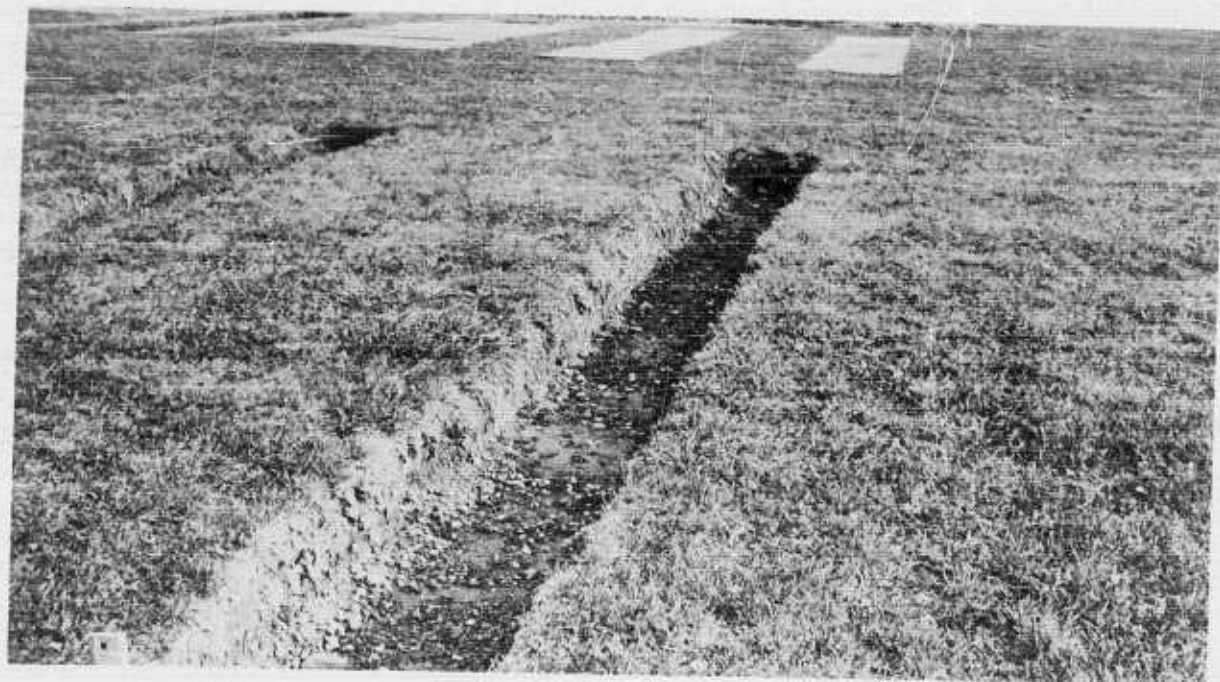
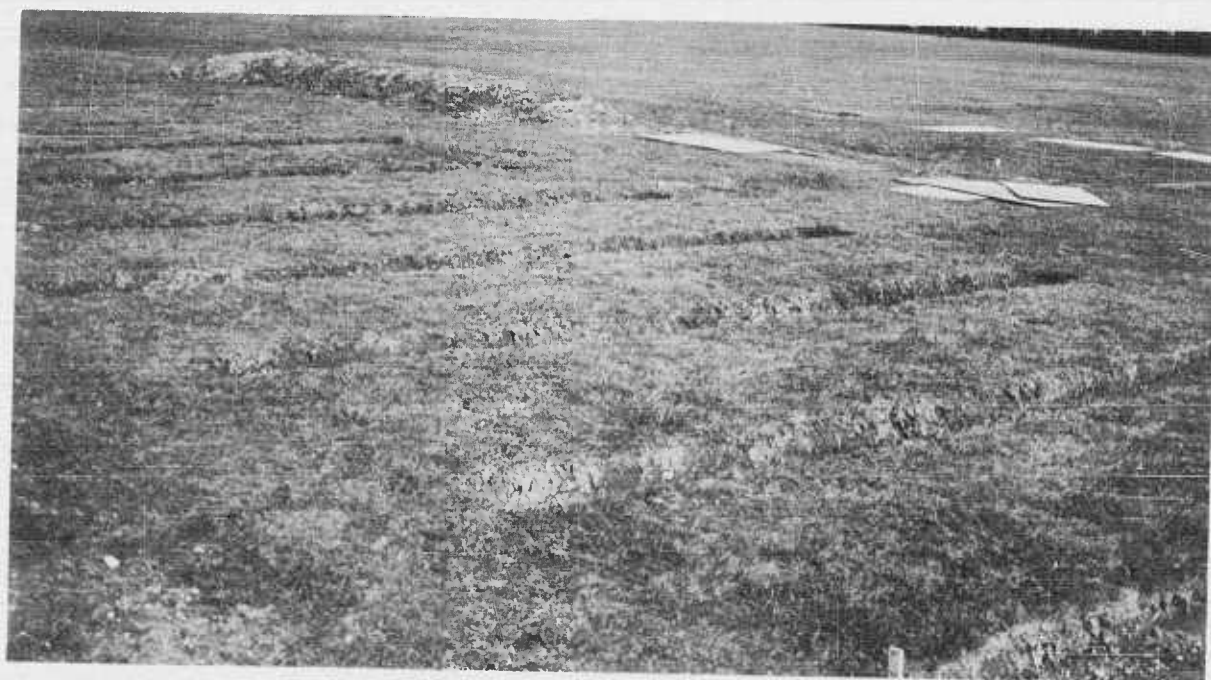


FIGURE 57b: A SCHEMATIC REPRESENTATION OF THE TEST TRACKS UTILIZED IN THE P-GEM TESTS



a. ONE OF A SERIES



b. OVERALL OF SERIES

FIGURE 58: SERIES OF 10 DITCHES 8 FEET APART, 2 FEET WIDE,
1 FOOT DEEP AND 30 FEET LONG



a. ONE OF A SERIES



b. OVERALL OF SERIES

FIGURE 59: SERIES OF 10 DITCHES 10 FEET APART, 4 FEET WIDE,
2 FEET DEEP AND 30 FEET LONG

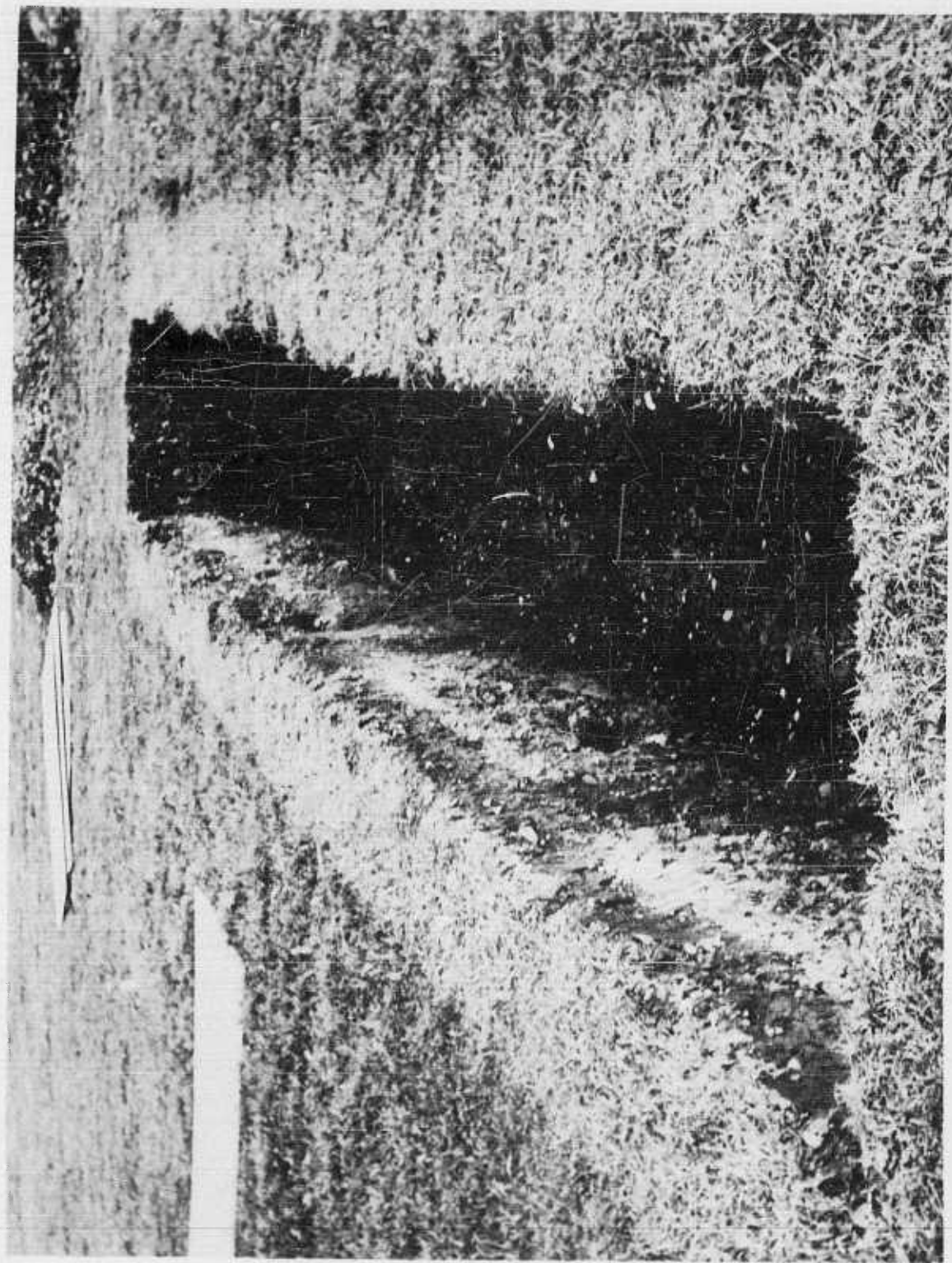


FIGURE 60: INDIVIDUAL DITCH 4 FEET WIDE, 4 FEET DEEP AND 30 FEET LONG

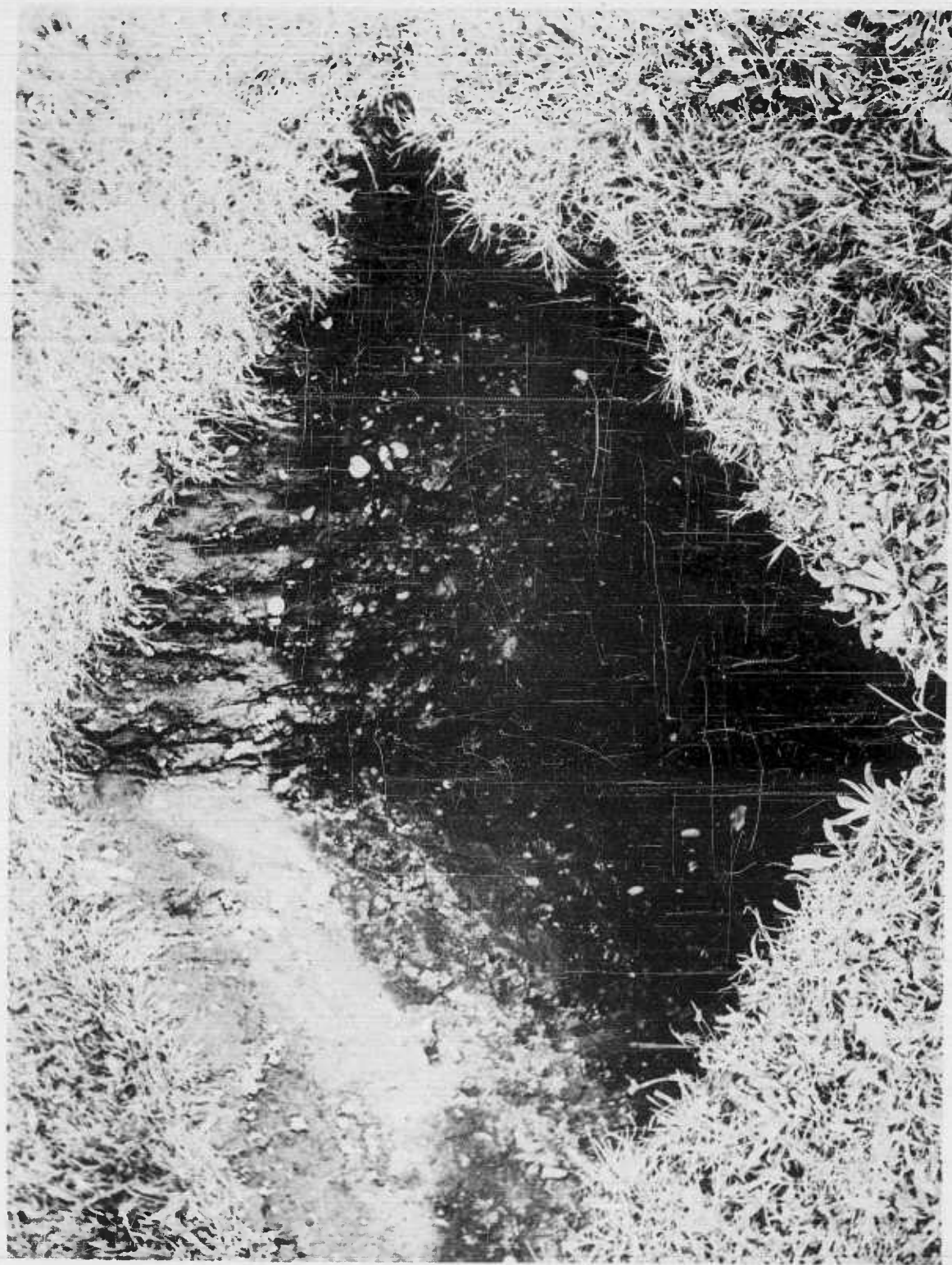


FIGURE 61: INDIVIDUAL HOLE, 4 FEET BY 4 FEET BY 4 FEET DEEP

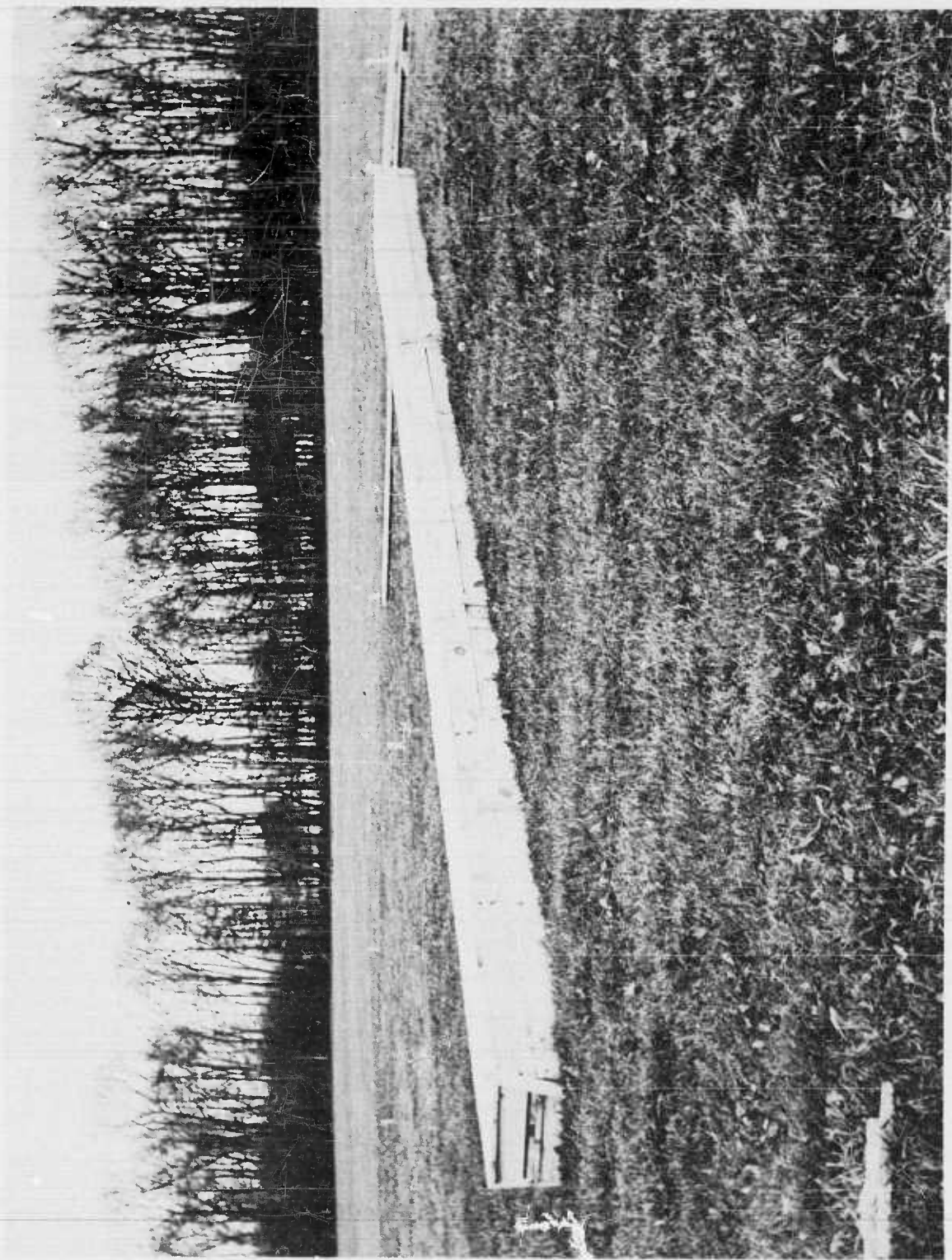


FIGURE 62: WOODEN FENCE, 12 INCHES HIGH, 24 INCHES THICK AND 30 FEET LONG



a. VIEW ALONG FURROWS



b. VIEW ACROSS FURROWS

FIGURE 63: PLOWED FIELD, .75 FOOT DEEP X 1.5 FEET SPACING
NEGOTIATED BY THE P-GEM

DISTRIBUTION

Army War College	(1)
USA Aviation School	(1)
The Research Analysis Corporation	(1)
ARO, OCRD	(2)
ARO, Durham	(1)
USA QM Research and Engineering Command	(1)
Chief of Transportation, DA	(2)
USA Transportation Combat Development Group	(1)
USA Transportation Board	(1)
USA Transportation Materiel Command	(18)
USA Transportation School	(1)
USA Transportation Research Command	(100)
USATRECOM Liaison Officer, USA Engineer Waterways Experiment Station	(1)
USATRECOM Liaison Officer, USA R&D Liaison Group (9851 DU)	(1)
TC Liaison Officer, USAERDL	(1)
USATRECOM Liaison Officer, Detroit Arsenal	(1)
USAERDL	(1)
Ordnance Tank Automotive Command	(2)
Aeronautical Research Laboratories	(1)
USA TC Liaison Officer, Airborne and Electronics Board	(1)
HQ AFSC (SCS-3)	(1)
Bureau of Ships	(1)
Naval Supply Depot	(1)
Chief of Naval Operations	(3)
Chief of Naval Research	(3)
Bureau of Naval Weapons	(6)
Asst. Chief for Research & Development (OW), Navy	(1)
US Naval Postgraduate School	(1)
David Taylor Model Basin	(2)
Hq, US Marine Corps	(1)
Marine Corps Schools	(3)
NASA, Washington, D. C.	(6)
George C. Marshall Space Flight Center, NASA	(4)
Langley Research Center, NASA	(3)
Ames Research Center, NASA	(1)
Lewis Research Center, NASA	(1)
US Government Printing Office	(1)

Library of Congress	(1)
US Army Standardization Group, U. K.	(1)
US Army Standardization Group, Canada	(1)
Canadian Army Liaison Officer, USA Transportation School	(3)
British Joint Services Mission (Army Staff)	(3)
Armed Services Technical Information Agency	(10)
Maritime Administration	(1)
OSD, Director of Defense Research and Engineering	(1)
Kellett Aircraft Corporation	(10)

Kellet Aircraft Corporation,
Willow Grove, Pa.

AN EXPERIMENTAL INVESTIGATION OF THE
RESPONSE CHARACTERISTICS OF TWO
MAN-CARRYING GROUND EFFECT MACHINES,
by A. A. Perlmutter and M. M. George
Report No. 212X90-2; TCREC Technical
Report 62-28, May 1962, 102p. incl.
illus, tables, Contract DA 44-177-
TC-733 Unclassified Report

An experimental investigation was
performed of the dynamic response
characteristics of the Princeton

(over)

1. Air Cushion
Vehicles

2. Contract
DA 44-177-TC-
733

Kellet Aircraft Corporation,
Willow Grove, Pa.

AN EXPERIMENTAL INVESTIGATION OF THE
RESPONSE CHARACTERISTICS OF TWO
MAN-CARRYING GROUND EFFECT MACHINES,
by A. A. Perlmutter and M. M. George
Report No. 212X90-2; TCREC Technical
Report 62-28, May 1962, 102p. incl.
illus, tables, Contract DA 44-177-
TC-733 Unclassified Report

An experimental investigation was
performed of the dynamic response
characteristics of the Princeton

(over)

1. Air Cushion
Vehicles

2. Contract
DA 44-177-TC-
733

Kellet Aircraft Corporation,
Willow Grove, Pa.

AN EXPERIMENTAL INVESTIGATION OF THE
RESPONSE CHARACTERISTICS OF TWO
MAN-CARRYING GROUND EFFECT MACHINES,
by A. A. Perlmutter and M. M. George
Report No. 212X90-2; TCREC Technical
Report 62-28, May 1962, 102p. incl.
illus, tables, Contract DA 44-177-
TC-733 Unclassified Report

An experimental investigation was
performed of the dynamic response
characteristics of the Princeton

(over)

1. Air Cushion
Vehicles

2. Contract
DA 44-177-TC-
733

Kellet Aircraft Corporation,
Willow Grove, Pa.

AN EXPERIMENTAL INVESTIGATION OF THE
RESPONSE CHARACTERISTICS OF TWO
MAN-CARRYING GROUND EFFECT MACHINES,
by A. A. Perlmutter and M. M. George
Report No. 212X90-2; TCREC Technical
Report 62-28, May 1962, 102p. incl.
illus, tables, Contract DA 44-177-
TC-733 Unclassified Report

An experimental investigation was
performed of the dynamic response
characteristics of the Princeton

(over)

1. Air Cushion
Vehicles

2. Contract
DA 44-177-TC-
733

20-foot annular jet Ground Effect Machine and the TRECOM 15-foot "Hula-Hoop". The tests ranged from dynamic stability and control responses to performance and for the P-GEM also the operation over specially prepared test tracks simulating various conditions of rough terrain. The P-GEM successfully negotiated all prepared obstacles. The calculated values of frequency and damping ratio from existing two-dimensional theories are found to be inadequate for the prediction of the dynamic characteristics of the test vehicles.

20-foot annular jet Ground Effect Machine and the TRECOM 15-foot "Hula-Hoop". The tests ranged from dynamic stability and control responses to performance and for the P-GEM also the operation over specially prepared test tracks simulating various conditions of rough terrain. The P-GEM successfully negotiated all prepared obstacles. The calculated values of frequency and damping ratio from existing two-dimensional theories are found to be inadequate for the prediction of the dynamic characteristics of the test vehicles.

20-foot annular jet Ground Effect Machine and the TRECOM 15-foot "Hula-Hoop". The tests ranged from dynamic stability and control responses to performance and for the P-GEM also the operation over specially prepared test tracks simulating various conditions of rough terrain. The P-GEM successfully negotiated all prepared obstacles. The calculated values of frequency and damping ratio from existing two-dimensional theories are found to be inadequate for the prediction of the dynamic characteristics of the test vehicles.

20-foot annular jet Ground Effect Machine and the TRECOM 15-foot "Hula-Hoop". The tests ranged from dynamic stability and control responses to performance and for the P-GEM also the operation over specially prepared test tracks simulating various conditions of rough terrain. The P-GEM successfully negotiated all prepared obstacles. The calculated values of frequency and damping ratio from existing two-dimensional theories are found to be inadequate for the prediction of the dynamic characteristics of the test vehicles.

Kellet Aircraft Corporation,
Willow Grove, Pa.

AN EXPERIMENTAL INVESTIGATION OF THE
RESPONSE CHARACTERISTICS OF TWO
MAN-CARRYING GROUND EFFECT MACHINES,
by A. A. Perlmutter and M. M. George

Report No. 212X90-2; TCREC Technical
Report 62-28, May 1962, 102p. incl.
illus, tables, Contract DA 44-177-
TC-733 Unclassified Report

An experimental investigation was
performed of the dynamic response
characteristics of the Princeton
(over)

1. Air Cushion
Vehicles

2. Contract
DA 44-177-TC-
733

Kellet Aircraft Corporation,
Willow Grove, Pa.

AN EXPERIMENTAL INVESTIGATION OF THE
RESPONSE CHARACTERISTICS OF TWO
MAN-CARRYING GROUND EFFECT MACHINES,
by A. A. Perlmutter and M. M. George

Report No. 212X90-2; TCREC Technical
Report 62-28, May 1962, 102p. incl.
illus, tables, Contract DA 44-177-
TC-733 Unclassified Report

An experimental investigation was
performed of the dynamic response
characteristics of the Princeton
(over)

1. Air Cushion
Vehicles

2. Contract
DA 44-177-TC-
733

Kellet Aircraft Corporation,
Willow Grove, Pa.

AN EXPERIMENTAL INVESTIGATION OF THE
RESPONSE CHARACTERISTICS OF TWO
MAN-CARRYING GROUND EFFECT MACHINES,
by A. A. Perlmutter and M. M. George

Report No. 212X90-2; TCREC Technical
Report 62-28, May 1962, 102p. incl.
illus, tables, Contract DA 44-177-
TC-733 Unclassified Report

An experimental investigation was
performed of the dynamic response
characteristics of the Princeton
(over)

1. Air Cushion
Vehicles

2. Contract
DA 44-177-TC-
733

Kellet Aircraft Corporation,
Willow Grove, Pa.

AN EXPERIMENTAL INVESTIGATION OF THE
RESPONSE CHARACTERISTICS OF TWO
MAN-CARRYING GROUND EFFECT MACHINES,
by A. A. Perlmutter and M. M. George

Report No. 212X90-2; TCREC Technical
Report 62-28, May 1962, 102p. incl.
illus, tables, Contract DA 44-177-
TC-733 Unclassified Report

An experimental investigation was
performed of the dynamic response
characteristics of the Princeton
(over)

1. Air Cushion
Vehicles

2. Contract
DA 44-177-TC-
733

20-foot annular jet Ground Effect Machine and the TRECOM 15-foot "Hula-Hoop". The tests ranged from dynamic stability and control responses to performance and for the P-GEM also the operation over specially prepared test tracks simulating various conditions of rough terrain. The P-GEM successfully negotiated all prepared obstacles. The calculated values of frequency and damping ratio from existing two-dimensional theories are found to be inadequate for the prediction of the dynamic characteristics of the test vehicles.

20-foot annular jet Ground Effect Machine and the TRECOM 15-foot "Hula-Hoop". The tests ranged from dynamic stability and control responses to performance and for the P-GEM also the operation over specially prepared test tracks simulating various conditions of rough terrain. The P-GEM successfully negotiated all prepared obstacles. The calculated values of frequency and damping ratio from existing two-dimensional theories are found to be inadequate for the prediction of the dynamic characteristics of the test vehicles.

20-foot annular jet Ground Effect Machine and the TRECOM 15-foot "Hula-Hoop". The tests ranged from dynamic stability and control responses to performance and for the P-GEM also the operation over specially prepared test tracks simulating various conditions of rough terrain. The P-GEM successfully negotiated all prepared obstacles. The calculated values of frequency and damping ratio from existing two-dimensional theories are found to be inadequate for the prediction of the dynamic characteristics of the test vehicles.

20-foot annular jet Ground Effect Machine and the TRECOM 15-foot "Hula-Hoop". The tests ranged from dynamic stability and control responses to performance and for the P-GEM also the operation over specially prepared test tracks simulating various conditions of rough terrain. The P-GEM successfully negotiated all prepared obstacles. The calculated values of frequency and damping ratio from existing two-dimensional theories are found to be inadequate for the prediction of the dynamic characteristics of the test vehicles.

UNCLASSIFIED

UNCLASSIFIED